AN EXPERIMENTAL INVESTIGATION OF FLASER AND WAVY BEDDING

by

NATHAN HAWLEY ©

B.S., University of Chicago

(1971)

M.S., University of Chicago

(1976)

SUBMITTED IN PARTIAL FULFILLMENT
OF THE REQUIREMENTS FOR THE
DEGREE OF

DOCTOR OF PHILOSOPHY

at the

MASSACHUSETTS INSTITUTE OF TECHNOLOGY

AUGUST 1978

Signature of Author.....
Department of Earth and Planetary Sciences
August 15, 1978

Certified by.....
Carl Wunsch

Accepted by.....
Lindgren

AN EXPERIMENTAL INVESTIGATION OF FLASER AND WAVY BEDDING

BY

NATHAN HAWLEY

Submitted to the Department of Earth and Planetary Sciences on August 15, 1978 in partial fulfillment of the requirements for the Degree of Doctor of Philosophy

ABSTRACT

Flume experiments simulating a 12.5 hour tidal cycle were performed to test the hypothesis that flaser and wavy bedding can be produced in shallow subtidal areas by tidal activity. The effects of clay composition, sand size, total amount of sediment deposited, compaction time, and peak current velocity were investigated. It was found that the resistance of a recently-deposited mud bed to subsequent erosion is determined primarily by the amount of overburden. The effect of a rippled sand bed on the erosion of an overlying mud bed is profound, causing erosion to occur at mean flow velocities substantially less than those required for erosion of a planar bed. The results indicate that successive deposition of thin mud layers during several consecutive slack-water periods cannot occur since the deposited mud will always be resuspended during the intervening high-velocity episodes. Although thick mud layers may accumulate during a single slack-water period, these beds are unlikely to be preserved due to the high rate of subsequent

reworking. It is concluded that the presence of flaser and wavy beds in shallow subtidal regions is most likely due to storm activity.

Thesis Supervisor: Dr. John B. Southard, Associate Professor, Department of Earth and Planetary Sciences

ACKNOWLEDGEMENTS

My thanks to R.L. Miller, L.F. McGoldrick, and J.B. Southard for advice, Molly Rauber for typing the manuscript, Mary Rodin for drafting the figures, Michael Cahen and Tamson Scott for assistance in the lab, and A.M. Ziegler, F.M. Richter, the University of Chicago, and the Massachusetts Institute of Technology for financial support. A special thanks to all those who listened to the gripes.

TABLE OF CONTENTS

	Page
ABSTRACT	2
TABLE OF CONTENTS	5
LIST OF SYMBOLS	7
LIST OF FIGURES	9
LIST OF TABLES	12
INTRODUCTION	13
BACKGROUND	20
Physical Properties of Water	20
Fluid Flow	22
Physical Properties of Sedimentary Particles	32
Previous Experimental Studies of Noncohesive Sediments	38
Previous Experimental Studies of Cohesive Sediments	41
DESCRIPTION OF APPARATUS	50
EXPERIMENTAL PROCEDURE	55

	Page
PRESENTATION OF THE EXPERIMENTAL RESULTS	67
General Observations	67
The "T"Runs	71
The "U" and "V" Runs	76
Calculation of u_*	88
Calculation of u_{50}	91
APPLICATION OF THE EXPERIMENTAL RESULTS TO NATURAL SETTINGS	94
CONCLUSIONS	99
REFERENCES CITED	104
APPENDIX A: DETAILED OBSERVATIONS OF THE EXPERIMENTAL RUNS	112
APPENDIX B: PHOTOGRAPHS OF THE EXPERIMENTAL RUNS	173
APPENDIX C: LISTINGS OF THE COMPUTER PROGRAMS USED IN THE INVESTIGATION	186
APPENDIX D: PROCEDURE FOR CALCULATING THE SHEAR VELOCITY	203

LIST OF SYMBOLS

b	flume width
c	concentration
C	Chézy coefficient
C_*	dimensionless Chézy coefficient
d	grain diameter
D	flow depth
f	Darcy-Weisbach friction factor
Fr	Froude number
g	acceleration due to gravity
k	coefficient
R	hydraulic radius
R'	grain hydraulic radius
R''	bed form hydraulic radius
Re	Reynolds number
S_b	bottom slope
S_e	energy slope
S_w	water-surface slope
t	time
T	temperature
u	horizontal flow velocity
$\bar{u}$	mean horizontal flow velocity
u_*	shear velocity
u_{*_c}	critical shear velocity

V_F fall velocity

v_f volume of fluid

v_s volume of sediment

v_{susp} volume of suspension

w vertical flow velocity

w' vertical turbulent velocity fluctuations

x horizontal coordinate

z vertical coordinate

κ von Karman's constant

θ sediment entrainment parameter

ρ density

ρ_f density of fluid

ρ_{susp} density of suspension

τ_0 shear stress

μ viscosity

μ_f viscosity of fluid

μ_{susp} viscosity of suspension

ν kinematic viscosity

LIST OF FIGURES

		Page
Figure 1:	Classification of Alternating Sand and Mud Beds	14
Figure 2:	Flaser Bedding, Caseyville Sandstone, Illinois	16
Figure 3:	Wavy Bedding, Twin Creek Limestone, Utah	16
Figure 4:	Reference Diagram Showing Symbols Used	23
Figure 5:	Occurrence of Bed Forms as a Function of Grain size and Flow Velocity	28
Figure 6:	Distribution of Average Shear Stress Across a Rippled Surface	29
Figure 7:	Fall Velocity of Quartz Spheres in Water as a Function of Diameter	34
Figure 8:	Erosion and Deposition of Sediment as a Function of Mean Flow Velocity and Grain Size	40
Figure 9:	Entrainment and Suspension Criteria as a Function of Grain Size	42
Figure 10:	Schematic of the Flume	51

		Page
Figure 11:	Calibration Curves of the Orifice Meter	53
Figure 12:	Grain-Size Distribution of the Sands Used	54
Figure 13:	Typical Mud Deposition at Ebb Tide	70
Figure 14:	Partial Erosion of Mud During Flood Current	70
Figure 15:	Mud Deposition at Flood Tide	72
Figure 16:	Mixed Erosion and Burial of Mud During Ebb Current	72
Figure 17:	Suspended-Sediment Concentration as a Function of Mineralogic Composition	74
Figure 18:	Suspended-Sediment Concentration as a Function of Initial Load	75
Figure 19:	Preservation of continuous Mud Bed During Flood Tide	78
Figure 20:	Partial Preservation of Mud Bed During Flood Tide	78
Figure 21:	Wavy Flaser Bedding	79
Figure 22:	Simple Flaser Bedding	79
Figure 23:	Suspended-Sediment Concentration as a Function of Grain Size	80

		Page
Figure 24:	Suspended-Sediment Concentration as a Function of Grain Size	81
Figure 25:	Suspended-Sediment Concentration as a Function of Grain Size	82
Figure 26:	Development of Wavy Bedding	83
Figure 27:	Occasional Flasers Buried by Migrating Sand	83
Figure 28:	Idealized Sequence Showing the Development of a Flaser Bed	85

LIST OF TABLES

		Page
Table 1	Previous Experimental Investigations on the Erosion of Cohesive Sediments	44
Table 2	Summary of Experimental Runs	57
Table 3	Suspended-Sediment Grain-Size Analyses	63
Table 4	Mean Values of u_* and Their Standard Deviations	89
Table 5	Mean Values of u_{50}	93

INTRODUCTION

The research described herein is concerned with the conditions of sediment supply and current velocity needed for the formation and preservation of alternating sand and mud beds. The investigation is experimental in nature because, in addition to the great difficulties involved in an observational study, it was felt that more useful results would be obtained by systematic variation of several key parameters than by making observations in a relatively uncontrolled environment.

Alternating sand and mud beds are a rather common feature of both the stratigraphic record and of Holocene environments. Reineck and Wunderlich (1968) have proposed a purely descriptive classification system based on the relative amounts of sand and mud (the latter defined as a material whose average grain size is less than 60 μm), and on the lateral continuity of the minor constituent (Fig. 1). Thicknesses of the individual layers commonly are of the order of millimeters or centimeters. These structures are thus rather small-scale features, probably formed in response to local conditions. An important limitation on these conditions is that the sand present is always rippled. Since ripples are formed only in response to well-defined conditions of current velocity and sand size, and since they are readily destroyed by current velocities higher than those responsible for their formation,

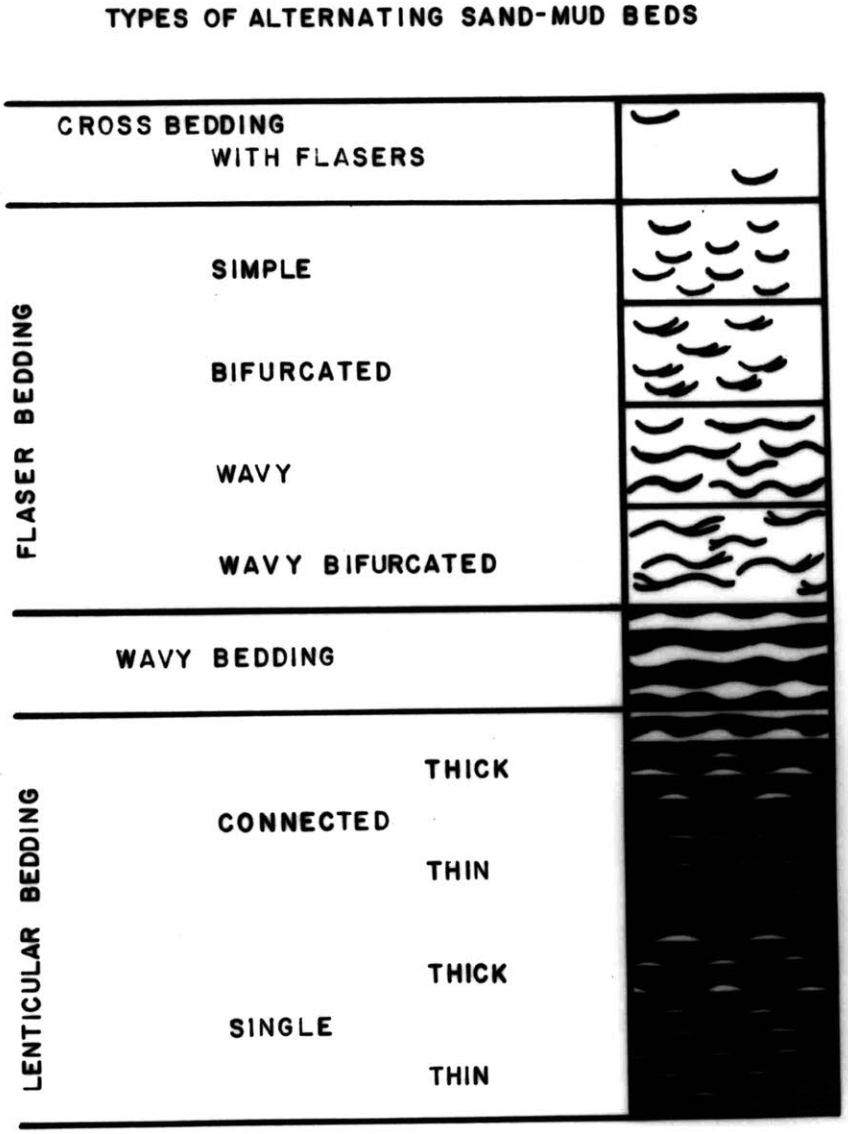

Figure 1: Classification of alternating sand and mud beds (after Reineck and Wunderlich,1968)

the range of current velocities that may exist during the formation of these structures is rather narrow. Reineck and Wunderlich stated that these structures form due to alternating periods of (relatively) high and low current activity, the sand being deposited during the high-velocity episodes and the mud during the more quiescent periods. Accordingly, for the formation of these deposits, there must exist not only abundant supplies of both sand and mud, but there must also be alternating periods of high and low current veloicty. Reineck and Wunderlich also noted that the sand could be rippled as a result of wave activity. Since the effects of waves were not examined in this study, such structures will not be considered further.

Based on their own and others' observations, Reineck and Wunderlich stated that the most likely areas for the formation of alternating sand and mud sequences are intertidal and shallow subtidal areas, where the alternating periods of high and low current velocity are due to the daily tidal cycles. They noted, however, that these deposits have also been reported from Holocene delta fronts, lakes, and lagoons.

The author has examined examples of these deposits from rocks formed in lacustrine, fluvial, deltaic (Fig. 2), and littoral (Fig. 3) environments, and has been shown photos of their occurrence in turbidite sequences. It seems, therefore, that these deposits can be preserved in a variety of

Figure 2: Flaser bedding in the Caseyville Sandstone, Illinois. Sample is 10 cm high.

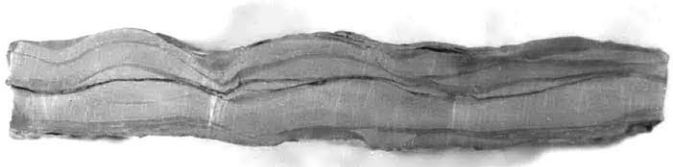

Figure 3: Wavy bedding in the Twin Creek Limestone, Utah. Sample is 5 cm high.

environmental settings. In addition to tidal activity, several other common processes, such as crevasse splaying, channel meandering, and storm activity could provide the necessary periods of alternating high and low current velocities.

Reineck (1960, 1963, 1967) and Reineck and Wunderlich (1969) have described the occurrence of these structures in both intertidal flats and subtidal channels of the North Sea. Reineck and Wunderlich (1967) have shown that these deposits can be formed during a single tidal cycle. In their later paper (Reineck and Wunderlich, 1969), however, they state that structures formed as the result of such conditions are not likely to be preserved since the areas in which they are formed (intertidal channels) are subject to substantial reworking during subsequent tidal cycles.

McCave (1970) concluded that, based on sediment budget calculations, alternating sand and mud beds could not form in either the open sea or in nearshore areas as the result of tidal activity. He stated that the results of Reineck and Wunderlich were the result of abnormally long slack-water periods and abnormally high sediment concentrations. McCave suggested that storm activity was a more likely candidate for the formation of these beds in both offshore and nearshore waters.

Terwindt and Breusers (1971) published the results of the only experimental investigation on the origin of alternating

sand and mud beds. They sought to explain the observed thickness of the mud beds (up to several centimeters) found in the Haringvliet Estuary in light of the fact that, according to their calculations, the maximum mud thickness that could be deposited in a single slack-water period was 0.3 cm. By determining the erodibility of muds collected from the area, they concluded that if the current velocity at a height of 50 cm above the bed did not exceed 60 cm/s a recently deposited mud bed would not be eroded. This observation led them to suggest that mud layers could be deposited during several consecutive slack-water periods occurring during the neap portion of the biweekly spring-neap tidal cycle. During this period the maximum current velocities would not be great enough to erode the mud deposited, while during the spring part of the cycle, when current velocities are higher, sand could be deposited over the mud.

When reading the above report, the author was struck by two points. First, in their flume experiments, Terwindt and Breusers used a planar bed. If a rippled surface was used, would this not lower the mean velocity needed to erode the mud? Since even the values reported by Terwindt and Breusers are almost always exceeded in natural settings, a further reduction in the minimum velocity needed for mud erosion would make their explanation untenable.

The second point relates to the rigidity of the mud beds

that they tested. In their experiments the mud bed was formed by depositing mud from a highly concentrated suspension in still water. Their experiments, as well as those of Migniot (1968), showed that the rigidity of the bed formed decreased as the concentration of the suspension from which it was deposited increased, due to the increased rate of deposition. Mud beds formed in natural tidal channels will accumulate more slowly than those formed by Terwindt and Breusers, due both to the smaller concentrations and to the higher current velocity that exists. The effect of this decrease in accumulation rate might lead to an increase in the resistance to erosion of the mud bed. Both of these effects should be considered before applying the results of Terwindt and Breusers.

An experimental program using a real-time tidal cycle of 12.5 hours was designed to investigate these effects. Initially the experiments were designed to reproduce the conditions reported by Terwindt and Breusers. Later, the range of conditions was expanded so that an investigation of the formation of flaser and wavy bedding in a variety of conditions was performed. Lenticular beds were not considered in this study.

Two previous investigations, those of Dillo (1960) and Bayazit (1968), have dealt with the response of rippled sand beds to tidal flow. Dillo, using a 12.5 hour tidal cycle, reported that when the flow direction was reversed the shape of the ripples quickly altered so that the bed was again in

equilibrium with the flow. He also stated that although the flow was unsteady, the ripples, because of the long time periods involved, behaved as though they had been formed in steady-flow conditions. Bayazit, using modeling techniques, came to a similar conclusion. He also reported that, as the number of tidal cycles increased, the response time of the ripples to adjust to the change in flow direction decreased.

BACKGROUND

Physical Properties of Water

The physical properties of both the fluid and the sediment are important in sediment transport studies. In addition, changes in the properties of the fluid as a result of suspended sediment may be important. In the present study, the two most important properties of water are its density (ρ) and its viscosity (μ). The value of these properties changes with both temperature and salinity. The data used in this paper are taken from Winegard (1970).

The effect of suspended particles on the viscosity of a fluid was expressed by Einstein (1906) as:

$$\mu_{susp}/\mu_f = 1 + kc \qquad (1)$$

where c is the concentration of the suspended particles and k is a coefficient equal to 2.5 for c less than or equal to three per cent. Einstein's equation is accurate for stable suspensions of spherical particles. For unstable suspensions and nonspherical particles, the value of k increases. In addition, for c greater than three percent, higher order terms must be added to equation 1. In the present study, c is one per cent or less, so equation 1 may be used in the form presented. However, the particles are nonspherical and the suspension unstable. Test calculations with an increase of ten per cent in the viscosity revealed that the resulting difference in shear velocity is less than two per cent. Given the other inaccuracies in the experiments, it was felt that this variation could be ignored. Viscosity measurements taken during Run U-8 with a Synchro-Lectric viscosimeter revealed no measurable difference in the viscosity from that of pure water.

The effect of suspended particles on the density of a fluid is given by:

$$\rho_{susp} = (\rho_f v_f + \rho_s v_s) \; / \; v_{susp} \qquad (2)$$

Solving equation 2 with the appropriate values gives a density difference of less than one per cent. This effect has also been ignored in the present study.

Fluid Flow

When a viscous fluid with a non-zero velocity u (Fig. 4) moves across a rigid boundary, the "no-slip" condition demands that the velocity of the fluid at the boundary equal the velocity of the boundary. Since the bulk of the fluid is moving with a different velocity, there must exist some region in which there is a velocity gradient. This region is known as a boundary layer. Initially the boundary layer will be restricted to a zone close to the bounding surface. As the flow progresses, the thickness of the boundary layer increases until it either intersects another boundary layer or until it occupies the entire volume of the flow. Schlichting (1968) presents an extensive review of boundary layers.

In turbulent flow, the boundary layer may be considered to consist of three zone:

1. The zone nearest the wall, where viscous forces are dominant, known as the viscous sublayer. Turbulent fluctuations are observed, but in this zone momentum transfer occurs primarily by molecular diffusion. The thickness of this zone is on the order of millimeters.

2. A thin zone called the intermediate or transition layer. Turbulent eddies appear to be produced more

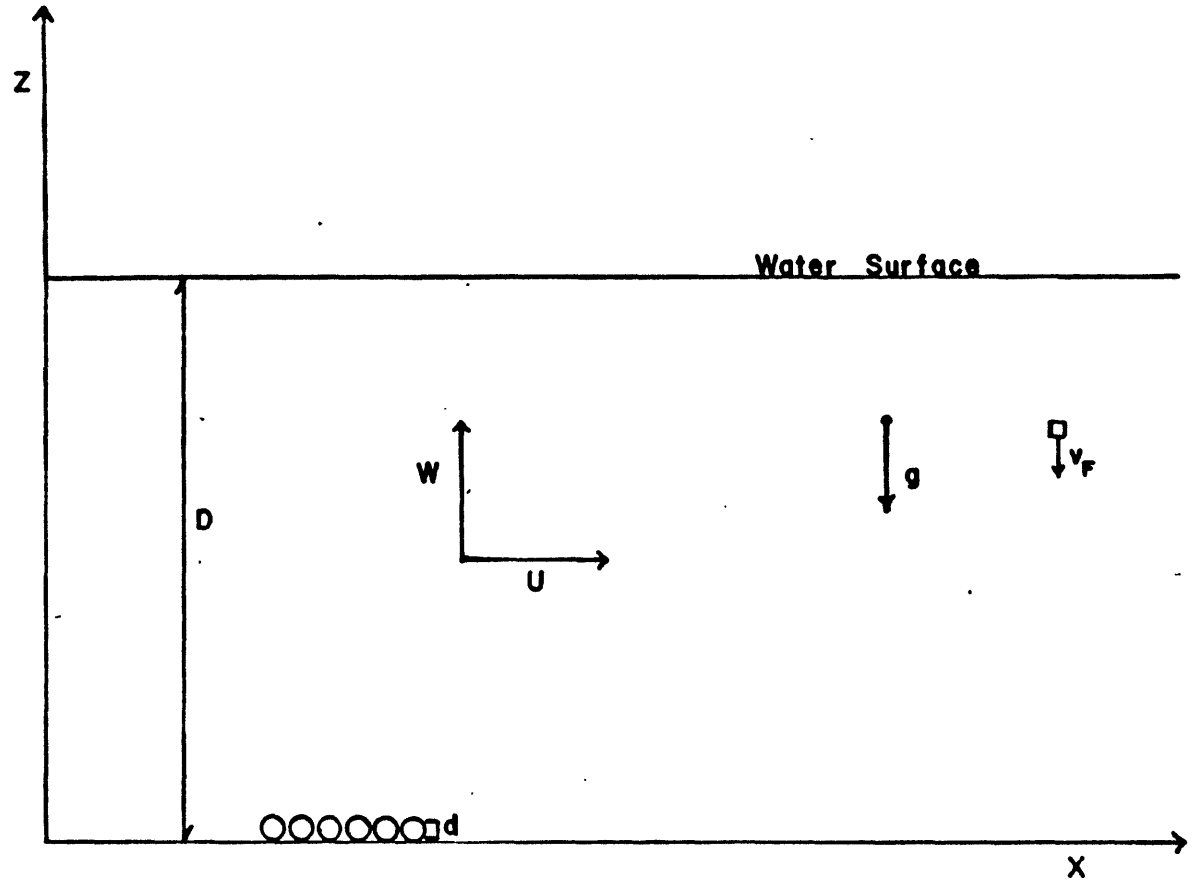

Figure 4: Reference diagram showing symbols used.

frequently in this zone than in the others and hence diffuse out into the adjoining regions.

3. The thick layer known as the outer zone. In fully developed turbulent flow this zone occupies most of the flow depth. This zone can be considered to consist of two sub-zones which differ in the shape of the velocity gradient observed. In the inner part, the velocity gradient can be described by a logarithmic function, the so-called "law of the wall." In the outer part, the gradient is described by the velocity defect law.

In sediment transport studies, the shear stress at the bed surface τ_0, in conjunction with the properties of the sediment, determines the mode of transport, if indeed transport occurs at all. The shear velocity is related to the shear stress by:

$$u_* = (\tau_0/\rho_f)^{1/2} \qquad (3)$$

A variety of formulas to calculate u_* exist, depending upon the types and locations of the quantities measured; only those formulas used in the present study will be reviewed here. All are based upon the two laws describing the velocity profile in the outer zone. Once u_* is known, τ_0 may be calculated

from equation 3.

The nature of the wall has a significant effect on the velocity profile developed in the fluid. For a planar bed a distinction between hydraulically smooth and hydraulically rough beds can be made. For hydraulically smooth beds the dimensions of roughness elements of the boundary are much smaller than the thickness of the viscous sublayer. Accordingly, any disturbance due to these elements will be dissipated before it can propagate into the outer zones of the flow. Equation 4, derived from Prandtl's mixing-length theory, is a method for determining u_* if u_z, the average velocity measured at a height z above the bed, is known:

$$u_z/u_* = \ln(u_* z/\nu) \; / \; \kappa + 5.5 \qquad (4)$$

where κ is von Karman's constant, an experimentally determined quantity whose value in clear water is 0.4. If there is a significant amount of suspended material in the flow, κ may vary to as low as 0.2 (Vanoni, 1975). In the present study, κ varied between 0.35 and 0.4.

If the roughness elements are of the same order as the thickness of the viscous sublayer, then disturbances generated by them will propagate into the flow. In this case, the roughness of the surface must be taken into account when computing u_*. Most flows over sand beds fall into this category. Equation 5 enables u_* to be calculated for a rough surface if

the particle diameter d is known:

$$u_z/u_* = \ln(30.2 \cdot z/d)/\kappa \qquad (5)$$

The presence of sediment in the flow can also affect the velocity profile. Einstein and Chien (1955) proposed a modification of equation 5 for sediment-laden flows:

$$u_z/u_* = \ln(z/35.45 \cdot d)/\kappa + 17.66 \qquad (6)$$

If the boundary is composed of discrete particles, and a velocity sufficient to transport these particles is achieved, the bed will not remain planar. Rather, it will start to deform and form undulations, known as bed forms. The resulting surface topography is known as a bed configuration. Reineck and Singh (1975) and Harms et al. (1975) provide good reviews of the experimental and observational work done on the formation and occurrence of bed forms. Kennedy (1969) provides a theoretical framework for their origin. In the present study only the bed form known as ripples will be considered.

When sediment movement is initiated, if the particle diameter is less than 0.6 mm, the first bed form to appear will be ripples (Southard and Boguchwal, 1973). As noted by Southard (1971), the three parameters which determine which of the several bed forms will develop are sediment size, flow depth, and fluid velocity. Except for very shallow depths (less than

8 - 10 cm), the occurrence of ripples is independent of flow depth. Thus the unidirectional flow conditions which produce ripples may be shown in a two-dimensional diagram (Fig. 5). Although many different types of ripples have been described, they all share certain characteristics. In profile they are roughly triangular with a crest-to-crest distance about ten times their height. Wavelengths are generally less than 30 cm. Ripples migrate downstream with a velocity far lower than that of the fluid. Ripples are found only in noncohesive sediments whose grain size is less than 0.6 mm, and are quickly altered to other bed forms as the flow velocity is increased. Due to the varying flow depth across a rippled surface, one would expect the average velocity, and hence the average shear stress, to vary also. Experiments by Raudkivi (1963) confirmed this (Fig. 6). In addition, Raudkivi also found that the instantaneous shear stress varied across the ripple profile, reaching a maximum in the ripple troughs.

The presence of any bed configuration generates another roughness, the form roughness, in addition to the bed roughness caused by the individual particles. The presence of this form roughness significantly affects the velocity gradient in the fluid and renders the use of equations 4-6 invalid.

The value of u_* is also related to the hydraulic radius (defined as the cross-sectional area of the channel divided by the wetted perimeter) and the energy slope by:

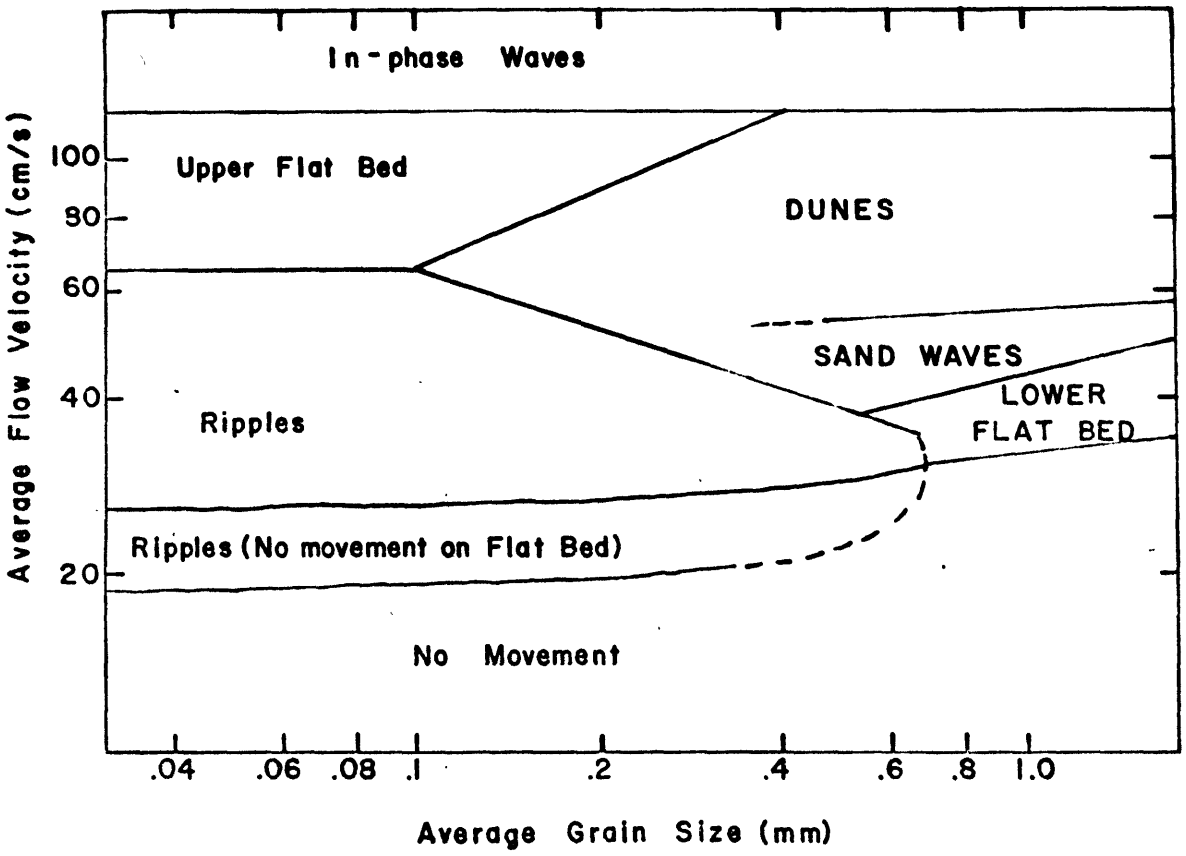

Figure 5: Occurrence of bed forms as a function of grain size and flow velocity. (after Harms et al., 1975)

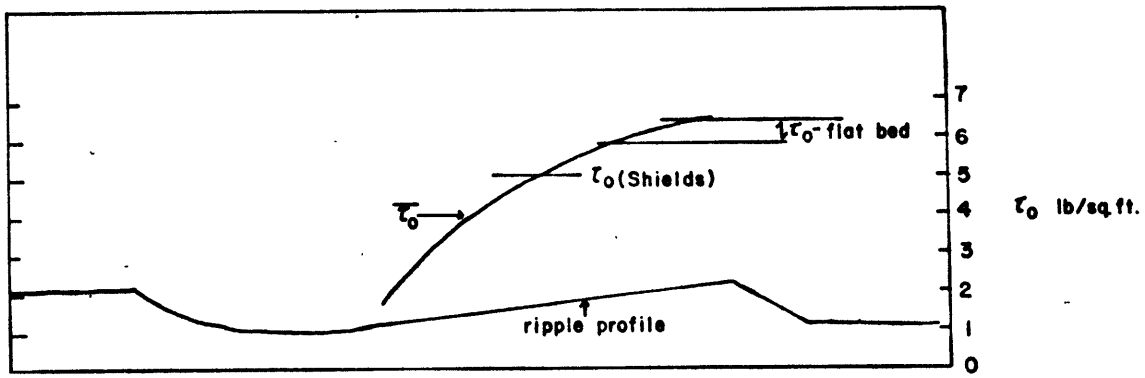

Figure 6: Distribution of average shear stress across a rippled surface. (after Raudkivi, 1963)

$$u_* = (gRS_e)^{1/2} \tag{7}$$

S_e is defined as

$$S_e = S_w - Fr^2 \ (S_w - S_b) \tag{8}$$

where S_w is the water-surface slope and S_b is the bed-surface slope.

In the presence of bed configurations, the value of R changes from its defined value, making the application of equation 7 more complex. Simons and Şentürk (1977) have reviewed a variety of methods for determining u_* in the presence of bed configurations. Most of these methods attempt to evaluate the effects of the form roughness and bed roughness separately and then combine them by adding the hydraulic radius computed for each roughness:

$$R = R' + R'' \tag{9}$$

where R' is the hydraulic radius associated with the bed roughness and R" is the hydraulic radius associated with the form roughness. Substitution of R into equation 7 then gives a value for u_*. These methods are cumbersome, and a knowledge of the grain size is needed. In the present study, where the bed is covered by mud, it is not at all clear what grain size should be used.

Another method, presented by Richardson and Simons (1967), is considerably easier to use, yields results as accurate as any of the other methods (Simons and Şentürk, 1977), and does not require knowledge of the appropriate bed roughness. Richardson and Simons state that the resistance to flow over a rippled bed is due almost entirely to the form roughness, a statement confirmed by Bayazit (1968). This fact, coupled with the narrow size range of sediments which form ripples, allowed Richardson and Simons to incorporate the effect of both roughnesses into a single equation:

$$u_z/u_* = (3.33 - (0.13/u_*)) \ln z + 14.3 \qquad (10)$$

where all quantities are measured in English units.

Hydraulic engineers have devised several formulas relating the average velocity of the total flow, u, to the resistance of the bed. Two of the most commonly used are the Darcy-Weisbach formula and the Chézy formula defined by:

$$u^2 = 8gRS_e/f \qquad (11)$$

and

$$u = C(RS_e)^{1/2} \qquad (12)$$

Combining equations 10 and 11 results in an expression relating

the Darcy-Weisbach friction factor and the Chézy coefficient:

$$C/(g)^{1/2} = (8/f)^{1/2} = C_* \qquad (13)$$

If one knows the mean velocity and the bottom and surface slopes, one can calculate u_* for a rippled bed from the following relation, also presented by Richardson and Simons:

$$C_* = (7.66 - (0.3/u_*)) \log D + 0.13/u_* + 11.0 \qquad (14)$$

where D, the flow depth, is measured in feet.

Physical Properties of Sedimentary Particles

Sediments may be classified into two groups, cohesive and noncohesive. Cohesive sediments generally consist of materials which have large surface charges, such as clay minerals. In saline solutions, this surface charge leads to the formation of strong electrochemical bonds between the individual particles. Due to this bonding, the density, size, and shape of the individual particles is less important than the respective properties of the agglomerates into which they form. Individual particles of cohesive materials are generally very small (less than 2 μm), but the resulting agglomerates can be much larger (up to over 60 μm).

Noncohesive sediments are formed of minerals, such as quartz and feldspar, without strong surface charges so interparticle bonds are negligible. In general, beds of noncohesive sediments have grain sizes above 60 μm, although noncohesive beds with grain sizes as small as 15 μm have been reported (Rees, 1966).

The most important particle property in sediment transport studies is fall velocity v_F. Because of its importance, fall velocity has been the subject of extensive research. Good reveiws may be found in Graf (1971) and Raudkivi (1976).

The fall velocity of any particular particle will depend on the density, shape, and size of the particle. Due to the irregular shape of most sedimentary particles, it has become common practice to define fall velocity in terms of the diameter of a quartz sphere whose fall velocity is equivalent to that of the particle. This practice has two advantages: it combines the effects of particle shape, size, and density, and it gives a measure of how the particle actually behaves. In water, for particles whose diameter is less than 60 μm, the fall velocity can be calculated from Stokes' Law. For larger particles, the velocity may be determined from the table of Zeigler and Gill (1959). Figure 7 presents the fall velocity as a function of particle diameter.

The data of Zeigler and Gill, and the use of Stokes' Law, are, strictly speaking, valid only for single particles falling through an infinitely broad, quiescent fluid. Such a case is

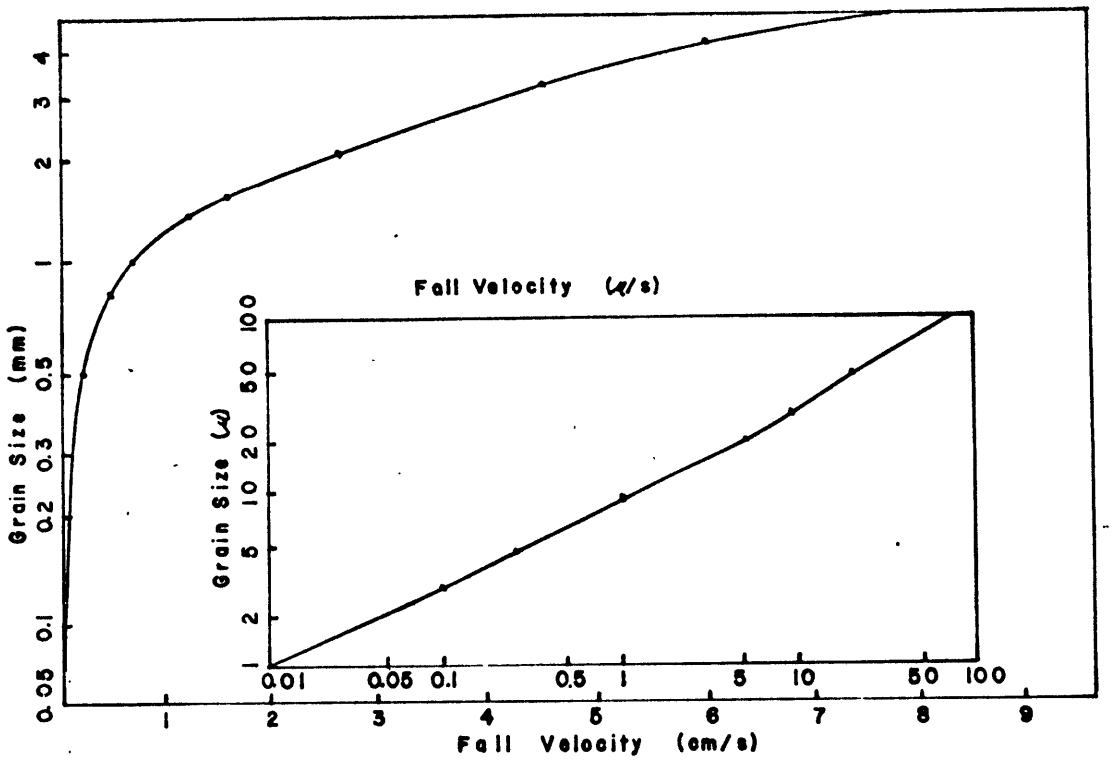

Figure 7: Fall velocity of quartz spheres in water as a function of grain diameter.

far removed from most real situations. Many studies have been done on the effects of the proximity of side walls, particle concentration, and heterogeneous size distributions. Unfortunately, it has not yet been possible to formulate a comprehensive theory to take these complications into account. Rather, one must evaluate each factor separately and then attempt to deduce how they interact with each other.

In the experiments described below, two deviations from the ideal situation are important. Both have to do with the settling velocities of clay materials. As noted above, clay particles have strong surface charges. In saline solutions the particles tend to form aggregates by a process known as flocculation. The rate at which flocculation occurs is governed by the frequency of inter-particle collisions. These collisions may result from Brownian motion, local shearing, or differential settling velocities. The equations describing the rates at which these processes occur may be found in Einstein and Krone (1962). Einstein and Krone compared flocculation rates for these three mechanisms and concluded that for natural situations the most important cause of interparticle collisions is differential settling velocities due to varying grain sizes. In flume experiments, however, the sediment is commonly recirculated both through the pump and through pipes whose cross-sectional area is much less than that of the flume channel. This leads to the generation of very high local shear stresses which are

great enough to break the interparticle bonds, thus at least partially negating any flocculation that takes place in the flume. Thus, the particle size in flume experiments may be considerably less than that in natural situations. This of course leads to a reduction in the fall velocity of the particles. More importantly, though, it may lead to an increase in the shear strength of the deposited bed over that found in natural settings. Krone (1963) has described flocculated particles in terms of the order of the agglomerates. In his terminology, a first-order agglomerate is composed of several primary particles, a second-order agglomerate is composed of several first-order particles, and so on. Krone (1972), reasoned that the agglomerates which settle to the bed form, in effect, an agglomerate of order n + 1 where n is the order of the individual agglomerates. Since the strength of the interparticle bonds decreases with increasing agglomerate order, a bed consisting of particles whose order is low will be able to resist a higher shear stress than a bed consisting of higher-order agglomerates. If the order of the agglomerates found in flume studies is lower than that found in natural settings, it follows that the resulting beds will exhibit greater resistance to erosion than the natural beds.

The second consideration is the effect of concentration of the fall velocity of the particles. In general the fall velocity will decrease with increasing particle concentration.

McNown and Lin (1952) reported that a sediment concentration of one per cent leads to a reduction in the fall velocity of twenty per cent for particles with a diameter of 0.1 mm. The results of Steinour, summarized by Maude and Whitmore (1958), exhibit a similar trend for particles in the silt size range for concentrations of less than one per cent. If the particle concentration exceeds one per cent, a phenomenon known as hindered settling occurs. Hindered settling is characterized by the fact that the particles tend to settle as a group, producing a distinct interface in the fluid with clear liquid above it and the suspended material below. This interface gradually settles to the bed surface as the sediment is deposited. Einstein and Krone (1962) noted the occurrence of this phenomenon, as did Migniot (1968), who showed that the shear strength of the deposited mud bed decreased with increasing rates of deposition.

All of the above observations were made in still water; extensive research on the behavior of falling bodies in flowing water has not as yet, been done. Owen (1971) reported that the observed fall velocity of silt-sized particles measured in the River Thames exceeded the values measured in the laboratory by as much as thirty per cent. Experiments by Murray (1971), on the other hand, show that because of the turbulence associated with moving water, the fall velocity of the particles can be reduced by as much as thirty per cent. It seems likely

that the results of Owen are the result of an increase in particle size due to flocculation caused by local shearing in the flow. Thus, even though the fall velocity of a particle of any given size would be reduced, the increased particle size would more than compensate for it, resulting in a net increase in fall velocity. Krone (1972) has stated that flocculation due to local shearing is more important in natural settings than that due to either Brownian motion or differential settling, except at the lowest flow velocities.

Previous Experimental Studies of Noncohesive Sediment

The flow conditions under which sediment will be eroded, transported, and deposited, and the various modes of transport, have been the subject of many studies (see Graf, 1971, and Raudkivi, 1976). Only a brief review is given here.

Commonly, three modes of transport are considered: traction, in which the sediment moves by rolling across the bed; saltation, in which the particles move in a series of jumps; and suspension, in which the particles are continuously supported by the fluid. Obviously, the dividing line between these modes is somewhat indistinct. For a given grain size, the order of the modes experienced as the fluid velocity increases is traction, saltation, and suspension. Grains transported by traction and

saltation are frequently grouped together as the bed load.

In 1936, Shields published experimental data relating his sediment entrainment parameter to the Reynolds number of the flow. Hjulström (1935) published a graph which related sediment movement to the average flow velocity (Fig. 8). Two points are of interest in Hjulström's figure. The first is that the velocity needed to initiate erosion reaches a minimum for grain sizes of about 0.2 mm. The second is that the velocity required for subsequent transportation of a given grain size is less than that required for its initial entrainment.

Just as there have been investigations of the conditions necessary for initiation of sediment movement, there also have been studies on the conditions necessary for suspension of sediment. Hjulström's plot is an early attempt at defining an appropriate criterion. A more recent approach is that of Bagnold (1966). Bagnold reasoned that in order for a particle to be suspended, the vertical turbulent velocity fluctuations must exceed the particle fall velocity. By examining experimental data of various workers, he concluded that an appropriate value of w' to maintain particles in suspension would be

$$w' = 0.8\ u_{*_c} \tag{15}$$

Using this value, he defined an entrainment parameter, similar

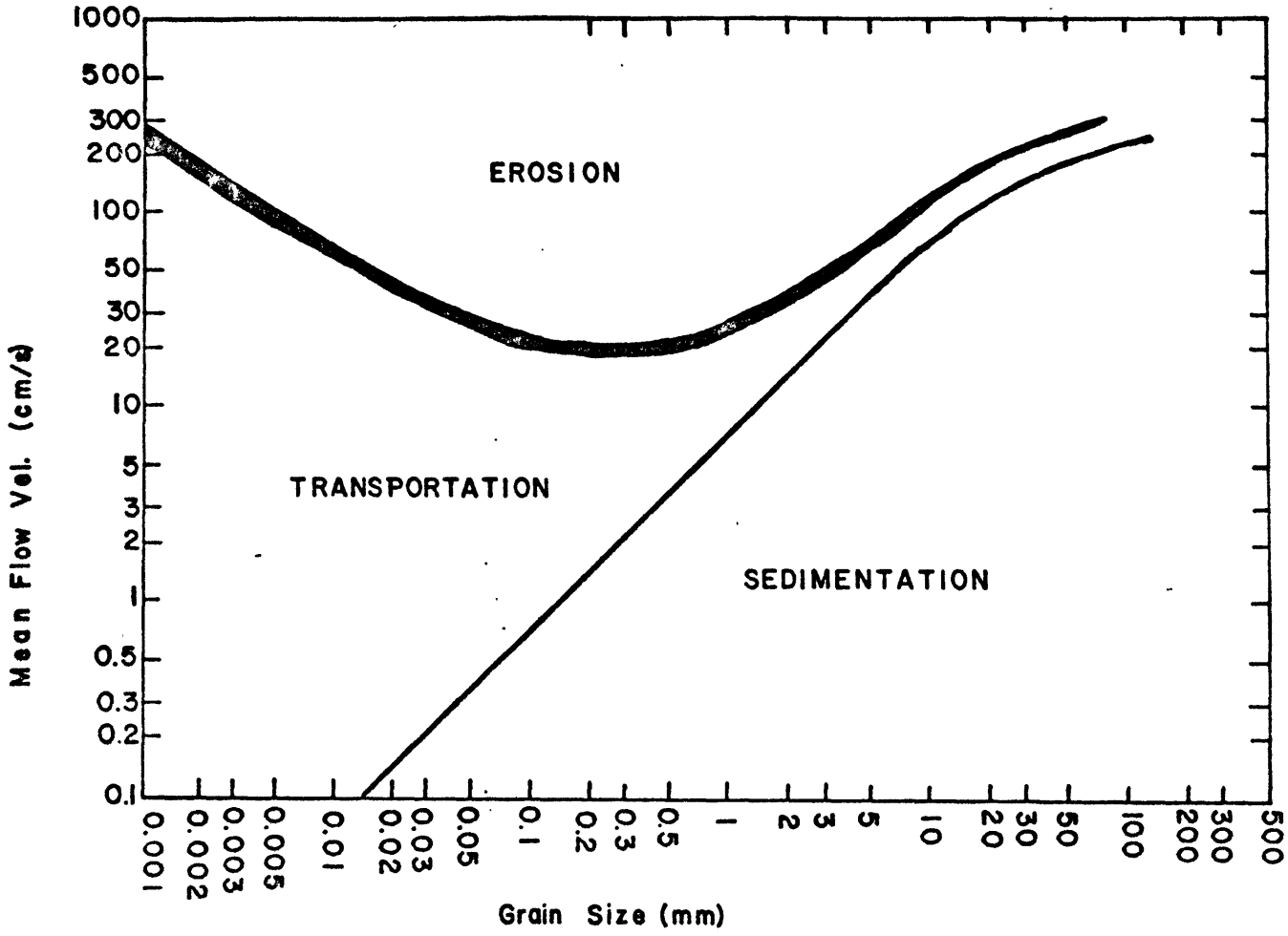

Figure 8: Erosion and deposition of sediment as a function of mean flow velocity and grain size. (after Hjulstrom, 1935)

in form to that of Shields, for the suspension of sediment:

$$\theta = 0.4\ w^2/gd \qquad (16)$$

A plot showing both θ and the Shields parameter is given as Figure 9. Since w' must equal zero when averaged over time, in theory the particle should eventually settle to the bottom, regardless of the value of w'. To circumvent this difficulty, Bagnold suggested that the vertical turbulence is anisotropic, with the upward fluctuations imparting a greater momentum flux than the downward fluctuations. This would imply that the upward fluctuations must occur as limited, violent bursts, with the downward fluctuations occurring over larger areas with smaller velocities. The phenomenon of turbulent bursting, reviewed by Jackson (1976), seems to fit this pattern.

Previous Experimental Studies of Cohesive Sediments

The criteria for erosion and deposition of noncohesive sediments have been more or less agreed on, as discussed above. For cohesive sediments far less experimental work has been conducted, so that the state of knowledge is far less complete. In particular, it has been far more difficult to establish uniform criteria for the entrainment of cohesive sediments

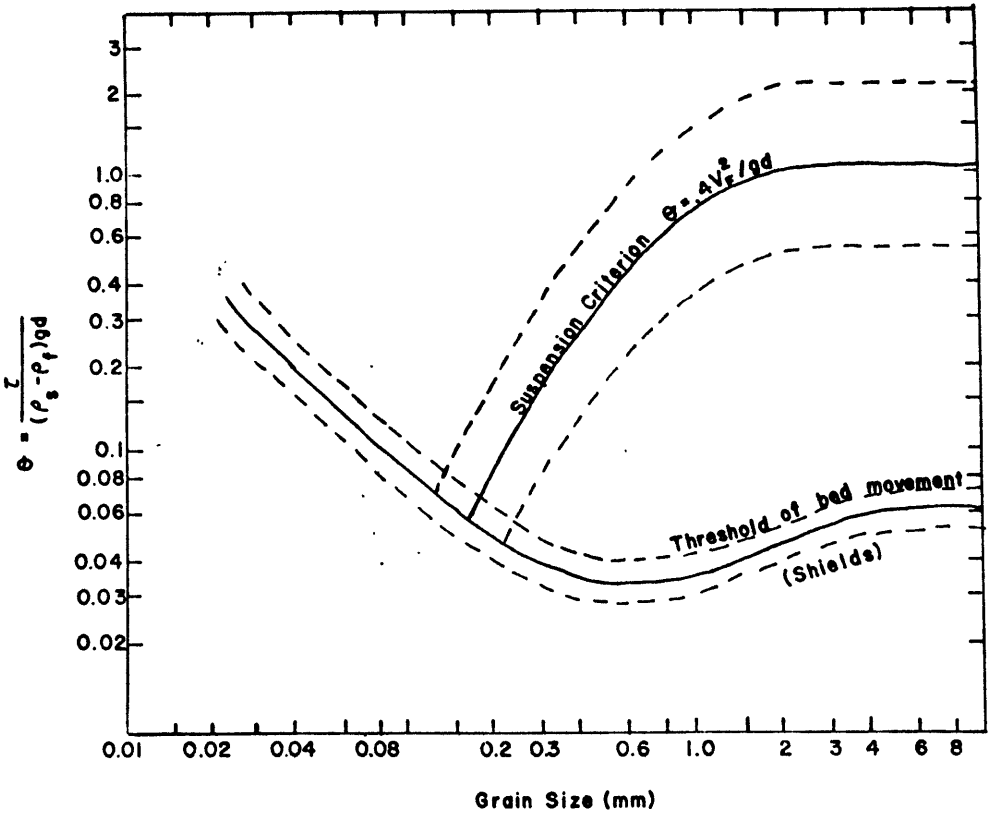

Figure 9: Entrainment and suspension criteria as a function of grain size. (after Bagnold, 1966)

because of both the variation in electrical properties with mineralogic composition and the continuously changing grain sizes caused by flocculation. In almost all cases, cohesive sediment moves only as suspended load. Only when large chunks of cohesive sediment are rolled along the bed can bed load movement be considered to occur for cohesive sediments. Since this phenomenon is of very minor importance, it will not be considered further.

Recent experimental results on the erosion of cohesive sediments are summarized in Table 1. Einstein and Krone (1962) reported the results of a series of experiments using a mud consisting primarily of illite and montmorillonite. They reported that for conce trations greater than 10 g/l (1 %) there was hindered settling, while for smaller concentrations it was not observed. The hindered settling consisted of two phases, the first lasting approximately two hours, during which the interface between clear water and the suspension settled to the bottom. The bulk concentration of the resulting sediment was 170 g/l. Einstein and Krone concluded that, based on viscosity measurements of lower concentrations, such a sediment should be able to withstand a shear stress of 10 dynes/cm^2. During the second phase of the deposition, the sediment compacted as interstitial water was squeezed out of the lower layers as a result of the pressure exerted by the upper layers of sediment.

Table 1

Previous Experimental Investigations
on the Erosion of Cohesive Sediments

Investigators	Mineral Composition	u_* (cm/s)	τ_0 (dynes/cm^2)
Einstein and Krone	Illite Montmorillionite Minor Kaolinite	0.7	0.49
Partheniades	Montmorillionite Illite	0.75, 2.19	0.57, 4.80
Terwindt and Breusers	70 % Illite 15 % Montmorillionite 15% Kaolinite	0.8-1.40 2.0	0.64-1.96 4.0
Gust	50% Illite 45% Kaolinite 5 % Chlorite	0.86 1.41	0.73 1.99

In flume studies using concentrations of 300 ppm or less, and low flow velocities, Einstein and Krone found that the decrease in sediment concentration was logarithmic with time. The rates of deposition were low, on the order of a few per cent per hour. By plotting deposition rates versus associated shear stress, they concluded that for particles 1.9 μm in diameter no deposition occurred if the shear stress exceeded 0.6 dynes/cm^2. They also reported that during deposition, material was exchanged between the suspended load and the bed.

Partheniades (1965) reported the results of a series of experiments using the same sediment as Einstein and Krone. Partheniades used two different mud beds, one collected and used at field moisture, and the other deposited directly from suspension in the flume. He found that although the measured shear strengths of the two beds varied by two orders of magnitude, the shear stress required to erode the beds was approximately the same (τ_0 = 0.57 dynes/cm^2). This value is very close to the value needed to inhibit deposition reported by Einstein and Krone. However, Partheniades stated that the value of the average velocity needed to inhibit deposition is 15 cm/s, considerably lower than that needed to initiate erosion (20 cm/s). On the basis of these results Partheniades stated that there can be no interchange of bed material and suspension material during episodes of deposition. Partheniades also found that when τ_0 exceeded 4.8 dynes/cm^2 the rate of erosion was

considerably increased. In addition, he noted that erosion rates were independent of both sediment concentration in the flow and the shear strength of the bed. In a subsequent series of papers (Partheniades and Kennedy, 1966, Partheniades et al., 1968, and Partheniades and Mehta, 1971), Partheniades and his co-workers have established the logarithmic settling behavior noted by Einstein and Krone for a wide range of flow velocities and suspended-sediment concentrations. They also found that the equilibrium suspended-sediment concentration reached is approximately equal to half the initial concentration, regardless of the actual value of initial concentration. Like the settling rate, this appears to depend only on the shear stress generated by the flow.

Both beds used by Partheniades were unconsolidated. Terwindt et al. (1968) reported the results of their investigation on the erosion of naturally occurring alternating sand and mud beds which showed that the clay layers were eroded only when τ_0 was between 10 and 60 dynes/cm^2. These results fit in well with previous reports of the shear stress needed to erode consolidated clay beds. These shear stresses are in fact higher than those needed to erode sand-sized noncohesive sediments.

Results reported by Migniot (1968) showed that the initial rigidity (shear strength) of unconsolidated mud beds varied with the mineralogic composition, grain size, rate of accumulation, and time allowed for compaction. Although the shear

stresses required for erosion varied widely, if the observation of Partheniades that the resistance to erosion of an unconsolidated mud bed is independent of its shear strength, then these variations should not be too important.

Terwindt and Breusers (1971) reported results of their investigation of alternating sand and mud bedding which showed that a pure mud bed would erode when u_* was between 0.8 and 1.4 cm/s, corresponding to τ_0 between 0.64 and 1.96 dynes/cm^2. For a mud with thirty-seven per cent sand-sized particles, they found that the critical shear velocity for erosion was 2.0 cm/s. This increase in resistance to erosion was also noted by Migniot, who found that the resistance peaked at a sand content of forty per cent.

Experiments by Southard et al. (1971) on erosion of calcareous ooze and by Lonsdale and Southard (1974) on abyssal clays give results similar in form to those shown in Table 1. However, the onset of mass erosion measured by Southard and Lonsdale is at a value of τ_0 considerably higher (10-60 dynes/cm^2) than that observed by Partheniades and in close agreement with that reported by Terwindt et al.(1968). This may be due to the longer time periods allowed for compaction before the experiments were initiated. The results of Southard et al. (1971) give values of τ_0 considerably lower than those reported by other workers. The sediment used in this sutdy is probably noncohesive, however.

Results reported by Postma (1967) indicate that mud resistance to erosion increases with decreasing water content. His results appear to be in qualitative agreement with the experimental results described above.

Recent research on drag resistance due to suspended particulate matter by Gust (1976) is of interest because if drag reduction occurs over rippled beds as well as over the planar beds studied by him, then the average velocities required to produce a given value of τ_0 may be increased by as much as forty per cent over that predicted by equations 4-6. That such drag reduction does occur over rippled beds is shown by the report of Simons et al. (1963), who showed that the value of C_* increased over fifty per cent with increasing suspended-sediment concentration. Gust reported that a planar mud bed collected from the field was eroded at a τ_0 of 0.73 dynes/cm^2, corresponding to a u_* of 0.86 cm/s. This result was determined from measurements made in the viscous sublayer. If u_* is computed from equation 4, as was done in the other studies, its value is 1.41 cm/s. This value is somewhat lower than that reported by Terwindt and Breusers for a mud with a similar sand content (40 %), but slightly higher than their value for a mud with with no sand. Why this discrepancy should exist is not clear. The most likely explanation is that the degree of consolidation was different because of the differing methods of forming the mud beds.

Although Gust's (1976) conclusion that turbulent drag reduction occurs in natural flows is undoubtedly correct, his statement that the occurrence of such drag reduction (Gust and Walger, 1976) will lead to an upward modification of the estimates of the mean velocity needed to erode naturally deposited mud beds does not necessarily follow. This is because the effects of drag reduction appear to be concentrated in a narrow zone near the bed surface, while the bulk of the flow remains Newtonian, and hence describable by the law of the wall. Since estimates of the value of u_* are generally computed from measurements of mean velocity made at some distance above the bed, the value of u_* may be inaccurate, but the mean velocity needed for erosion will still be correct. Only when the shear strength of the mud bed is measured directly, or when u_* is calculated from measurements taken in the viscous sublayer, are Gust's contentions valid.

A glance at Table 1 reveals that two different definitions of mud erosion appear to have been used, one based on an increase in suspended-sediment concentration, which would occur at very low velocities as individual particles begin to be resuspended (Einstein and Krone, Partheniades' lower value) and the other based on visible erosion of large chunks of deposited material (Terwindt and Breusers, Partheniades, and Gust). The onset of mass erosion is the more suitable definition for the purposes of this paper and is the one that will be used.

DESCRIPTION OF THE APPARATUS

The experiments described here were performed in a reversing, recirculating flume (Fig. 10). The flume is 10 m long with a cross-section 14.6 cm wide and 30 cm deep. The bulk of the flume is constructed of 0.75 inch plywood covered with resin-saturated fiberglass mat. The sides of the four-foot observation section, situated in the center of the flume, are of half-inch thick plexiglass. A centrifugal pump connected to a two-horse power motor drives the flow. A system of bypasses and valves was constructed so that the direction of the flow could be reversed. Discharge was regulated by a gate valve located just downstream of the pump outlet. Water temperature was partially regulated by means of a cooling jacket surrounding the return pipe. As the temperature of the cooling water increased, the cooling jacket became increasingly ineffective.

An instrument carriage containing a bed-leveling device and a rack-and-pinion point gauge was mounted on two one-inch diameter steel rods located above the sidewalls of the flume, and oriented parallel to the flume bottom. Although it is possible to vary the slope of the flume, all runs were carried out at zero slope.

Water discharge was measured with a calibrated U-tube mercury-water manometer connected to an orifice meter located in the return line. The manometer was calibrated by measuring

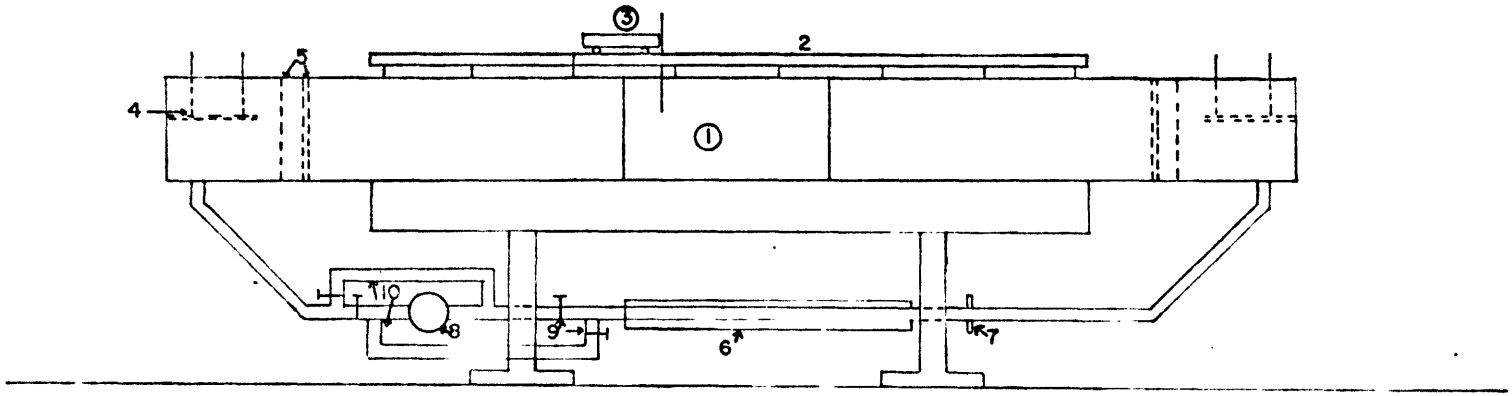

1. Observation area
2. Carriage rails
3. Instrument carriage
4. Wave dampers
5. Flow straighteners
6. Cooling jacket
7. Orifice meter
8. Pump
9. Gate valves
10. Bypass pipes

Figure 10: Schmatic of the flume.

the volume of water discharged in a ten-second interval for various pressure readings (Fig. 11).

To ensure fully developed turbulent flow, a series of one-half and one-quarter inch mesh screens were installed at both ends of the flume. It was found that smaller mesh sizes tended to act as a sediment trap, particularly at low velocities. Wave dampers, made of plexiglass sheets, were located directly above the pipe outlets at both ends of the flume.

Suspended-sediment concentrations were determined by using a 47 mm Nuclepore filtering system and 47 mm Nuclepore polycarbonate filters with a 0.4 μm pore opening.

All photos were taken on 35 mm Kodak Pan-X film (ASA 32) developed in undiluted Kodak Microdol-X. Three floodlights positioned below and behind the flume provided illumination. Exposures were at F4 for one-eighth of a second.

All calculations and plots were made using the MIT IBM 370/168 computer and a Calcomp plotter.

The two sands used in the experiments were obtained from the Holliston Sand Co., Holliston, Massachusetts. Microscopic examination revealed that both sands were composed of well-rounded grains, primarily quartz (over 95 %) with minor biotite and feldspar. Grain-size analyses, using the method of Folk (1966), are shown in Figure 12.

Three types of clay material were used in the experiments. The first is a Wyoming bentonite, composed almost completely

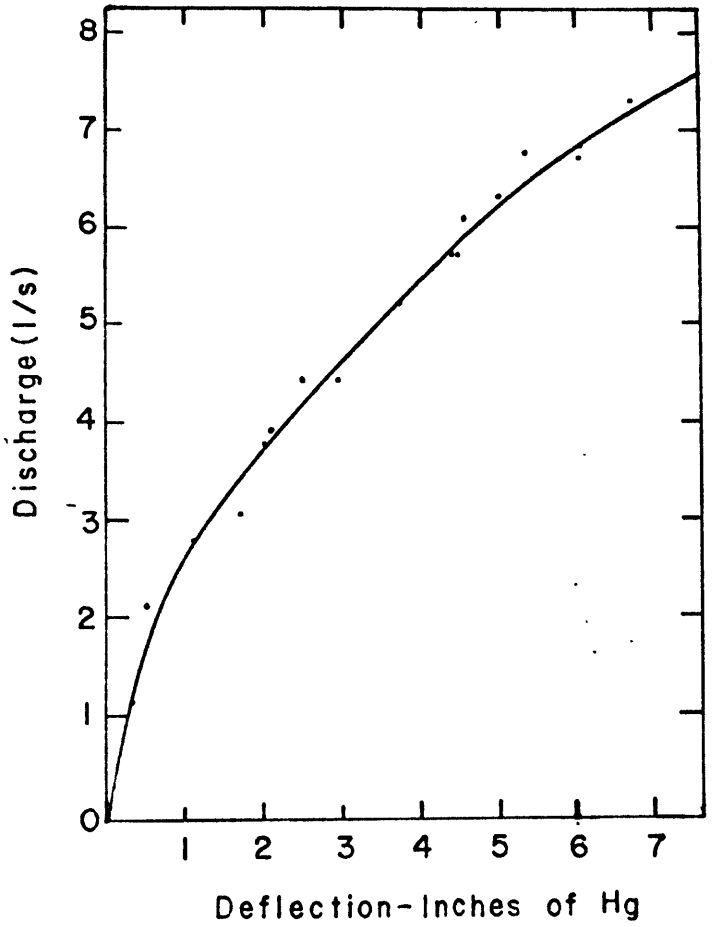

a

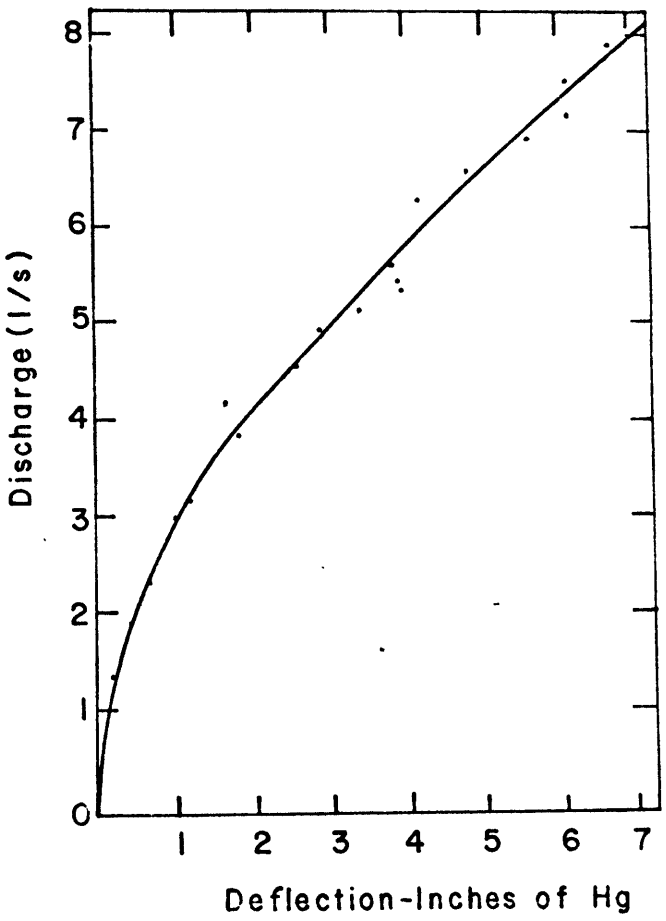

b

Figure 11: Calibration curves for the orifice meter. a-flow right to left, b-flow left to right.

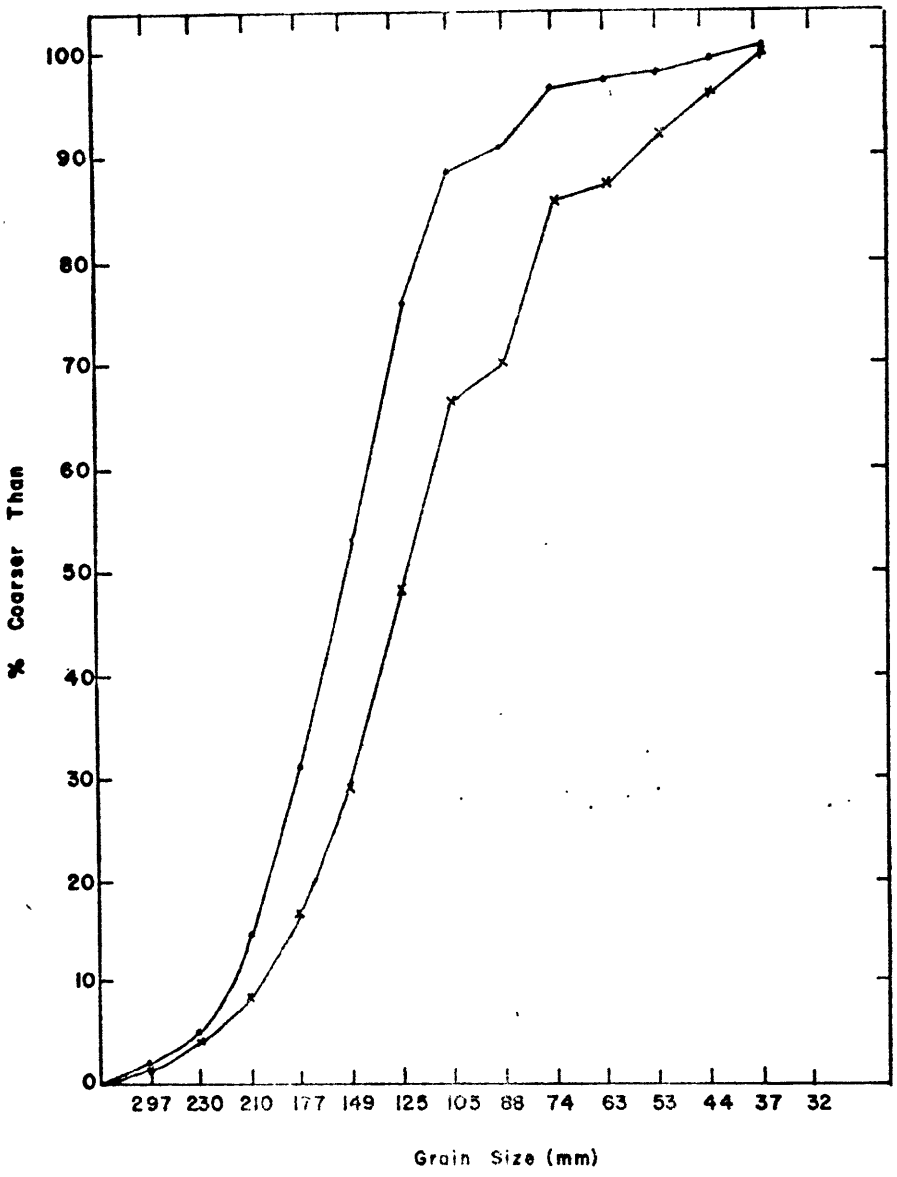

Figure 12: Grain-size distributions of the sands used.

of montmorillonite. The second clay was obtained from the Georgia Kaolin Co. packaged as Pioneer Kaolin. Analysis revealed that it is composed mostly of kaolinite with very minor amounts of other clay minerals. The third clay was obtained from the Gorham Brick Co., Gorham, N.H. Analysis revealed that the less than 60 μm size fraction contained significant amounts of quartz and feldspar, as well as chlorite and illite. The less than 2 μm size fraction was composed primarily of illite and chlorite. Because of the difficulties of separation, and the uncertainties of the composition, this clay was not used in any of the "U" runs. All analyses were done by X-ray diffraction.

The salt used to maintain the salinity of the solution at 15 ppt was commercial rock salt, obtained from a local distributor.

EXPERIMENTAL PROCEDURE

Two series of experiments were made. The first series, the "T" runs, was conducted in order to explore the effects of varying the initial sediment concentration, varying the sediment composition, varying the peak velocity, and varying the forcing function used to produce the tidal velocity profile.

The second series, the "U" runs, was then conducted in order to establish quantitatively the conditions necessary for the formation of wavy and flaser bedding. A short summary of the various runs is given in Table 2. Detailed descriptions of the runs are given in Appendix A.

All runs were based on a tidal cycle with a period of 12.5 hours. A computer program (see Appendix C) was written in order to create simulated tidal cycles with various maximum velocities and functional forms. Two different functional relations were used to generate the cycles. The first was a simple sine wave:

$$u = \sin(t) \tag{17}$$

This was used in runs T-1 through T-3. The other function used:

$$u = 2\sin(t) + \sin(2t) \tag{18}$$

more closely approximates a real tidal cycle, and is the form used for the rest of the runs. Due to the complexity of the interactions between the tidal generating forces and local bathymetry, almost any tidal-current velocity profile can exist. However, a large number of tidal velocity profiles closely resemble that described by equation 18. In particular, the tidal cycles during which observations referred to in this report (Gust and Walger, 1976; Postma, 1961; Reineck and Wunderlich, 1967, 1969; and Schubel, 1969, 1971) were made are similar

Table 2

Summary of Experimental Runs

Run #	Peak Velocities (cm/s)	Total Clay Added (g)	Remarks
T-1	+40,-40	100	No deposition observed
T-2	+40,-40	200	No deposition observed
T-3	+20,-20	400	Mud layer deposited, not re-eroded
T-4	+40,-40	400	Mud layer deposited, subsequently eroded
T-5	+20,-20	400	Mud layer deposited, not re-eroded
T-6	+30,-20	400	Mud layer deposited, mostly re-eroded
T-7	+30,-20	400	Mud layer deposited, mostly re-eroded
T-8	+30,-20	100	Mud layer deposited, subsequently eroded
T-9	+30,-20	2200	Mud layer deposited, mostly re-eroded
T-10	+30,-20	800	Mud layer deposited, mostly re-eroded

Table 2 (cont.)

Run #	Peak Velocities (cm/s)	Total Clay Added (g)	Remarks
U-1	+30,-20	3000	Mud layer deposited and preserved
U-2	+30,-20	1000	Occasional mud flasers preserved
U-3	+24,-24	1000	Some mud lenses preserved
U-4	+30,-24	1000	Occasional mud flasers Preserved
U-5	+30,-20	1000	Semi-continuous mud layer preserved
U-6	+24,-24	1000	Continuous mud layer preserved
U-7	+30,-20	1000	Occasional mud flasers preserved
U-8	+30,-24	1000	Occasional mud flasers preserved
V-1	+24,-24	1500	Almost continuous mud layer preserved

Note: Positive flow velocities are from left to right, negative flow velocities are from right to left. All runs began and ended with positive flow velocities.

to those produced by this equation.

Since the pump used was not a variable-speed pump, discharge had to be controlled by means of a gate valve. This made it impossible to continuously vary the current velocity. It was decided to change the velocity in increments of 2 cm/s. This increment is considered to be small enough to closely approximate the continuously varying flow present in real tidal systems and yet large enough to be accurately measured by the manometer. In addition, during some parts of the runs, when the velocity changed rapidly, more frequent velocity adjustments would have made it impossible to collect the other data being recorded. It should be noted that on all of the velocity profiles, the time indicated is the time that the velocity was changed to that velocity.

Prior to each run a new bed of fresh sand 4 cm thick was placed in the flume and leveled. In the entrance and exit regions the thickness was gradually reduced to zero. Water was added until a water depth of 12 cm was achieved. The flume was then turned on anr run at a velocity of 30 cm/s for approximately one hour so that a fully rippled bed was developed. Six kilograms of salt were added during this period to achieve the desired salinity of 15 ppt. The flume was then turned off and left overnight.

The next morning the flume was turned on and the velocity adjusted to that desired for the beginning of the run. A given

weight of dry clay was then added in small amounts over a period of about ten minutes. The clay was added at the downtstream end of the flume so that the action of the pump would destroy any large clumps. After addition of the clay the flume was allowed to run for a specified time before the formal initiation of the run. In the case of the "T" runs this period was one hour, at the end of which time, according to Patheniades, an equilibrium suspended sediment concentration was established. It was found that, when large quantities of clay were added, substantial amounts would be deposited and covered by migrating sand before the initiation of the run. In order to minimize this, a shorter time period elapsed before the initiation of the "U" runs, one-half hour. An unfortunate but unavoidable effect of this time reduction was to superimpose two depositional trends during the early hours of the run: that due to the deposition before equilibrium in a steady flow was reached, and that due to the varying current velocity.

The formal part of the run was always begun at a velocity somewhat below the maximum reached during the run. The velocity was then raised and lowered according to the table generated by the computer for that particular run. Photographs of the observation area were taken every half hour. During the "T" runs, suspended sediment samples were taken from 10 cm above the bed every hour. Temperature readings were also taken every hour during the "T" runs. When velocities greater than

30 cm/s were reached, significant amounts of sand were found in the suspended-sediment samples. In these cases the entire sample was wet-sieved to remove the sand, which was then dried and weighed separately. The rest of the sample was filtered through the apparatus described above, and then dried at a temperature of 30°C. This removed all interstitial water, but not that which was chemically bound to the clay particles. It is not possible to determine at what temperature the samples were dried in other reports (Postma, 1961; Gust and Walger, 1976). If their samples were dried at temperatures high enough to remove the hydrated water as well as the interstitial water (greater than 300°C) then the comparable concentrations of their samples are considerably higher than those in this report. During the "U" runs suspended sediment samples and temperature readings were taken every half hour. The size of the suspended sediment sample was governed by the capacity of the filter. During all of the "U" runs and during Run V-1 and Run T-9, the high suspended-sediment concentrations permitted a sample volume of only 50 ml to be used. During the "T" runs in which the total amount of suspended sediment was much lower, a larger sample volume of one liter was used.

In an effort to determine whether or not the grain size changed during the runs, grain-size analyses were made during several of the runs using the pipette method of Folk (1966). The results are somewhat variable, but the average grain size

appears to be fairly constant, both from run to run and within individual runs (Table 3).

As a check on whether the suspended sediment affected the fluid viscosity, a series of measurements were made during Run U-8 using a Synchro-Lectric Viscosimeter. No significant variations were noted.

Water-surface profiles were measured during the "U" runs by taking measurements at intervals of one meter at five positions centered about the midpoint of the observation area. Five measurements, using the point gauge, were taken at each point and averaged. The resulting five values were then fit using a least-squares fitting program to determine the water-surface slope. The results of Rathburn and Guy (1967) show that such a procedure gives an accurate slope determination. During several of the runs ten or more observations were taken at each point, but the average value did not vary significantly from that obtained using only five measurements. Water-surface profiles were measured at the following flow velocities: 12, 16, 20, 24, 26, 28, and 30 cm/s.

The runs were terminated at various times, but never until the maximum velocity reached shortly after the beginning of the run had been reached for a second time. After termination of the run, the flume was drained and cleaned prior to the next run.

Table 3

Suspended-Sediment Grain-Size Analyses
Per Cent Fine Than

Run #	T-7		T-8			U-8		
Velocity (cm/s)	30	0	30	0	20	0	24	30
Grain Size								
ϕ Microns								
4 62	100	100	100	100	100	100	100	100
5 32	100	100	100	100	100	100	100	100
6 16	100	100	100	100	100	100	100	100
7 8	100	86	67	50	67	25	50	100
8 4	25	25	0	0	0	0	0	0
9 2	8	16	-	-	-	-	-	-

All data were stored on punched cards and analyzed using the program listed in Appendix C.

When considering the experiments described here, several limitations of the apparatus should be considered. The most significant limitations are those imposed by the dimensions of the flume.

The flume used is narrow (14.6 cm) and at the flow depth used (12 cm) has a width-to-depth ratio of only 1.22. Williams (1971) has suggested that for the effect of the sidewalls to be negligible the width-to-depth ratio should be at least 3:1. At the small ratio used, the resistance of the sidewalls is a significant percentage of the total resistance of the flume. In addition, the presence of the sidewalls initiates the formation of secondary currents which may modify the flow structure so that it differs from that found in natural channels. In order to apply the experimental results to natural situations it is necessary to employ a sidewall correction procedure. Two different methods were used. The first is the method of Johnson (1942) as described by Vanoni (1975). Johnson's method involves determining the resistance of the sidewalls and subtracting it from the total resistance as measured from the energy slope in order to determine the resistance of the bed.

The second method was proposed by Williams (1970), who multiplied the measured energy slope by the factor:

$$S_e = S_e \, [1/(1 + 0.18(D/b^2))] \qquad (19)$$

to eliminate the sidewall effects.

Although the flume is short (10 m), it is long enough for fully developed turbulent flow to exist in the observation area.

A more serious limitation is the shallow depth of the flume (12 cm). Since the depth is much less than that found in tidal channels (2-6 m), in order for the total amount of sediment deposited to be equal to that found in natural settings the concentration must be considerably higher. An upper bound on the concentrations that may be used is set by the occurrence of hindered settling at concentrations of greater than 1 per cent.

Since it was the observations of Terwindt and Breusers that were being tested, at least originally, their calculations of the amount of sediment deposited during a tidal cycle were the ones used. Terwindt and Breusers calculated that a layer of sediment 0.3 cm thick could form during a single tidal cycle. This calculation was based on the observed bulk sediment concentration near the bed during slack water. Other observations directly measuring suspended sediment concentrations during tidal cycles reveal, not surprisingly, that the amount of suspended sediment can vary over several orders of magnitude (Krone, 1972; Postma, 1961; Schubel, 1969, 1971a; Gust and Walger, 1976). When compared with these observations, the amounts calculated by Terwindt and Breusers are very low.

It was observed that a mud layer 0.3 cm thick could easily be eroded at low flow velocities (Runs T-4, T-6, T-7, T-8, T-10). Accordingly, larger amounts of sediment were used in subsequent runs. Hindered settling occurred in Run U-1, so smaller amounts of sediment were used in the following runs. Mud layers up to 1 cm thick were produced in Runs U-2 through U-8.

The shallow flow depth also meant that the sediment would deposit more quickly than in real tidal areas, provided the grain sizes were equal. Fortunately, the grain sizes in the flume runs were considerably less than those reported from natural settings. This, plus the reduction in fall velocity due to the increased concentrations, resulted in settling behavior quite similar to that observed by Postma (1961) and by Gust and Walgar (1976). One notable difference between the field and experimental observations is that in the tural settings the water was never completely free of sediment while in the flume it was. This is probably due to two factors: first, the presence of wave activity in the natural channels, and second, the greater depths of the channels so that even in the absence of wave activity not all of the finest material could settle out.

The mineralogy of the sediment in most of the runs was composed only of kaolinite and/or montmorillionite, whereas natural sediments will have compositions considerably more complex. In particular, natural sediments will contain some proportion of organic material, which might increase the shear

strength of the sediment. However, organic-matter content of nearshore sediments appears to be low. Both Young and Southard (1978) and Einstein and Krone (1962) reported organic-matter contents of about three per cent, and Krone (1972) characterized an organic-matter content of ten per cent as high. Given these data, it was felt that the organic-matter content could be neglected. The possible effects of non-organic binding agents such as iron compounds should also be considered. Because of the low iron contents and the lengths of time required for them to increase the rigidity of the mud (Partheniades, 1965), this effect has also been neglected.

PRESENTATION OF THE EXPERIMENTAL RESULTS

General Observations

Detailed observations of the individual runs are given in Appendix A; only the results of the runs, and the conclusions deduced from them, are given here. Some general observations which apply to all of the runs can be made first.

1. It is difficult to define exactly when erosion of a mud bed begins. As noted above, for this study it is the onset of mass erosion that is of interest. This was defined to occur when the mud surface began to become ragged. This usually

occurred when the mean velocity was 24 cm/s. However, the onset of mass erosion did not guarantee that a significant portion of the mud bed would be removed, since the rate of erosion at this velocity was low. As soon as the velocity was increased to 26 cm/s the erosion rate increased rapidly.

2. The deposited mud formed two distinct layers corresponding to the two phases of deposition noted by Einstein and Krone (1962) and Migniot (1968). The unconsolidated upper layer was always resuspended at relatively low flow velocities (less than 16 cm/s) leaving the lower, more consolidated layer molded over the rippled sand bed.

3. Erosion of the consolidated mud layer occurred first on the stoss side of the ripples. Once the sand was exposed, the rate of mud erosion was increased as the sand began to be transported, thus undermining the remaining mud layer.

4. The thickness of the mud layer varies with the amount of clay added to the flume. In general, the thicker the layer, the greater its resistance to erosion. The 0.3 cm thickness calculated by Terwindt and Breusers was almost completely eroded by the time the velocity reached 24 cm/s.

5. Substantial amounts of mud were deposited during the period corresponding to low water and were not resuspended. This does not agree with the observations of Postma (1961), and allows longer compaction times than found in nature. It was found, however, that even allowing a mud layer to lie

undisturbed for up to two days did not increase its resistance to erosion.

6. The ratio of mud deposition generally increased substantially when the velocity was lowered below 18 cm/s. The precise value of this change in rate depended to some extent on the total suspended-sediment concentration, with higher concentrations depositing at higher velocities than lower concentrations.

7. The sequence of deposition and erosion of the mud followed the same general trend throughout all of the runs, differing only in degree. During the first part of the run, when the velocity increased to its maximum, most of the mud was in suspension. As the velocity decreased below 18 cm/s deposition began and continued through the first still-water period until the velocity was increased to about 10 cm/s (Fig. 13; Note: grid is 1 cm, flow left to right unless noted). During this first still-water episode, corresponding to low tide, most of the mud was deposited. During the subsequent high-velocity period, most, but not all, of the mud would be resuspended. If enough mud was not resuspended, consolidation of the remaining mud would begin to occur (Fig. 14). During the second still-water period, which corresponded to high tide and was much longer than the first, all of the mud would be deposited, forming thick layers of both unconsolidated and

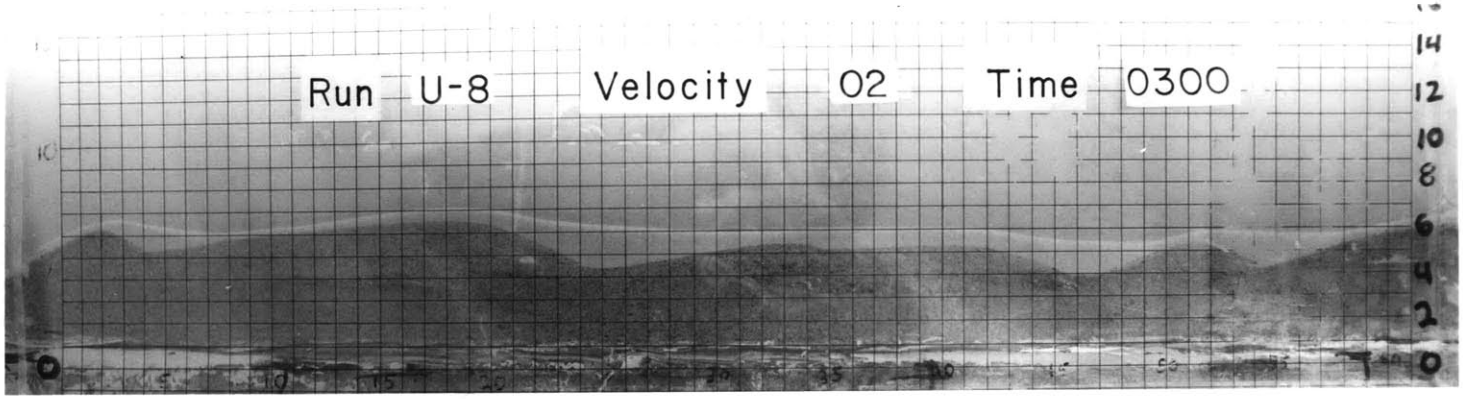

Figure 13: Typical mud deposition at low water. Flow right to left.

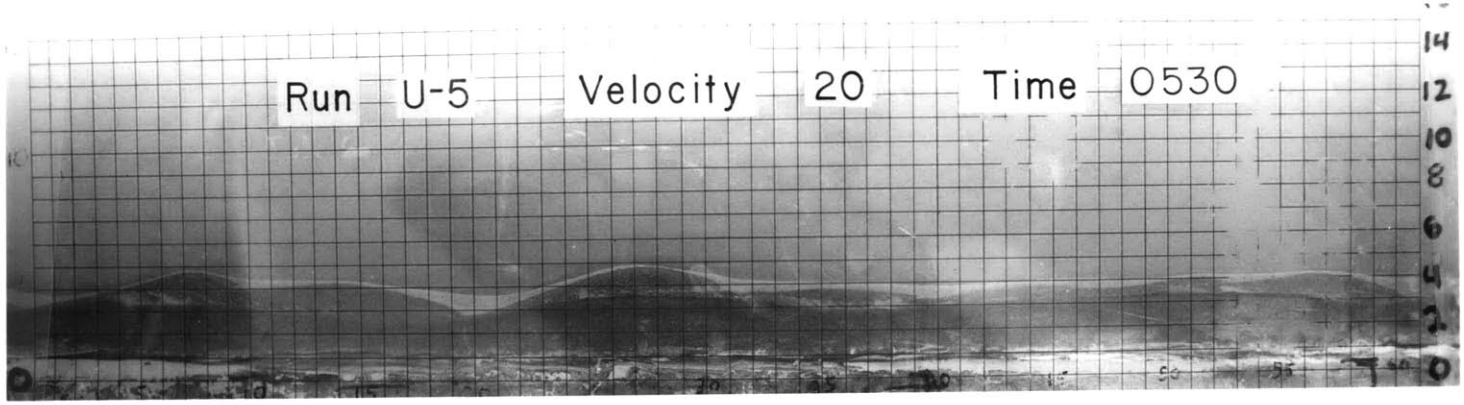

Figure 14: Partial erosion of mud during flood tide. Flow right to left.

consolidated mud (Fig. 15). As the current velocity was increased, first the unconsolidated layer and then the consolidated layer would be eroded. Mass erosion of the consolidated layer began at current velocities approximately equal to those needed to initiate sand movement. As the mud was eroded (at first only on the stoss side of the ripples), the exposed sand would begin to migrate, partially covering the portions of the mud bed not yet eroded (Fig. 16). Depending upon the velocities used it was possible to bury varying amounts of the mud bed. Details of each run are given in Appendix A, and the results are discussed in the following sections.

The "T" Runs

Runs T-1 through T-5 were primarily exploratory. These runs were conducted in order to determine how much clay should be added and what maximum current velocities would be needed to produce mud deposition and erosion. It was found that if a tidal cycle with peak current velocities of more than 24 cm/s was used, and enough mud was added to produce a layer 0.3 thick, the mud would deposit during the period corresponding to high water and be eroded during the subsequent period of high current velocity. This was true for both tidal profiles used. Runs T-3 and T-5 showed that if the maximum velocity did not exceed 20 cm/s, the mud would not be eroded.

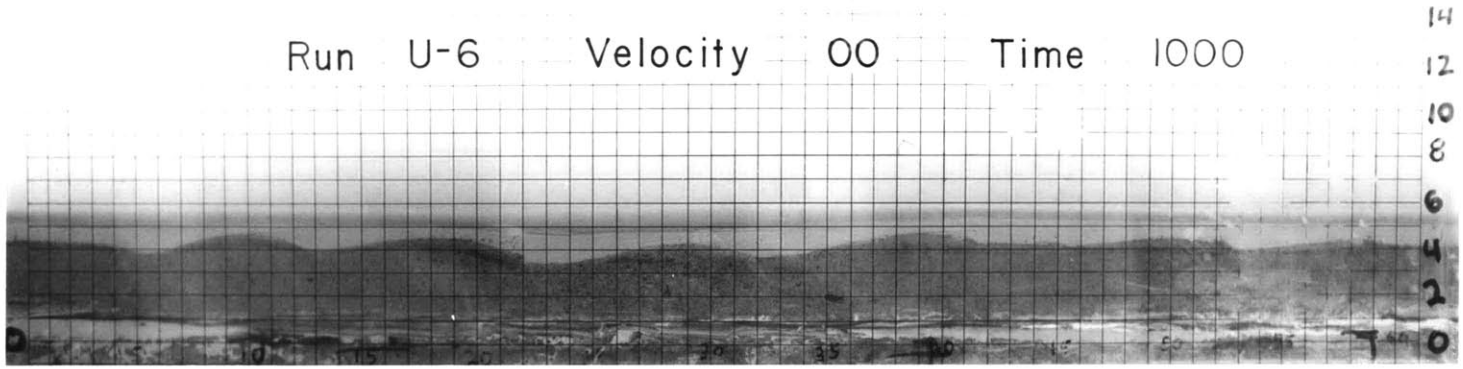

Figure 15: Mud deposition at high water.

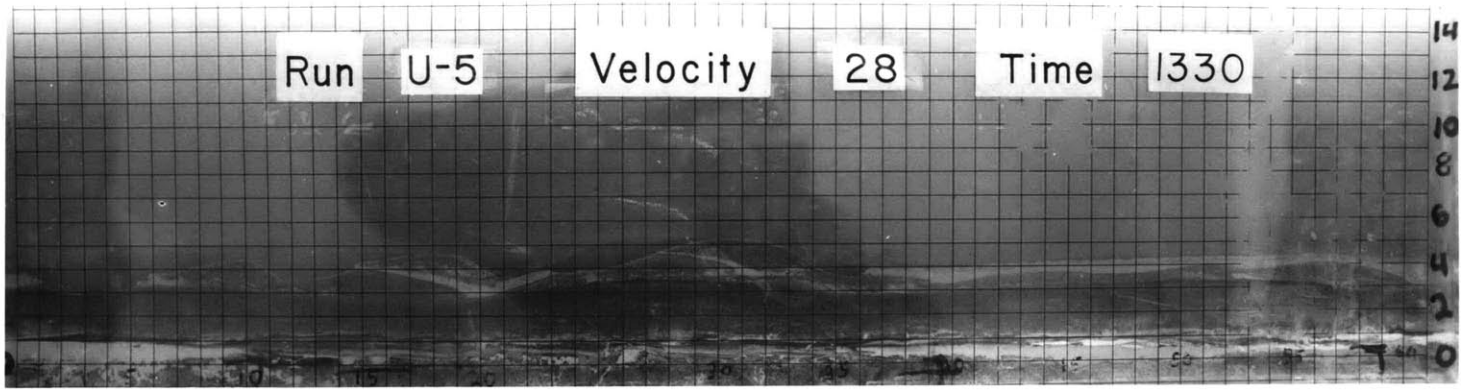

Figure 16: Mixed burial and erosion of mud by ebb current.

The value of u_* corresponding to a mean velocity of 24 cm/s is 1.75 cm/s. This value is considerably less than the value Terwindt and Breusers claimed is needed to erode a mud bed (u_* = 2.0 cm/s). The results of these initial runs, which are supported by the results of runs T-6, T-7, and T-10, which had similar suspended-sediment concentrations, show that only flasered beds can be preserved if the mean velcoity exceeds cm/s. Accretion over subsequent tidal cycles producing mud layers several centimeters thick is impossible.

Runs T-6, T-7, and T-10 were conducted to determine the effect of various mineralogic compositions on depositional and erosional behavior. The results for the three minerals tested show that for the short time periods used in this study the minerals behaved identically (Fig. 17), although for longer periods Einsele et al. (1974) have reported marked differences in consolidation rates for different clay minerals. The higher concentration of illite material is due to the substantial amounts of quartz and feldspar in the sediment. This did not appear to affect the behavior. Nevertheless, the illite sediment was not used in any of the subsequent runs.

The purpose of runs T-8 and T-9 was to see if the suspended sediment concentration had an effect on the rates of deposition. Figure 18 shows that for the concentrations used, depositional behavior did not vary with total concentration.

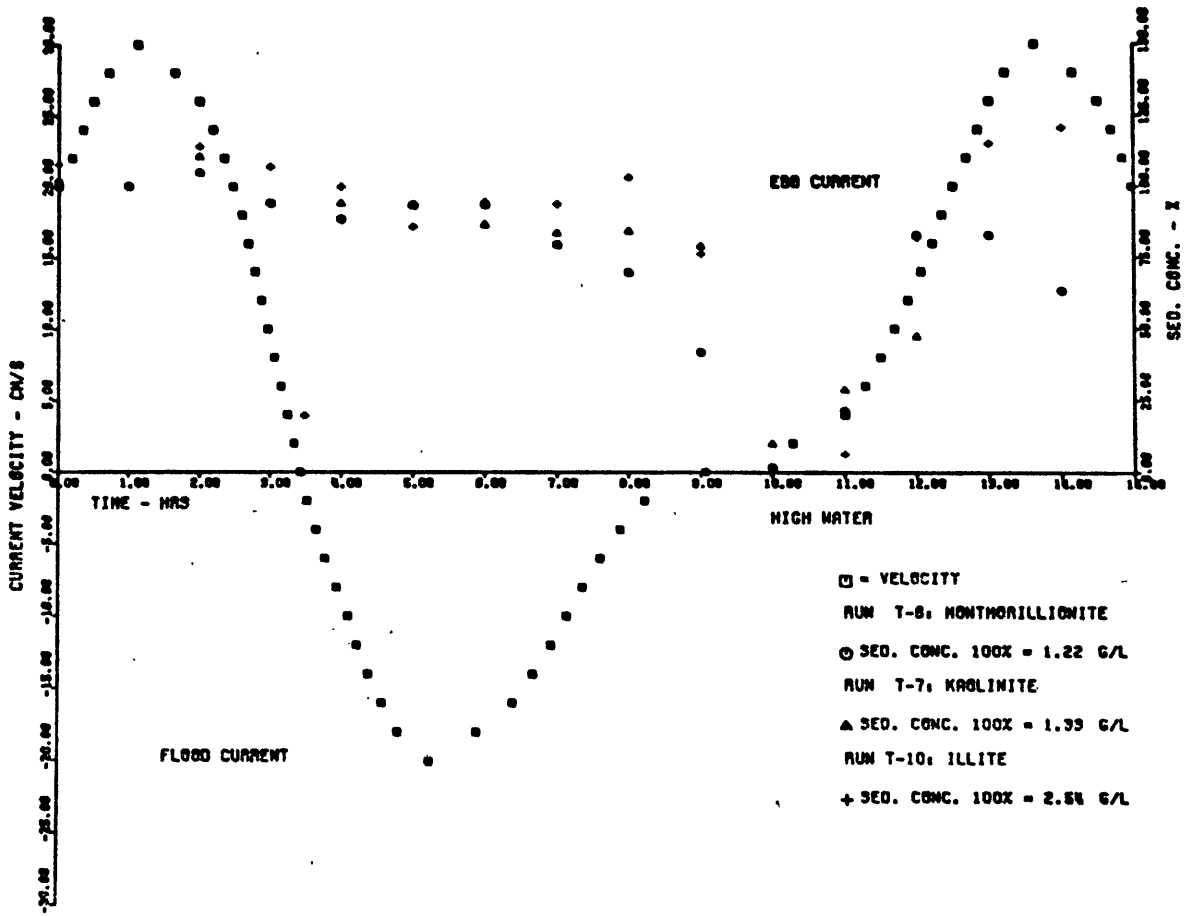

Figure 17: Suspended-sediment concentration as a function of mineralogy.

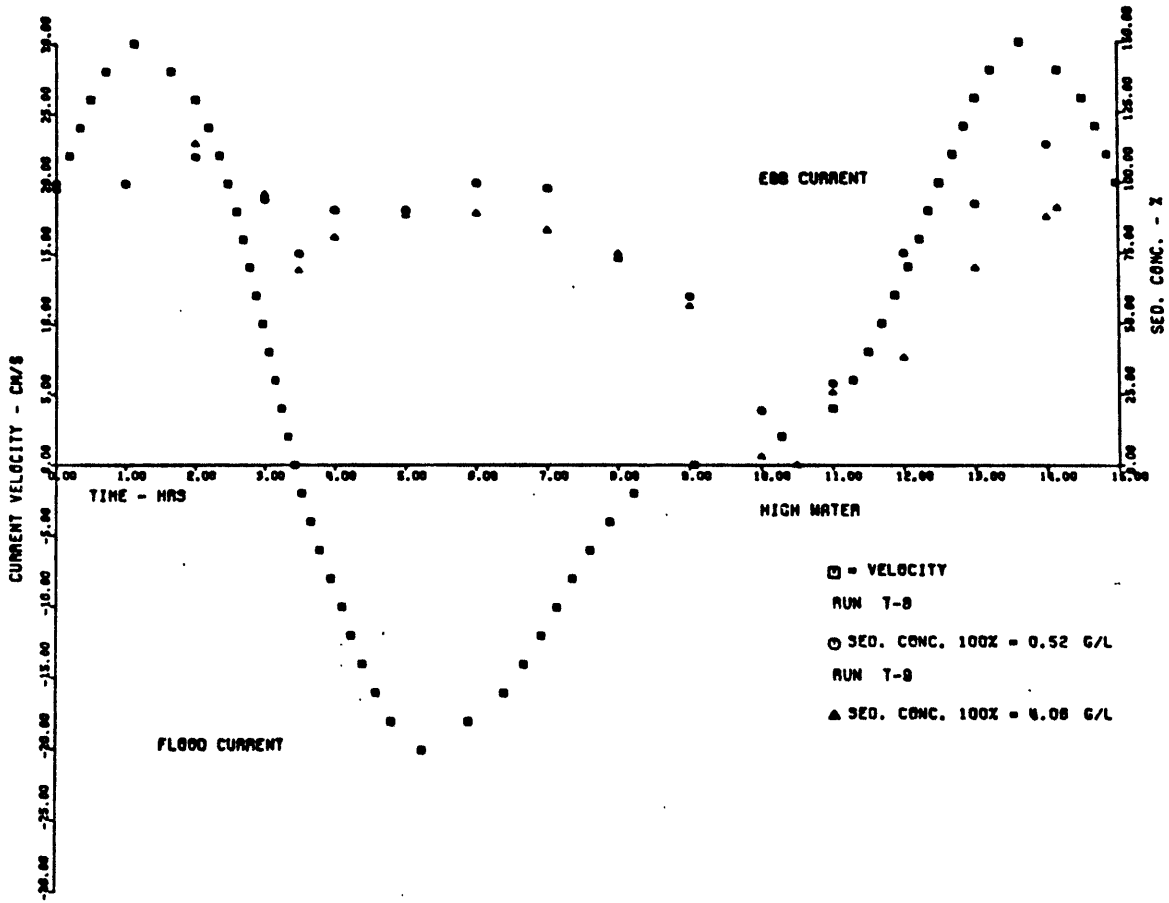

Figure 18: Suspended-sediment concentration as a function of initial load.

The "U" and "V" Runs

Run U-1 was conducted with a very large amount of sediment. It was found that a substantial amount of the clay was deposited very quickly after it was introduced into the flume. In addition, when the flow velocity was reduced, hindered settling occurred. For these reasons it was decided to use smaller amounts of sediment in subsequent runs.

Run V-1, was conducted with less sediment than Run U-1, but substantial amounts of sediment were still deposited shortly after it was introduced into the flume. At the end of both of these runs, which were ended early, an almost continuous mud layer covered the sand bed.

Runs U-2 through U-8 were all conducted with the same amount of clay added. Because of difficulties with the point gauge, the results of run U-2 had to be discarded. The run was repeated as run U-8. The object of these runs was to determine the minimum velocity needed to inhibit the preservation of a continuous mud layer and the effect of changing the sand size. The mud layers deposited were over 1 cm thick. It was found that if the maximum velocity did not exceed 24 cm/s, an almost continuous mud layer could be preserved. The differing velocity profiles between runs U-4 and U-5 (or U-7 and U-8) tested whether a difference in the secondary velocity maximum would have an effect on the erosional behavior of the bed.

If the velocity during flood tide reached only 20 cm/s, there was very little erosion and the mud layer remained continuous (Fig. 19). If the maximum velocity was 24 cm/s, mud erosion progressed to the point that sand was exposed in places. Subsequent bed-load movement buried portions of the mud layer (Fig. 20) as the ripples adjusted to the change in flow direction.

Varying the sand size also had an effect on the erosional process. Since the finer sand was transported at lower velocities than the coarser, as soon as it was exposed (due to partial erosion of the mud layer) it migrated more actively, leading to more rapid undermining of the remaining mud. At the same time it buried other portions of the mud bed more quickly than did the coarser sand. The net result was to produce more continuous flasers than were formed with the coarser sand (Figs. 21, 22). This occurred even though the total amount of mud resuspended did not vary with the sand size (Fig. 23, 24, 25).

In one case, run U-6, the mud layer was never eroded, allowing a continuous mud layer to be preserved until the end of the run (Fig. 26). If the maximum mean velocity exceeded 24 cm/s, the mud bed was always eroded, leading to the preservation of only occasional mud flasers (Fig. 27).

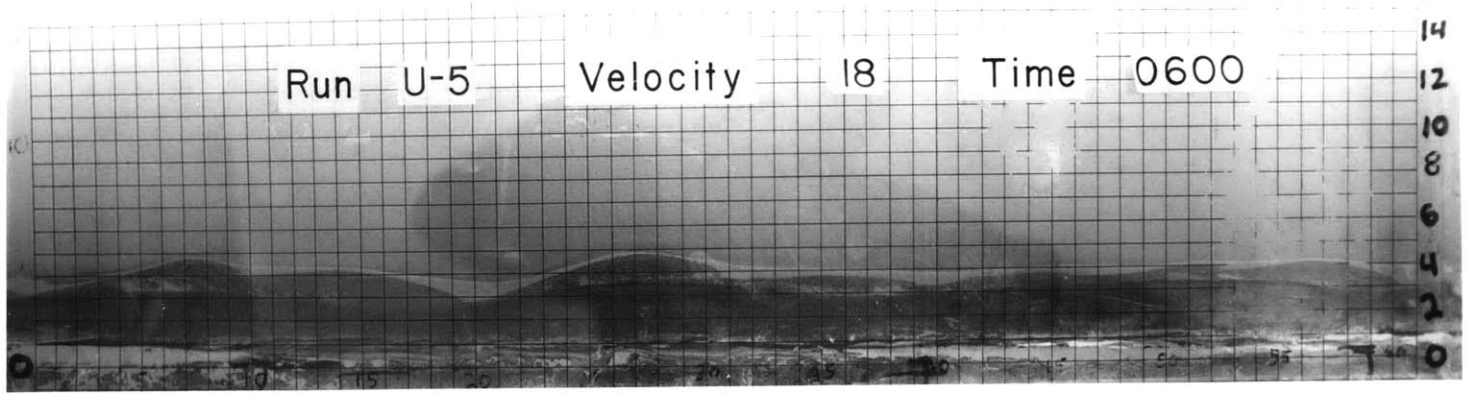

Figure 19: Preservation of continuous mud layer during flood tide. Maximum velocity was 20 cm/s at 0530. Flow right to left.

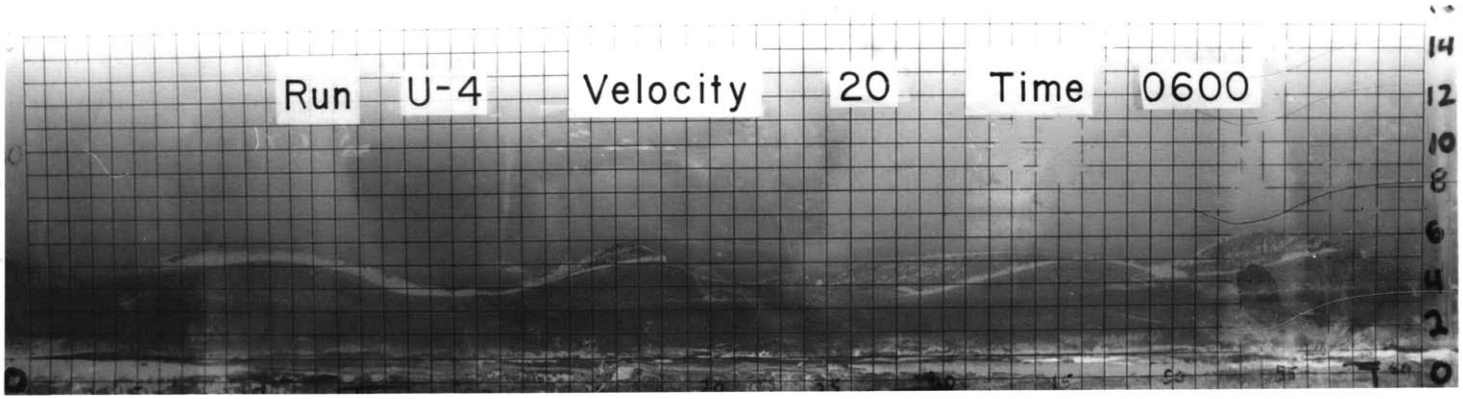

Figure 20: Partial preservation of mud layer during flood tide. Maximum velcoity was 24 cm/s at 0530. Flow right to left.

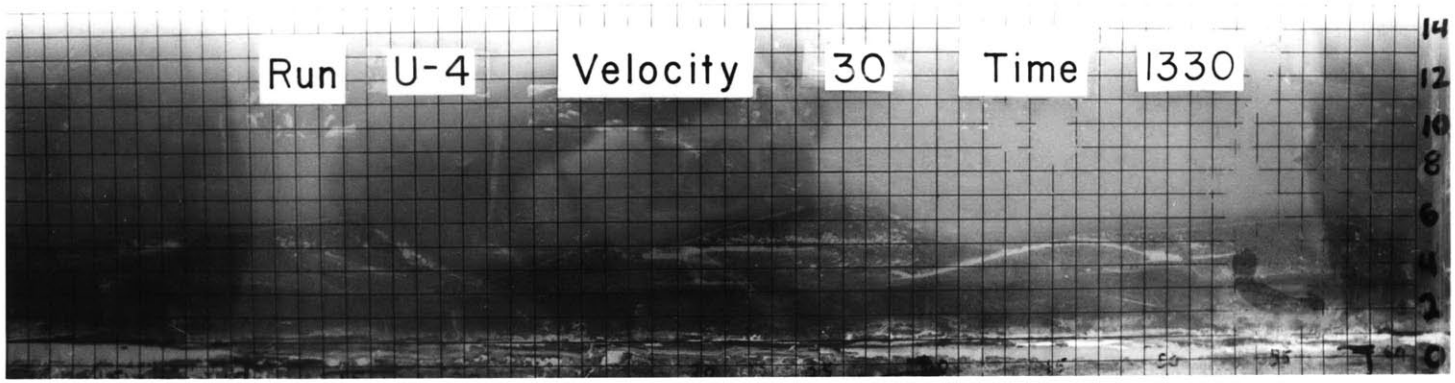

Figure 21: Wavy flaser bedding. Sand size 0.0129 cm.

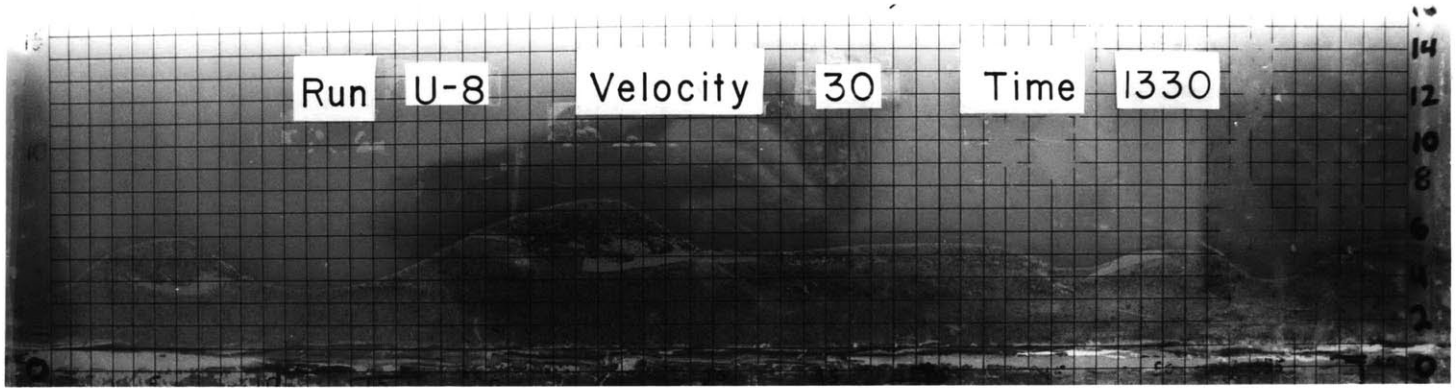

Figure 22: Simple flaser bedding. Sand size 0.0156 cm.

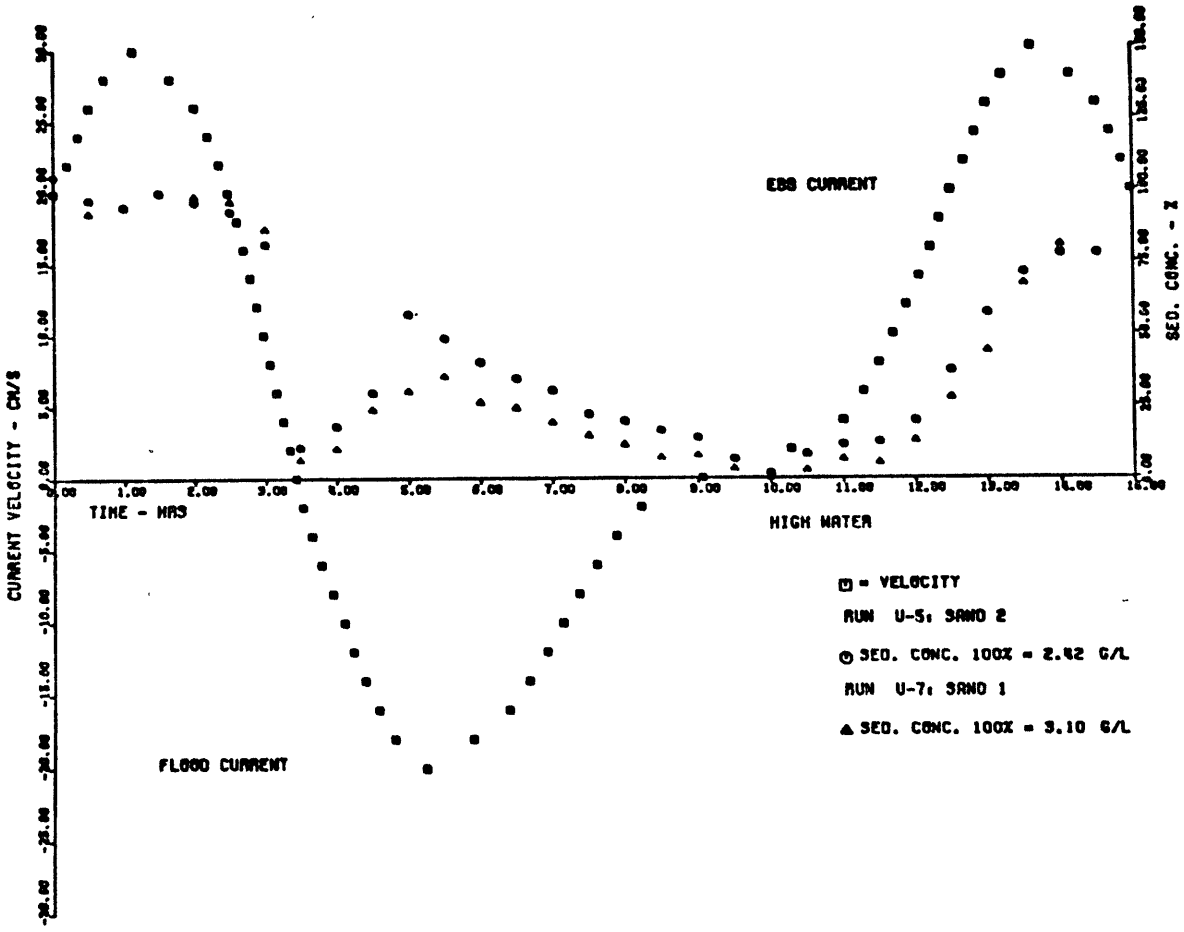

Figure 23: Suspended-sediment concentration as a function of bed grain size.

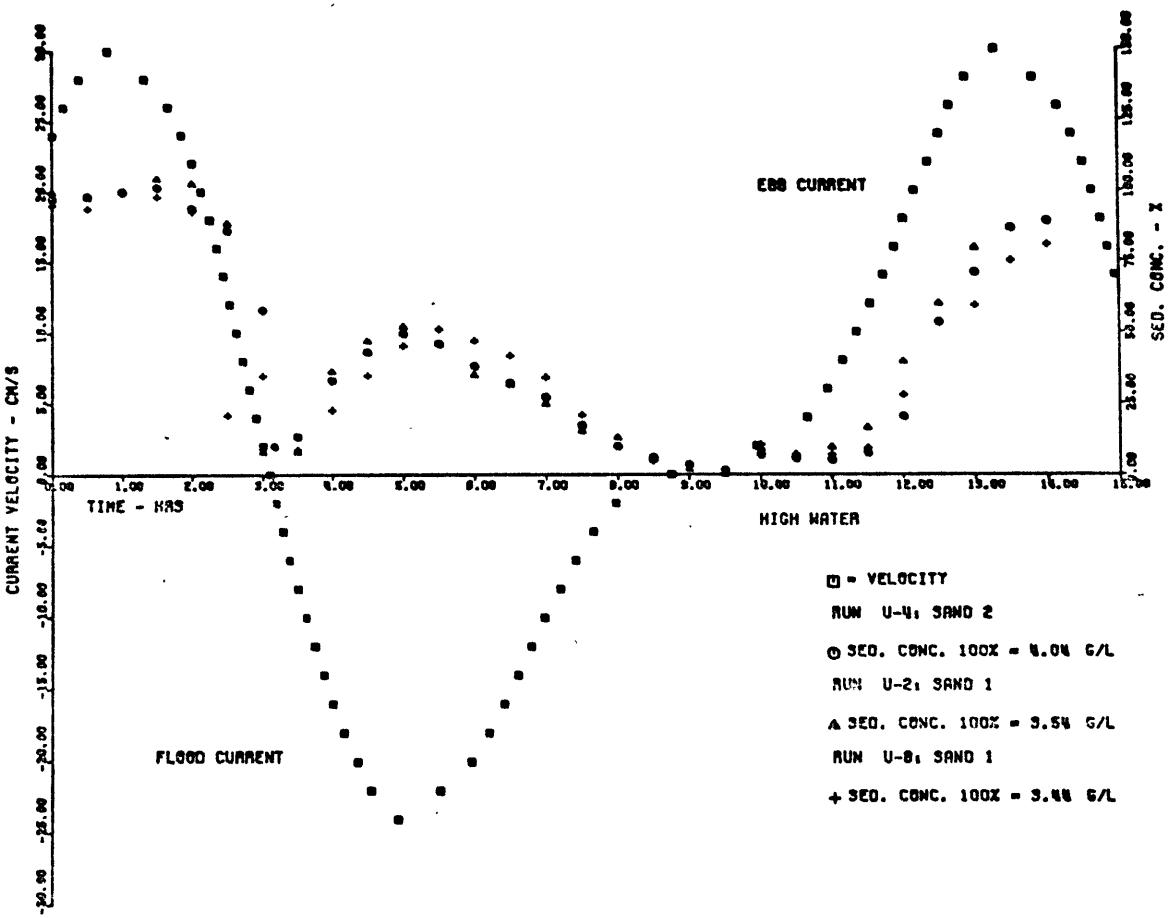

Figure 24: Suspended-sediment concentration as a function of bed grain size.

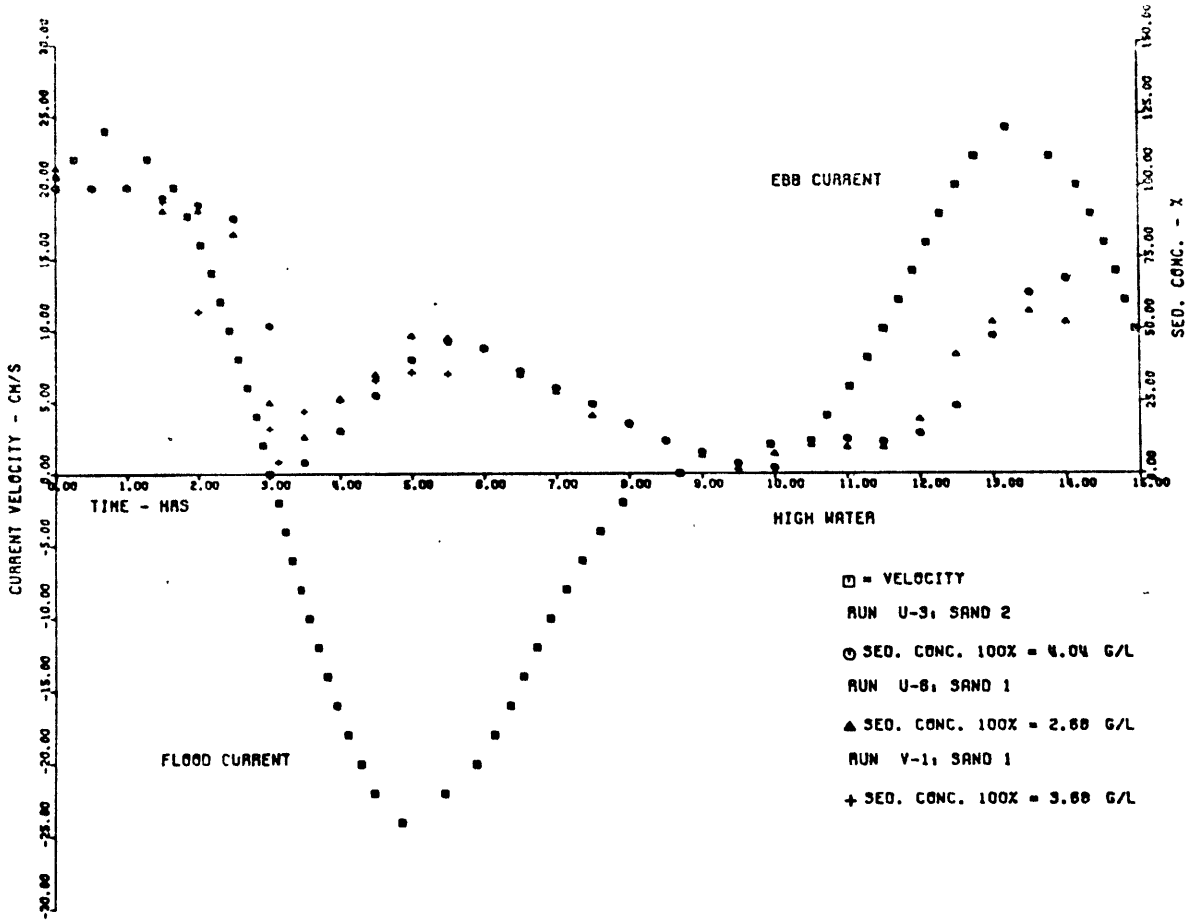

Figure 25: Suspended-sediment concentration as a function of bed grain size.

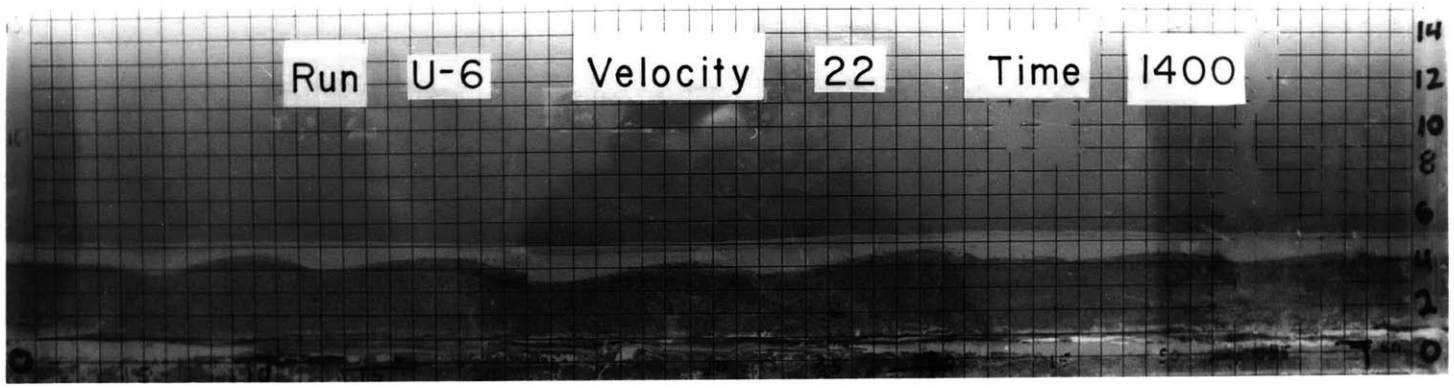

Figure 26: Development of wavy bedding.

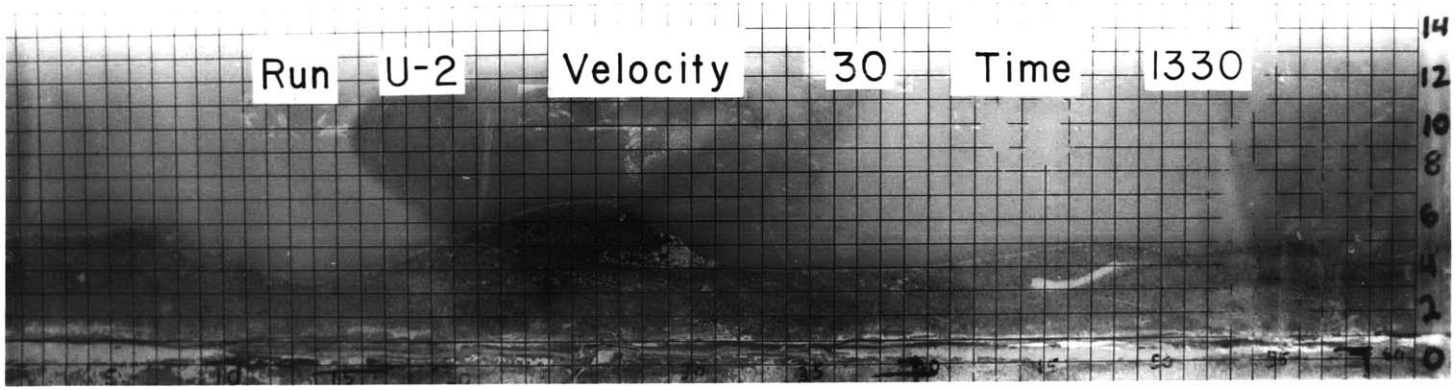

Figure 27: Occaisional flasers buried by migrating ripples.

Figure 28 is a schematic representation of how a flasered bed is formed. As the flow velocity decreases (steps a through c), an increasing amount of mud is deposited forming an unconsolidated layer across the rippled sand; initially this layer conforms to the bed topography (b), but gradually fills in the troughs as the accumulation increases (c). The total amount of mud reaches a maximum at slack water (d), and if accumulation is significant, a consolidated layer begins to form. As the flow velocity increases, the unconsolidated layer is removed (e). A further increase in velocity results in partial removal of the consolidated layer on what are now the stoss sides of the ripples (f). As the sand is exposed, and if the current velocity is large enough, sand movement begins and the uneroded portions of the mud layer become buried by transported sand (g). As sand transport continues, and the ripples begin to migrate, the remaining mud patches are at first buried but then re-eroded as the ripples migrate across them (h through j).

Differences in the shear stress needed to erode the mud as compared to that needed to move the sand will lead to varying amounts of mud being preserved. If the shear stress required to erode the mud is much lower than that required to initiate sand movement (as in runs T-4, T-6, T-7, T-8, and T-10) no mud will be preserved if that shear stress is reached. If the shear stress required to erode the mud is greater than that needed to initiate sand movement, a wavy mud bed will be

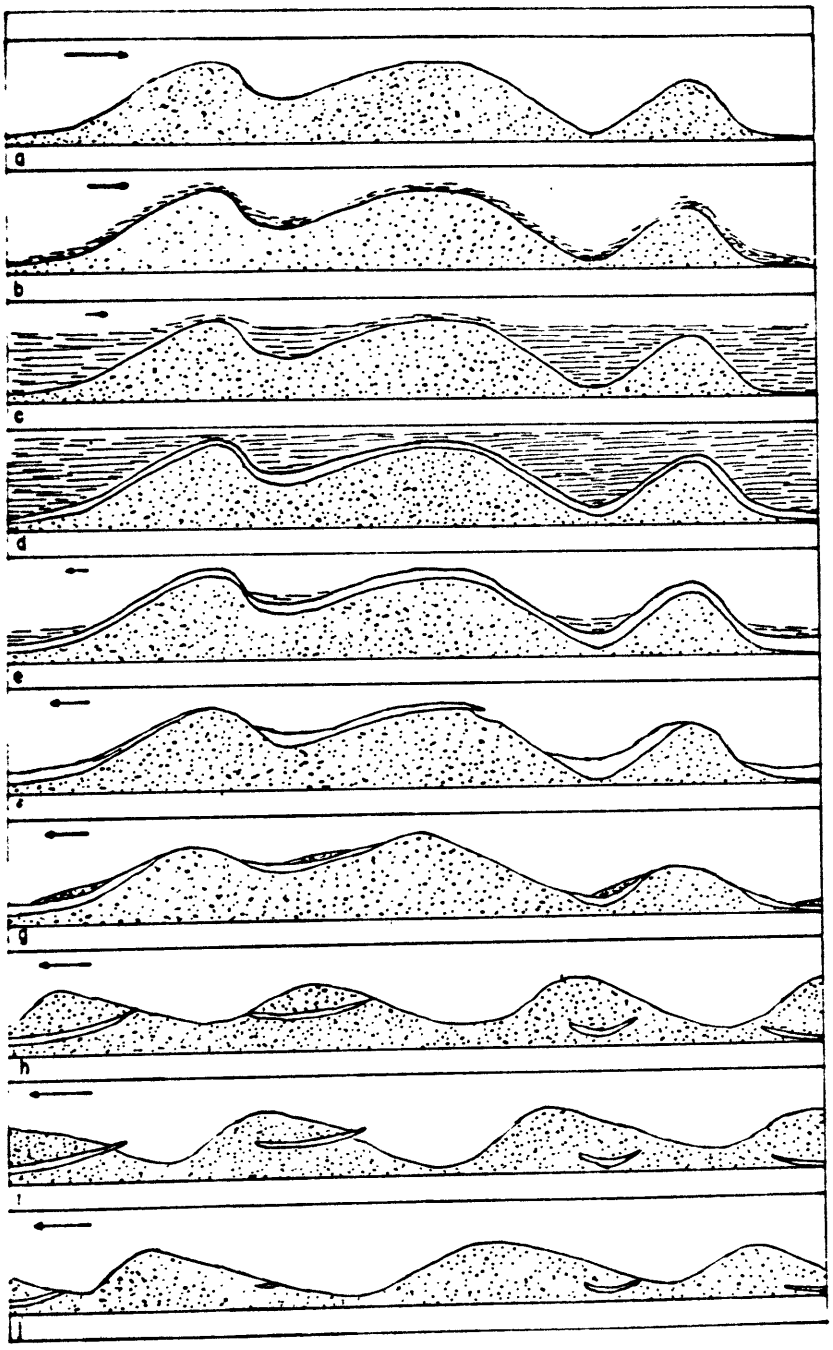

Figure 28: Idealized sequence showing the development of a flaser bed.

preserved (Run U-6). If active bed-load transport of sand occurs at about the same shear stress needed to erode the mud, fairly continuous flaser mud beds (wavy flaser bedding in the terminology of Reineck and Wunderlich, 1968, see Fig. 1) will be formed (Runs U-3, U-4, U-5). If bed-load movement is less active at the shear stress which erodes the mud, more of the mud will be eroded before it can be buried by migrating sand, leading to the formation of simple flaser beds (Runs U-3, U-8, and U-7). The difference between the shear stress required for mud erosion and sand transport will depend upon the grain-size of the sand and the degree of consolidation of the mud. Very small variations in the values of these stresses may produce substantial changes in the types of bedding formed. In the present study, the shear stress needed to initiate movement of the two sands used is practically identical, yet the bedding produced is substantially different (see Fig. 21 and Fig. 22).

Comparison of Figures 17 and 18 with Figures 23, 24, and 25 reveals that considerable amounts of sediment were not resuspended during the secondary velocity maximums in the "U" runs. Part of this descrepancy is caused by the method of calculating the percentage of sediment in suspension. Since the concentration used as 100% was that measured during the first velocity maximum, and because of the lograithmic settling behavior noted by Partheniades, the difference in time between

the introduction of the clay and the initiation of the run between the "T" and "U" runs makes a difference in the calculations. In the "T" runs, because of the longer time period, the sediment had more closely approached its equilibrium value. Because of the shorter time period used during the "U" runs the equilibrium value had not been achieved by the time the velocity maximum had been reached. Experiments and calculations show that the reference concentration for the "U" runs should be reduced by about 30% in order to compare the results with those from the "T" runs. When this reduction is made, the resulting curves appear much more similar. This does not, however, completely explain either the discrepancy or the observation that during the "T" runs only minor amounts of mud were not resuspended whereas during the "U" runs significant amounts of sediment remained deposited. Perhaps the early deposition of large amounts of sediment during the "U" runs allowed the sediment to become more compacted, thus increasing its resistance to erosion.

In order to compare the results of the flume runs to natural conditions some common parameter is necessary. The shear velocity u_* is readily calculated, and because of its relationship to τ_0, is a useful measure describing the flow field near the sediment-fluid interface.

Calculation of u_*

Three different methods of calculating u_* were applied to the experimental results. The results of these methods are listed in Table 1 of Appendix A. U*(1) was determined by the method of Johnson, U*(2) by the equation presented by Richardson and Simons, and U*(3) by the sidewall correction procedure given by Williams. The resulting values of u_* vary considerably, both from run to run and according to the method used. Although some differences due to differing topography from run to run and experimental errors were expected, nothing like this diversity of values was anticipated. In view of the critical importance of the value of u_*, a detailed description of its method of determination is presented in Appendix D.

In order to determine which of the methods gives the most accurate and consistent results, u_* was calculated for each slope measurement by each method. The determinations were then grouped together by mean velocity and averaged. The results, with their standard deviations, are shown in Table 4. Surface slopes measured at a velocity of 12 cm/s were frequently so low that u_* could not be determined. For this reason, values for this velocity are not listed in Table 4. Of the three methods used, that of Williams gives the most consistent results. The values calculated by the Johnson method have high standard deviations, as well as large values of u_*. The results of

Table 4

Mean Value of u_* and their Standard Deviations (S.D.) as Calculated by the Methods of Johnson (U*1), Richardson and Simons (U*2), and Williams (U*3).

u(cm/s)	U*1 (cm/s)	S.D.	U*2 (cm/s)	S.D.	U*3 (cm/s)	S.D.
16	1.78	0.57	1.75	0.70	1.16	0.22
20	2.01	0.44	1.72	0.75	1.36	0.20
24	2.72	0.61	2.23	1.19	1.75	0.29
26	2.62	0.66	1.76	1.00	1.82	0.31
28	3.03	0.51	1.84	0.68	1.97	0.25
30	3.42	0.53	2.02	0.64	2.19	0.25

the Richardson and Simons technique are extremely variable, sometimes predicting a reduction in u_* as the mean velocity is increased. Because of this variability, the results of this method were rejected, although the results for low velocities are attractive. The third method gives by far the most consistent values, as can be seen by comparing the standard deviations.

Two checks can be made on the accuracy of the values of u_*. The first involves the observation that no sand was in suspension at velocities less than or equal to 30 cm/s. Applying Bagnold's criterion for the suspension of sediment, one finds that a τ_0 of 3.36 dynes/cm^2 is sufficient to suspend sand of the size used in the experiments. This value is less than that predicted by Johnson's method for a mean velocity of 30 cm/s. Accordingly, if Johnson's method is accurate, there should be sand in suspension at this velocity. Since there is not, it is felt that the values calculated by this method are inaccurate.

A second check can be made by measuring the slope and mean velocity needed to initiate sediment movement on a flat bed. For the coarser sand the resulting value of u_* read from the Shields diagram is 1.35 cm/s. From measurements made in the flume, u_* was calculated as 1.57 cm/s when using the method of Johnson, and 1.42 when using the procedure described by Williams. It is felt, then, that the most accurate determinations of u_* are those made using Williams' method.

Calculation of u_{50}

Once u_* is determined, it remains to see what values of u_z will produce these values. Four equations (4,5,6, and 10) have been presented which, for a given u_*, enable u_z to be calculated. Values of u_{50} have been calculated using each of these equations; these values are shown in Table 1 of Appendix A. (U501 is calculated from equation 4, U502 from equation 5, U503 from equation 6, and U504 from equation 10.) For these calculations a water temperature of 15°C and a salinity of 15 ppt has been used. The grain diameter used is 0.0129 cm.

The use of equations 4, 5, and 6 is valid only when a planar bed is present. When a rippled bed is present, as is the case when wavy and flasered beds are being formed, use of these equations will result in values of u_z that are too high. This is because for a given u_z the corresponding u_* is less over a planar surface than over a nonplanar surface. Accordingly, for a given value of u_*, equations assuming a planar bed will give values of u_z that are higher than those not assuming a planar bed.

Equation 10 was developed specifically for use over rippled beds. The values obtained by using this equation are distinctly lower than those using the other equations, as would be expected, Although equation 10 was developed for use with noncohesive

sediments, it should be applicable in this investigation. This is because the resistance to flow over a rippled bed is due almost entirely to the form roughness (Richardson and Simons, 1967; Bayazit, 1968).

It should be noted that the results of equations 4, 5, and 6 depend on the value of κ that is used. For natural flows with suspended-sediment concentrations of up to 380 mg/l, Gust and Walgar (1976) noted that κ remained constant at 0.4. This is the value that has been used in the calculations.

Table 5 presents the values of u_{50} calculated using the equations mentioned above and the values of U*(3) presented in Table 4. It can be seen that the values obtained using equations 4, 5, and 6 are approximately equal, and quite a bit higher than those obtained using equation 10. It can be seen that the effect of a rippled bed is to reduce the flow velocity needed to produce a given u_* when compared to that needed over a planar bed.

Examination of Table 1 in Appendix A shows that even the highest value of u_{50} calculated is only about 70 cm/s, not a great deal higher than that calculated by Terwindt and Breusers. The highest value of u_{50} calculated form equation 10 is only about 45 cm/s. These low values of u_{50}, in conjunction with the large amounts of mud eroded at these velocities, seem, to preclude the possibility of continuous mud deposition over

Table 5

Mean values of u_{50} calculated from equations 4 (U501), 5(U502), 6(U503), and 10 (U504).

u (cm/s)	u_* (cm/s)	U501 (cm/s)	U502 (cm/s)	U503 (cm/s)	U504 (cm/s)
16	1.16	31.01	33.81	34.08	16.19
20	1.36	36.90	39.63	39.96	21.65
24	1.75	48.58	51.00	51.42	32.22
26	1.82	50.70	53.04	53.48	34.22
28	1.97	55.27	57.41	57.88	38.32
30	2.19	62.02	63.82	64.35	44.34

succesive slack-water periods, although the results of Runs U-1, V-1, and U-6, in which continuous mud layers resisted subsequent erosion, suggest that if enough mud is deposited, the mechanism suggested by Terwindt and Breusers may be feasible. It should be noted, though, that for these runs the total accumulation is considerably greater than that calculated by Terwindt and Breusers. The results of these runs are actually more in accord with the observations of Reineck and Wunderlich (1967), who noted substantial accumulations of mud in a single slack-water period. It now remains to compare the experimental conditions with those observed in nature in order to determine under what circumstances conditions similar to those used in the experiments might occur.

APPLICATION OF THE EXPERIMENTAL RESULTS TO NATURAL SETTINGS

The report by Postma (1961) seems to be the most appropriate set of data to use when attempting to apply the experimental data to natural situations. Postma collected both suspended-sediment concentration and current velocity data from each of 16 stations located throughout the Wadden Sea over the course of a single tidal cycle. Similar observations made by other workers were either made in areas where sand was absent (Krone, 1972; Schudel, 1969, 1971a) or did not extend over a

complete cycle (Gust and Walgar, 1976). The area studied by Postma is close to that studied by Terwindt and Breusers, and not far from those studied by Reineck and by Gust and Walger. Sediment textures and grain-size characteristics, as well as wave and current activity, seem to be fairly similar in all of the areas studied (Reineck, 1975, Terwindt, 1975). Reineck (1975) states that flaser and wavy bedding is most common in subtidal channels and in the central portions of the tidal flats. In earlier papers (1967, 1972) Reineck has pointed out that preservation of structures located on the tidal flats is much less likely than in the channels due to the high levels of bioturbation on the flats. He also states that deposits formed on channel floors are more likely to be preserved than those on the flats since they are likely to be deposited and subsequently buried more quickly. Since the structures are, in fact, observed on the tidal flats, the question becomes how were they formed and preserved there.

Postma has observed that almost all sand transport in shallow subtidal and intertidal areas, at least in his study region, occurs in the tidal channels. Thus it seems unlikely that the flaser and wavy beds observed on the tidal flats formed under normal conditions. Two other possibilities suggest themselves:

1. The deposits are relics that were formed when the area in which they are found was the floor of a channel and

have been preserved as the channel migrated to a new location.

2. The deposits formed as the result of some abnormal situation when sand was actively transported across the tidal flat and deposited, killing any organisms present in the sediment.

The data of Postma may be used to determine whether, in fact, it is likely that such deposits will form in tidal channels under any conditions. The peak mean velocities measured by Postma are on the order of 80-150 cm/s. Since the exact water depth is not known, it is not possible to calculate u_*. Two other observations can be used, however. First, the total sediment load is considerably higher than that used in the experiments. Run U-1 was, in fact, an attempt to observe whether a mud bed could be deposited given the sediment available according to Postma's observations. It will be recalled that Run U-1 resulted in a mud bed that resisted subsequent erosion at the velocities used. Postma's observations show that nearly all of the mud was resuspended during the subsequent high-velocity period. This implies that the value of u_* is considerably greater in the areas where Postma made his observations than it was in the flume experiments. A second point that reinforces this conclusion is that Postma found significant amounts of sand suspended in the water column. This could occur only if the value of u_* exceeded that measured in the flume experiments. If, in addition to this, one considers the statement of Reineck

and Wunderlich (1969) that channel floor deposits are subject to considerable physical reworking, it seems extremely unlikely that deposits could be formed and preserved during the conditions that prevailed when these observations were made. An additional consideration might also be mentioned. Gordon (1975) has reported that, due to the adverse pressure gradient present during decelerating flow, the Reynolds stress and average kinetic energy of the flow increase significantly over that observed for a steady flow at the same velocity. Thus, for significant periods of time, the actual value of τ_0 in natural tidal flows may exceed that measured in the flume experiments even if the mean flow velocities are equal.

Given the unlikeliness of "every-day" events being responsible for the formation and preservation of these deposits, a more catastrophic mechanism seems to be indicated. McCave (1970) suggested that storm activity was responsible for the formation of these beds in offshore areas. There seems to be no reason why this should not also be possible in nearshore waters.

Terwindt (1967) has observed that the total amount of sediment in suspension along the Dutch coast increases during the winter due to storm activity, and reaches a peak during the spring freshet when there is a combination of storm activity and high sediment discharge from the rivers. Schubel (1971b) has observed that over 70 % of the sediment influx into the

northern Chesapeake Bay occurs during two months during the spring, and that most of the sediment transport observed during the remainder of the year is merely reworking of this sediment. In addition, Postma's observations were made during a period during the summer when there was a minimum of wave activity and suspended-sediment concentrations were about half those observed during the winter.

Storms in shallow water produce both high wave activity and strong currents. Experiments by Kennedy and Locher (1972) have shown that wave activity can suspend significant amounts of sandy material, and the observations of Anderson (1972) showed that fine-grained sediments may be suspended by very small waves. With these arguments in mind the following sequence of events is proposed as a likely mechanism for the formation of wavy and flaser bedding.

During the spring large amounts of sediment are discharged by rivers into nearshore waters. As the clay material enters more saline water, it flocculates, increases in grain size, and eventually settles to the bottom. Storms occurring during this period, which generate both large waves and strong currents, can erode and resuspend substantial amounts of both sand and mud. As the storms subside, the sand, which has been carried in suspension over the tidal flats, deposits first and is formed into rippled beds by the dwindling currents. As the velocity declines further the mud is deposited on top of

the sand where, due to the thick overburden the lower layers consolidate sufficiently to resist erosion. These deposits are then buried by subsequent movement of sediment across the flat during more quiescent periods.

CONCLUSIONS

The results of this investigation indicate that mass erosion of recently deposited mud beds over a rippled surface will begin at an average velocity (for a 12 cm flow depth) of 24 cm/s. This corresponds to a u_* of 1.75 cm/s and a τ_0 of 3.00 dynes/cm^2. The rate of erosion increases significantly if the mean velocity is increased to 26 cm/s, corresponding to a u_* of 1.82 cm/s and a τ_0 of 3.24 dynes/cm^2. These values are somwhat below those reported by Partheniades (1965) (τ_0 = 4.80 dynes/cm^2), but are higher than those reported by Terwindt and Breusers (1971) for a pure mud bed (u_* = 0.8 - 1.4 cm/s). Since the mud beds tested by Terwindt and Breusers (1971) were deposited from highly concentrated suspensions, which settle quickly, and since Migniot (1968) has shown that the initial rigidity of a mud bed is inversely proportional to its rate of deposition, it is believed that the values of Terwindt and Breusers for the pure mud beds are probably too low. It should be noted though that the value of u_* used by Terwindt and Breusers for

calculating u_{50} is that for a bed with 40 % sand.

The consolidated mud layers produced in the experiments were up to 1.2 cm thick, considerably greater than the thickness that Terwindt and Breusers calculated could be deposited in a single slack-water period (0.3 cm). During those runs when a mud layer 0.3 cm thick was deposited, it was almost completely eroded at velocities lower than 24 cm/s. It is concluded that the hypothesis of continuous mud deposition during consecutive slack-water periods advanced by Terwindt and Breusers cannot explain the thickness of the mud beds observed by them.

If thicknesses greater than 0.3 cm accumulate during a single slack-water period, the hypothesis of Terwindt and Breusers might be valid if the bed is planar. However, due to the rippled nature of the bed, the value of u_{50} required to erode mud beds up to 1 cm thick is about 32 cm/s, not 60 cm/s. Accordingly, since a value of over 50 cm/s for u_{50} is invariably reached, at least in the areas they studied, it seems impossible for mud beds to accumulate during successive slack-water periods. The observations of Reineck and Wunderlich (1967, 1969), who noted the deposition of mud beds over 1 cm thick during a single slack-water period, are more in line with the experimental results.

It appears that the most important factor determing the resistance of a mud bed to erosion is the thickness of the bed.

The thicker the bed, the greater the degree of consolidation and the greater its resistance to erosion. This factor appears to be more important than either the mineralogy of the mud, or the time allowed for consolidation, at least for the range of values studied.

For most of the runs, the rate of deposition increased rapidly when the current velocity decreased below 18 cm/s. This value is somewhat higher than that reported by Postma (1967), who measured an increase in depositional rate when the velocity was lowered below 14 cm/s.

The results of this study, and those of Partheniades, suggest that deposition in an unsteady flow should not be considered to be a simple system in which the value of the flow velocity acts as an on-off switch determining whether or not sedimentation will occur. The system appears to be more complex, with sedimentation proceeding at various rates depending upon both the flow velocity and the time which that velocity has persisted.

Flaser beds may be formed by migrating sand ripples covering partially eroded mud beds. The grain size of the sand is important since it determines at what value of u_* sand transport will be initiated. Most occurrences of flaser and wavy bedding have sand that is either fine or very fine-grained. It appears unlikely that these beds would develop in the presence of coarser-grained sand since the velocity needed to

initiate movement of the sand is far higher than that needed to erode the mud. In the present study, the velocities needed to erode the mud and to move the sand are approximately equal. This allows sand movement to occur once the mud layer has been partially removed. Sand is then transported and buries those portions of the mud bed which are still present. At the same time, sand underlying exposed portions of the mud may be removed, thus undermining the mud and leading to its erosion. The different grain sizes used in this study appeared to have a qualitative effect on the nature of the mud beds preserved, with the finer-grained sand producing preservation of more continuous mud layers.

The formation of wavy bedding requires an intact mud layer. This requires a sand source outside the immediate vicinity and transport of the sand across the mud layer. For transport to occur the resistance of the mud bed to erosion must be higher than that obtained in the experiments.

In light of the above considerations, it appears that tidal action, on either a daily or biweekly basis, is unlikely to cause the preservation of flaser or wavy beds. Although a flasered bed may be formed as the result of deposition during a single slack-water period, the structure is unlikely to be preserved since it most likely will be subjected to considerable reworking.

It appears that a situation in which large amounts of sand and mud can be deposited quickly and then allowed to consolidate is required for the formation of flaser and wavy bedding. In shallow subtidal areas, storm action, particularly during the spring, seems to be the most likely mechanism.

REFERENCES CITED

Anderson, F.E. 1972, Resuspension of estuarine sediments by small amplitude waves. J. Sed. Petr., 42, p. 602-607

Bagnold, R.A. 1966, An approach to the sediment transport problem from general physics. USGS Professional Paper #422-I, 37 p.

Bayazit, M. 1969, Resistance to reversing flow over movable beds. J. Hydraulics Division, Proc. Am. Soc. Civil Eng., 95, p. 1110-1127

Carver, R.E. (ed) 1971, Procedures in Sedimentary Petrology, Wiley-Interscience, New York, 653 p.

Dillo, H.-G. 1960, Sandwanderung in tideflussen. Mitteilung Franzius Institut, Grund-Wasserbau Technische Hochschule Hanover, 17, p. 135-253

Einsele, G., Overbeck, R., Schwarz, H.U., and Unsold, G. 1974, Mass physical properties, sliding and erodability of experimentally deposited and differentially consolidated clayey beds. Sedimentology, 21, p. 339-372

Einstein, A. 1906, Eine neue bestimmung der molekuldimensionen. Annalen der Physik, Vierte Folge, 19, p. 289-306

Einstein, H.A., and Chien, N. 1955, Effects of heavy sediment concentration near the bed on velocity and sediment distribution. Univ. California at Berkeley and U.S. Army Eng. Div. Omaha, Nebraska, MRD Sediment Series 8, 76 p.

Einstein, H.A., and Krone, R.B. 1962, Experiments to determine modes of cohesive sediment transport in salt water. J. Goephys. Res., 67, p. 1451-1461

Gordon, C.M. 1975, Sediment entrainment and suspension in a turbulent tidal flow. Marine Geology, 18, p. M57-M64

Graf, W.H. 1971, Hydraulics of Sediment Transport, McGraw-Hill, New York, 513 p.

Gust, G. 1976, Observations on turbulent-drag reduction in a dilute suspension of clay in sea-water. J. Fluid Mechanics, 75, p. 29-47

Gust, G. and Walgar,E. 1975, The influence of suspended cohesive sediments on boundary-layer structure and erosive activity of turbulent seawater flow. Marine Geology, 22, p. 189-206

Harms, J.C., Southard, J.B.,Spearing, D.R., and Walker, R.G. 1975, Depositional Environments as interpreted from primary sedimentary structures and stratification sequences. Short Course #2 Lecture Notes, Soc. Econ. Paleon. and Mineral., 161 p.

Hjulström, F. 1935, Studies of the morphological activity of rivers as illustrated by the River Fyris. Bull. Geol. Inst. Uppsala, 25, p. 221-557

Jackson, R.G. 1976, Sedimentological and fluid-dynamic implications of the turbulent bursting phenomenon in geophysical flows. J. Fluid Mechanics, 77, p. 531-560

Johnson, J.W. 1942, The importance of considering side-wall friction in bed-load investigations. Civil Eng., 12, p. 329-331

Kennedy, J.F. 1969, The formation of sediment ripples, dunes, and antidunes. Ann. Rev. of Fluid Mechanics, 1, p.147-168.

Kennedy, J.F. and Locher, F. 1972, Sediment suspension by water waves in Waves on Beaches, Meyer, R.E. (ed). Academic Press, New York, p. 249-295.

Krone, R.B. 1962, Flume studies of the transport of sediment in estuarial shoaling processes. Final Report, June 1962, Hydraulic Eng. Lab. & Sanitary Eng. Res. Lab., University of California, Berkeley, 110 p.

Krone, R.B. 1972, A field study of flocculation as a factor in estuarial shoaling processes. Technical Bulletin #1a, Committee on Tidal Hydraulics, Corps. of Eng., U.S.Army, 62 p.

Lonsdale, P. and Southard J.B. 1974, Experimental erosion of north pacific red clay. Marine Geology, 17, p. M51-M60

Maude, A.D. and Whitmore, R.L. 1958, A generalized theory of sedimentation. British J. of Appl. Phys., 9, p. 477-482.

McCave, I.N. 1970, Deposition of fine-grained suspended sediments from tidal currents. J. Geophys. Res., 75, p. 4151-4159.

McNown, J.S. and Lin P.-N. 1952, Sediment concentration and fall velocity. Proc. 2nd Midwestern Conf. on Fluid Mechanics, p. 401-411.

Migniot, C. 1968, Étude des propriétés physiques de différents sédiments très fins et de leur comportement sous des actions hydrodynamiques. Houille Blance, 23, p. 591-620.

Murray, S.P. 1970, Settling velocities and vertical diffusion of particles in turbulent water. J. of Geophys. Res., 75, p. 1647-1654.

Owen, M.W. 1971, The effect of turbulence on the settling velocities of silt flocs. Proc. of the 14th Congress of the Internat. Assoc. for Hydraulic Res., 4, p. 27-32

Partheniades, E. 1965, Erosion and Deposition of cohesive soils. J. of the Hydraulics Div., Proc. of the ASCE, 91, p. 105-139.

Partheniades, E., Cross, R.H.III, and Ayora A. 1968, Futher results of the deposition of cohesive sediments. Proc. of the 11th Conf. on Coastal Eng., 1, p. 723-742.

Partheniades, E. and Kennedy, J.F. 1966, Depositional behavior of fine sediment in a turbulent fluid motion. Proc. of the 10th Conf. on Coastal Eng., 1, p. 707-729.

Partheniades, E. and Mehta, A.J. 1971, Rates of deposition of fine cohesive sediments in turbulent flows. Proc. 14th Cong. Internat. Assoc. for Hydraulic Res., 4, p. 17-26.

Postma, H. 1961, Transport and accumulation of suspended matter in the Dutch Wadden Sea. Netherlands J. for Sea Res., 1, p. 148-190.

Postma, H. 1967, Sediment transport and sedimentation in the estuarine environment in Estuaries, Lauff, G. (ed.), Am. Assoc. Adv. Sci. Publ. 83, Washington, D.C. p. 158-179.

Rathburn, R.E. and Guy, H.P. 1967, Measurement of hydraulic and sediment transport variables in a small recirculating flume. Water Resources Res., 3, p. 107-122.

Raudkivi, A.J. 1963, Study of sediment ripple formation. J. Hydraulic Div., Proc. ASCE, 89, p. 15-33.

Raudkivi, A.J. 1976, Loose Boundary Hydraulics, Pergamon Press Oxford, 397 p.

Rees, A.I. 1966, Some flume experiments with a fine silt. Sedimentology, 6, p. 209-240.

Reineck H.E. 1960, Über die entstehung von linsen-und flaserschichtung. Abhandlung der Deutschen Akademie Wissenschaftlichen, Berlin, Klasse III, 1, p. 369-374.

Reineck, H.E., 1963, Sedimentgefüge in bereich der südlichen Nordsee. Ablandlungen der Senckenbergischen Naturforschenden Gesellschaft, 505, 138 p.

Reineck, H.E. 1967, Layered sediments of tidal flats, beaches, and shelf bottoms of the North Sea. in Estuaries, Lauff, G. (ed.), Am. Assoc. Adv. Science, Washington, D.C. p. 191-206.

Reineck, H.E., 1972 Tidal flats, in Recognition of Ancient Sedimentary Environments, Rigby, J.K. and Hamblin, W.K., (eds.), Soc. Econ. Paleon. and Mineral. Spec. Pub., 16, p. 146-159

Reineck, H.E. 1975, German North Sea tidal flats, in Tidal Deposits, Ginsburg, R.N. (ed.), Springer-Verlag, New York, p. 5-12.

Reineck, H.E., and Singh, I.B. 1975, Depositional Sedimentary Environments, Springer-Verlag, New York, 439 p.

Reineck, H.E. and Wunderlich, F. 1967, Zeitmessungen an Gezeitenschichten. Natur und Museum, 97, p. 193-197

Reineck, H.E. and Wunderlich, F. 1968, Classification and origin of flaser and lenticular bedding. Sedimentology, 11, p. 99-104

Reineck, H.E. and Wunderlich, F. 1969, Die entstehung von schichten und schichtbanken im Watt. Senckenbergiana Maritima, 1, p.85-106

Richardson, E.V. and Simons, D.B. 1967, Resistance to flow in sand channels. Proc. 12th Cong. of Int. Assoc. Hyd. Res., 1, p. 141-150

Schlichting, H. 1968, Boundary-layer Theory, 6th ed., McGraw-Hill, New York, 748 p.

Schubel, J.R. 1969, Size distributions of the suspended particles of the Chesapeake Bay turbidity maximum. Netherlands J. Sea Res., 4, p. 283-309

Schubel, J.R. 1971a, Tidal variation of the size distribution of suspended sediment at a station in the Chesapeake Bay turbidity maximum. Netherlands J. Sea Res., 5, p. 252-266

Schubel, J.R. 1971b, The Estuarine Environment, Short Course Lecture Notes, Am. Geological Inst., Falls Church, Virginia

Shields, A. 1936, Anwendung der Ähnlichkeitsmechanik und der Turbulenzforschung auf die Geschiebewegung. Mitteilung der Prussichen Versuchssanstelt fur Wasserbau Erdbau und Schiffbau, #26

Simons, D.B. ,Richardson, E.V., and Hauschild, W.L., 1963, Some effects of fine sediment on flow phenomena. USGS Water Supply Paper 1498-G, 45 p.

Simons, D.B. and Şentürk, F. 1977, Sediment Transport Technology Water Resources Publications, Fort Collins, 807 p.

Southard, J.B. 1971, Representation of bed configurations in depth-velocity-size diagrams. J. Sed. Petr., 41, p. 903-915

Southard, J.B. and Boguchwal, L.A. 1973, Flume experiments on the transition from ripples to lower flat bed with increasing grain size. J. Sed. Petr.,43, p. 1114-1121

Southard, J.B., Young, R.A., and Hollister, C.D. 1971, Experimental erosion of calcareous ooze. J. Geophys. Res., 76, p. 5903-5909

Terwindt, J.H.J. 1967, Mud transport in the Dutch Delta area and along the adjacent coastline. Netherlands J. Sea Res., 3, p. 503-531

Terwindt, J.H.J. 1975, Sequences in inshore tidal deposits in Tidal Deposits, Ginsburg, R.N. (ed), Springer-Verlag, New YOrk, p. 85-91

Terwindt, J.H.J. and Breusers, H.N.C. 1971, Experiments on the origin of flaser, lenticular and sand-clay alternating bedding. Sedimentology, 19, p. 85-98.

Terwindt, J.H.J., Breusers,H.N.C., and Svasek, J.N. 1968, Experimental investigation on the erosion sensitivity of a sand-clay lamination. Sedimentology, 11, p. 105-114.

Vanoni, V.A.(ed.) 1975. Sedimentation Engineering. Am. Soc. of Civil Eng., New York, 745 p.

Williams, G.P. 1970, Flume width and water depth effects in sediment transport experiments. USGS Professional Paper 562-H, 37 p.

Williams, G.P. 1971, Aids in designing laboratory flumes. USGS Open File Report, 294 p.

Winegard, C.I. 1970, Settling velocity of grains of quartz and other minerals in sea water versus pure water. USGS Professional Paper 700-B, p. B161-166.

Young, R.N., and Southard, J.B. 1978, Erosion of fine-grained marine sediments: seafloor and laboratory experiments. Bull. Geol. Soc. Am., 89, p. 663-672

Zeigler, J.M., and Gill, B. 1959, Tables and graphs for the settling behavior of quartz in water, above the range of Stokes' law. Woods Hole Ocean. Inst. Reference 59-36, 13 p.

APPENDIX A: DETAILED OBSERVATIONS OF THE EXPERIMENTAL RUNS

(Note: All figures referred to are in Appendix B. Velocity profiles are given in Table 2, suspended-sediment concentrations in Table 3.)

Run T-1

Run T-1 used a sinusoidal velocity profile with maximum velocities of ± 40 cm/s (positive values indicate flow from left to right, negative values flow from right to left). Due to the small amount of sediment added, no visible mud accumulation was observed. Active ripple migration took place whenever the average flow velocity exceed 24 cm/s. At velocities above 32 cm/s, significant amounts of sand were suspended. Due to the high velocities, the ripples were exceedingly irregular in shape.

Run T-2

This run used the same velocity profile as run T-1. The amount of clay added was doubled, but again no deposition was observed. As in run T-1, the ripple forms were irregular, and significant suspended sand was observed at velocities greater than 32 cm/s.

Run T-3

Run T-3 also used a sinusoidal profile but the peak velocities were ± 20 cm/s. Four hundred grams of montmorillonlite were used in this run. Due to the low maximum velocities, no sand movement was observed during the run (compare Fig. 1 and 2). A small amount of mud was deposited during the first low-velocity period. Some of this sediment was resuspended, but not all. During the second low-velocity period, more mud was deposited. This layer resisted subsequent erosion. Note that the suspended sediment concentration measured at 0200 is probably incorrect.

Run T-4

This run was done to compare the effects of a longer low-velocity period on the sedimentation and compaction of the mud. The generating function used for this and all subsequent runs was $u = 2 \sin(t) + \sin(2t)$. Peak velocities used in this run were ± 40 cm/s. Four hundred grams of clay were added. No deposition was observed during the first low-velocity period. During the second low velocity period the two distinct mud layers corresponding to the two phases of deposition noted by Einstein and Krone were observed. Both layers were eroded as the current velocity was increased: the unconsolidated layer

when the velocity was 12 cm/s, and the consolidated layer at 22 cm/s. The unconsolidated layer appeared to diffuse into the water whereas the consolidated layer was torn up in chunks. By the end of the run no mud layer could be seen. As in the previous runs when the peak velocities exceeded 30 cm/s, the ripple forms were quite irregular and sand in suspension was observed.

Run T-5

Run T-5 was similar to run T-4 except that the maximum velocities were ± 20 cm/s. Unfortunately the photographs taken during this run were ruined. As in run T-3, a very thin mud layer was deposited during the first slack-water period. This layer was eroded as the velocity was increased. During the second, longer, low-velocity period, a 2 mm thick consolidated layer formed. This layer was not eroded as the velocity was increased. Due to the low velocities used, there was no sand movement during this run. The suspended sediment concentration measurement made at 0900 is wrong.

Run T-6

Runs T-6 through T-10 all used the same velocity profile with peak velocities of + 30 and -20 cm/s. Minor bed-load

movement was observed when the velocity exceeded 26 cm/s. During the first low-velocity period, a very thin mud layer was deposited. This layer was eroded as the velocity was increased. During the second period of low velocity both a consolidated and an unconsolidated layer formed. The unconsolidated layer was completely removed by the time the velocity had been increased to 10 cm/s. The consolidated layer began eroding when the velocity reached 24 cm/s. As the velocity was further increased, the rate of erosion also increased. Parts of the mud layer were buried by migrating ripples (Fig.3).

Run T-7

Run T-7 was identical to Run T-6 except that the mineralogy of the clay was different. The sequence of events observed was very similar to those seen in Run T-6 except that erosion was initiated at slightly lower velocities (20 cm/s for the consolidated layer). The end results were very similar (Fig. 4).

Run T-8

The purpose of runs T-8 and T-9 was to investigate the effect of suspended-sediment concentration on depositional behavior. Run T-8 was run with a very low suspended-sediment concentration. During the first low-velocity period a thin

unconsolidated layer was deposited. This layer was subsequently eroded as the current velocity was increased. As in all of the runs in which the secondary velocity maximum was 20 cm/s, sand movement was minimal during the interval between the two slack-water periods. During the second slack-water both a consolidated and an unconsolidated layer were formed, although both layers were eroded by the time the velocity had reached 12 cm/s. Subsequent sand transport, which began at a velocity of 26 cm/s buried some small patches of mud which had not been eroded (Fig. 5).

Run T-9

In Run T-9 the total amount of suspended sediment added was approximately equal to what might be deposited in a natural setting (based on Postma's (1961) observations). By the beginning of the run a substantial clay layer had already been deposited (Figure 6). Subsequent sand movement first buried, and then re-exposed these deposits so that most of them had been eroded before the first low-velocity episode (Fig. 7 and 8). Thick layers, both unconsolidated and consolidated, formed during this period (Fig. 9). The unconsolidated layer had been eroded by the time the velocity had reached 14 cm/s (Fig. 10). Most of the consolidated layer was eroded by the flood current but some remained in the troughs (Figure 11). During

the second low-velocity period a thick mud layer was deposited, the consolidated layer reaching a thickness of 0.5 cm (Fig. 12). Much of this layer was eroded when the velocity was increased to more than 24 cm/s, but some was buried by the sand (Fig. 13).

Run T-10

Run T-10 was done using an illite mixture to compare its behavior to that of montmorillinite (Run T-6) and kaolinite (Run T-7). The results were similar to those described for those runs.

Run U-1

Run U-1 was similar to Run T-9 in that an attempt was made to approximate the total amount of sediment that might be deposited during a single tidal cycle. So much sediment was added that a large amount deposited at any velocity less than 30 cm/s. For this reason the run was begun at this velocity. A consolidated layer 1 cm thick was deposited during the first low-velocity period and was not eroded when the velocity was re-increased. Even more mud was deposited during the second slack water period, forming a second consolidated layer. At the end of the run, these layers had almost completely resisted erosion, leaving an almost continuous mud

layer (Fig. 14).

Run V-1

Run V-1 used less sediment than U-1 in an attempt to eliminate the deposition at high velocities and the hindered settling which had been observed during that run. The attempt was not completely successful since some sediment deposited before the beginning of the run. Since lower peak velocities were used sand transport was much less extensive. This resulted in a consolidated layer forming during the first slack-water period which eroded only slightly during the following high-velocity episode. The run was terminated at this point.

All of the following runs used the same amount and type of clay material. Since run U-8 was a rerun of U-2, they are discussed together.

Runs U-2 and U-8

The results of the two runs were very similar. By the beginning of both runs some mud had already been deposited. As the velocity was increased, bed-load movement became more active, re-exposing some of the mud that had already been buried. During the first slack-water period, a large amount

of mud was deposited, forming a thick unconsolidated layer and a thinner consolidated layer (about 1 cm thick). The unconsolidated layer was eroded before the velocity reached 12 cm/s, while the consolidated layer was partially eroded and partially buried during the subsequent increase in current velocity. More mud was deposited during the second low-velocity period, but most of this was eroded when the velocity was re-increased. Only a small amount of mud was preserved at the end of the runs (Fig. 15).

Run U-3

Run U-3 used peak velocities of ± 24 cm/s. During the first high-velocity period, some of the mud that had already been deposited was buried by migrating sand (Fig. 16). As the velocity decreased, more mud was deposited, producing a consolidated layer about 1 cm thick, but thicker in the troughs (Fig. 17). As the velocity increased, this layer was partially eroded and then buried by sand movement (Fig. 18). During the second slack-water period more mud was deposited. This formed another consolidated layer which was not quite as thick as the one formed previously since less mud was available (Fig. 19). Erosion of this layer was evident when the velocity reached 16 cm/s. By the time the velocity was 24 cm/s, much of the

second mud layer had been eroded or buried by the sand. This resulted in a complex series of sand and mud layers (Fig. 20).

Run U-4

The initial portion of this run was much like that of runs U-2 and U-8. Erosion was more pronounced during the flood tide than in those runs. This is probably due to the change in the sand size. The sand in this run was smaller than in runs U-2 and U-8, so presumably it was transported more actively, thus leading to increased undermining of the mud layers (Fig. 21). Another mud layer was deposited during the second low-velocity period and was eroded as the velocity was increased.

Run U-5

As in all of the "U" runs, some mud had been deposited and buried before the beginning of the run. As the velocity was increased, most of this mud was exposed and eroded. During the first low-velocity episode, a consolidated layer varying from 0.3 to 1 cm in thickness formed. Only small portions of this layer were eroded as the velocity was increased. During the second slack-water period a second consolidated layer formed. As the velocity was increased above 24 cm/s both of these consolidated layers were in part eroded and in part buried by the

sand (Fig. 22).

Run U-6

Very little of the mud deposited before the beginning of the run was either eroded or buried during the first high-velocity episode. During the first slack-water period a 1 cm thick consolidated layer formed. Very little of this layer was eroded as the velocity was increased (Fig. 23). More sediment deposited during the second low-velocity period and was only slightly eroded later. This run was the only one in which a continuous mud layer was produced.

Run U-7

The mud deposited before the beginning of the run was mostly eroded during the first high-velocity period. A 0.7 cm thick consolidated layer formed during the first slack-water period and was not eroded as the velocity was increased. More mud deposited during the second slack-water period but both layers were mostly eroded as the velocity was increased to 30 cm/s (Fig. 24).

Table 1 lists the measured surface slope (SW), the energy slope (SE), the Froude number (FR), the friction factor (F), r^2 (R2), u_* calculated by the three methods described, u_{50} as calculated from equations 4 (U50(1)), 5 (U50(2)), 6 (U50(3)), and 10 (U50(4)). The value of τ_0 corresponding to $u_*(3)$ is also given.

Table 2 shows the velcoity profiles used for the various runs. Table 3 shows the suspended-sediment concentrations measured.

TABLE 1 SUMMARY OF DATA FOR RUN U-8

DEPTH = 12 CM HYDRAULIC RADIUS = 4.54 CM SAND SIZE = 0.016 CM

VELOCITY (CM/S)	TEMP. (DEG. C)	VISCOSITY (STOKES)	REYNOLDS NUMBER	SURFACE SLOPE	R2	F	U*(1) (CM/S)	U*(2) (CM/S)	U*(3) (CM/S)
24.0	21.0	0.102E-01	0.283E+05	0.560E-03	0.979E+00	0.035	1.90	1.05	1.38
26.0	21.0	0.102E-01	0.307E+05	0.874E-03	0.957E+00	0.046	2.57	1.45	1.72
28.0	22.0	0.993E-02	0.338E+05	0.942E-03	0.961E+00	0.043	2.64	1.33	1.79
30.0	22.0	0.993E-02	0.363E+05	0.153E-02	0.994E+00	0.060	3.60	2.12	2.28
30.0	22.0	0.993E-02	0.363E+05	0.170E-02	0.992E+00	0.067	3.86	2.55	2.40
28.0	22.0	0.993E-02	0.338E+05	0.139E-02	0.993E+00	0.063	3.45	2.28	2.17
26.0	22.0	0.993E-02	0.314E+05	0.118E-02	0.996E+00	0.062	3.16	2.23	2.00
24.0	22.0	0.993E-02	0.290E+05	0.114E-02	0.991E+00	0.071	3.16	2.79	1.97
20.0	22.0	0.993E-02	0.242E+05	0.704E-03	0.998E+00	0.063	2.41	2.25	1.55
-16.0	23.0	0.971E-02	0.198E+05	0.348E-03	0.997E+00	0.048	1.60	1.55	1.09
-20.0	23.0	0.971E-02	0.247E+05	0.570E-03	0.995E+00	0.051	2.09	1.64	1.39
-24.0	23.0	0.971E-02	0.297E+05	0.103E-02	0.986E+00	0.064	2.96	2.31	1.87
-24.0	23.0	0.971E-02	0.297E+05	0.119E-02	0.992E+00	0.074	3.25	3.04	2.01
-20.0	23.0	0.971E-02	0.247E+05	0.760E-03	0.994E+00	0.068	2.54	2.57	1.61
-16.0	23.0	0.971E-02	0.198E+05	0.486E-03	0.992E+00	0.068	2.01	2.57	1.29
16.0	25.0	0.925E-02	0.208E+05	0.310E-03	0.999E+00	0.043	1.47	1.34	1.03
20.0	25.0	0.925E-02	0.259E+05	0.490E-03	0.983E+00	0.044	1.88	1.36	1.29
24.0	26.0	0.907E-02	0.318E+05	0.810E-03	0.986E+00	0.050	2.53	1.62	1.66
30.0	27.0	0.888E-02	0.405E+05	0.168E-02	0.997E+00	0.067	3.85	2.50	2.39
30.0	27.0	0.888E-02	0.405E+05	0.183E-02	0.981E+00	0.072	4.05	2.92	2.49
30.0	27.0	0.888E-02	0.405E+05	0.175E-02	0.959E+00	0.069	3.95	2.69	2.44

TABLE 1 SUMMARY OF DATA FOR RUN U-8

VELOCITY (CM/S)	U*(3) (CM/S)	FR	SE	TAU DYNES/ CM**2)	U50(1) (CM/S)	U50(2) (CM/S)	U50(3) (CM/S)	U50(4) (CM/S)
24.0	1.38	0.05	0.560E-03	1.87	37.48	39.55	39.88	20.04
26.0	1.72	0.06	0.874E-03	2.91	47.78	49.40	49.82	25.52
28.0	1.79	0.07	0.942E-03	3.14	49.77	51.29	51.72	26.57
30.0	2.28	0.08	0.153E-02	5.09	64.71	65.28	65.83	34.35
30.0	2.40	0.08	0.170E-02	5.67	68.63	68.90	69.48	36.36
28.0	2.17	0.07	0.139E-02	4.64	61.51	62.30	62.83	32.69
26.0	2.00	0.06	0.118E-02	3.94	56.31	57.45	57.93	30.00
24.0	1.97	0.05	0.114E-02	3.81	55.27	56.47	56.95	29.45
20.0	1.55	0.03	0.704E-03	2.35	42.46	44.34	44.71	22.70
-16.0	1.09	0.02	0.348E-03	1.16	28.90	31.17	31.44	15.38
-20.0	1.39	0.03	0.570E-03	1.90	37.84	39.90	40.23	20.23
-24.0	1.87	0.05	0.103E-02	3.44	52.25	53.63	54.08	27.87
-24.0	2.01	0.05	0.119E-02	3.98	56.57	57.70	58.18	30.13
-20.0	1.61	0.03	0.760E-03	2.54	44.27	46.07	46.46	23.67
-16.0	1.29	0.02	0.486E-03	1.62	34.68	36.84	37.15	18.53
16.0	1.03	0.02	0.310E-03	1.04	27.13	29.42	29.67	14.41
20.0	1.29	0.03	0.490E-03	1.64	34.84	36.99	37.30	18.62
24.0	1.66	0.05	0.810E-03	2.71	45.84	47.56	47.96	24.49
30.0	2.39	0.08	0.168E-02	5.63	68.27	68.58	69.15	36.18
30.0	2.49	0.08	0.183E-02	6.12	71.39	71.45	72.05	37.78
30.0	2.44	0.08	0.175E-02	5.85	69.72	69.91	70.49	36.92

TABLE 1 SUMMARY OF DATA FOR RUN U-7

DEPTH = 12 CM HYDRAULIC RADIUS = 4.54 CM SAND SIZE = 0.016 CM

VELOCITY (CM/S)	TEMP. (DEG. C)	VISCOSITY (STOKES)	REYNOLDS NUMBER	SURFACE SLOPE	R2	F	U*(1) (CM/S)	U*(2) (CM/S)	U*(3) (CM/S)
20.0	21.0	0.102E-01	0.236E+05	0.450E-03	0.992E+00	0.040	1.75	1.23	1.24
24.0	21.0	0.102E-01	0.283E+05	0.726E-03	0.987E+00	0.045	2.32	1.41	1.57
26.0	21.0	0.102E-01	0.307E+05	0.788E-03	0.993E+00	0.041	2.38	1.28	1.64
28.0	21.0	0.102E-01	0.331E+05	0.982E-03	0.989E+00	0.045	2.72	1.39	1.83
30.0	21.0	0.102E-01	0.354E+05	0.135E-02	0.985E+00	0.053	3.31	1.76	2.14
30.0	21.0	0.102E-01	0.354E+05	0.128E-02	0.966E+00	0.051	3.21	1.65	2.09
28.0	21.0	0.102E-01	0.331E+05	0.125E-02	0.984E+00	0.057	3.22	1.94	2.06
26.0	21.0	0.102E-01	0.307E+05	0.111E-02	0.987E+00	0.059	3.04	2.02	1.94
24.0	21.0	0.102E-01	0.283E+05	0.690E-03	0.988E+00	0.043	2.23	1.32	1.53
20.0	21.0	0.102E-01	0.236E+05	0.536E-03	0.974E+00	0.048	2.00	1.52	1.35
16.0	21.0	0.102E-01	0.189E+05	0.384E-03	0.991E+00	0.053	1.71	1.77	1.14
-16.0	22.0	0.993E-02	0.193E+05	0.314E-03	0.996E+00	0.044	1.48	1.36	1.03
-20.0	22.0	0.993E-02	0.242E+05	0.430E-03	0.994E+00	0.038	1.69	1.17	1.21
-20.0	22.0	0.993E-02	0.242E+05	0.360E-03	0.990E+00	0.032	1.45	0.97	1.11
-16.0	22.0	0.993E-02	0.193E+05	0.356E-03	0.996E+00	0.049	1.62	1.59	1.10
16.0	23.0	0.971E-02	0.198E+05	0.240E-03	0.990E+00	0.033	1.18	1.01	0.90
20.0	23.0	0.971E-02	0.198E+05	0.240E-03	0.948E+00	0.0	0.0	0.0	0.0
24.0	23.0	0.971E-02	0.297E+05	0.800E-03	0.994E+00	0.049	2.50	1.59	1.65
26.0	23.0	0.971E-02	0.321E+05	0.650E-03	0.100E+01	0.034	2.06	1.04	1.49
28.0	23.0	0.971E-02	0.346E+05	0.101E-02	0.973E+00	0.046	2.78	1.44	1.85
30.0	23.0	0.971E-02	0.371E+05	0.106E-02	0.986E+00	0.042	2.87	1.30	1.90

TABLE 1 SUMMARY OF DATA FOR RUN U-7

VELOCITY (CM/S)	U*(3) (CM/S)	FR	SE	TAU DYNES/ CM**2)	U50(1) (CM/S)	U50(2) (CM/S)	U50(3) (CM/S)	U50(4) (CM/S)
20.0	1.24	0.03	0.450E-03	1.50	33.26	35.45	35.75	17.76
24.0	1.57	0.05	0.726E-03	2.42	43.18	45.03	45.40	23.09
26.0	1.64	0.06	0.788E-03	2.63	45.15	46.91	47.30	24.13
28.0	1.83	0.07	0.982E-03	3.27	50.91	52.37	52.81	27.17
30.0	2.14	0.08	0.135E-02	4.50	60.49	61.36	61.87	32.17
30.0	2.09	0.08	0.128E-02	4.28	58.91	59.88	60.38	31.35
28.0	2.06	0.07	0.125E-02	4.18	58.16	59.18	59.67	30.96
26.0	1.94	0.06	0.111E-02	3.71	54.47	55.73	56.19	29.04
24.0	1.53	0.05	0.690E-03	2.30	42.00	43.90	44.26	22.46
20.0	1.35	0.03	0.536E-03	1.79	36.59	38.69	39.01	19.56
16.0	1.14	0.02	0.384E-03	1.28	30.49	32.75	33.02	16.25
-16.0	1.03	0.02	0.314E-03	1.05	27.32	29.61	29.86	14.51
-20.0	1.21	0.03	0.430E-03	1.43	32.44	34.65	34.94	17.31
-20.0	1.11	0.03	0.360E-03	1.20	29.44	31.71	31.97	15.68
-16.0	1.10	0.02	0.356E-03	1.19	29.26	31.53	31.79	15.58
16.0	0.90	0.02	0.240E-03	0.80	23.58	25.89	26.11	12.44
20.0	0.0	0.0	0.0	0.0	0.0	0.0	0.0	0.0
24.0	1.65	0.05	0.800E-03	2.67	45.53	47.27	47.66	24.33
26.0	1.49	0.06	0.650E-03	2.17	40.65	42.61	42.96	21.74
28.0	1.85	0.07	0.101E-02	3.37	51.69	53.11	53.55	27.58
30.0	1.90	0.08	0.106E-02	3.54	53.07	54.41	54.86	28.30

TABLE 1 SUMMARY OF DATA FOR RUN U-6

DEPTH = 12 CM HYDRAULIC RADIUS = 4.54 CM SAND SIZE = 0.016 CM

VELOCITY (CM/S)	TEMP. (DEG. C)	VISCOSITY (STOKES)	REYNOLDS NUMBER	SURFACE SLOPE	R2	F	U*(1) (CM/S)	U*(2) (CM/S)	U*(3) (CM/S)
20.0	10.0	0.135E-01	0.178E+05	0.386E-03	0.989E+00	0.034	1.50	1.04	1.15
24.0	10.0	0.135E-01	0.214E+05	0.560E-03	0.992E+00	0.035	1.85	1.05	1.38
20.0	10.0	0.135E-01	0.178E+05	0.480E-03	0.991E+00	0.043	1.80	1.33	1.28
16.0	10.0	0.135E-01	0.142E+05	0.200E-03	0.950E+00	0.028	0.94	0.85	0.82
-16.0	20.0	0.104E-01	0.142E+05	0.200E-03	0.937E+00	0.0	0.0	0.0	0.0
-20.0	20.0	0.104E-01	0.231E+05	0.366E-03	0.982E+00	0.033	1.47	0.99	1.12
-24.0	20.0	0.104E-01	0.277E+05	0.570E-03	0.976E+00	0.035	1.92	1.07	1.39
-24.0	20.0	0.104E-01	0.277E+05	0.504E-03	0.982E+00	0.031	1.80	0.94	1.31
-20.0	20.0	0.104E-01	0.231E+05	0.470E-03	0.967E+00	0.042	1.81	1.29	1.26
-16.0	20.0	0.104E-01	0.185E+05	0.198E-03	0.994E+00	0.028	0.97	0.84	0.82
16.0	30.0	0.888E-02	0.216E+05	0.300E-03	0.965E+00	0.042	1.44	1.29	1.01
20.0	30.0	0.888E-02	0.270E+05	0.420E-03	0.993E+00	0.037	1.67	1.14	1.19
24.0	30.0	0.888E-02	0.270E+05	0.420E-03	0.931E+00	0.0	0.0	0.0	0.0

TABLE 1 SUMMARY OF DATA FOR RUN U-6

VELOCITY (CM/S)	U*(3) (CM/S)	FR	SE	TAU DYNES/ CM**2)	U50(1) (CM/S)	U50(2) (CM/S)	U50(3) (CM/S)	U50(4) (CM/S)
20.0	1.15	0.03	0.386E-03	1.28	30.58	32.83	33.11	16.30
24.0	1.38	0.05	0.560E-03	1.86	37.48	39.55	39.88	20.04
20.0	1.28	0.03	0.480E-03	1.59	34.45	36.61	36.92	18.41
16.0	0.82	0.02	0.200E-03	0.66	21.34	23.64	23.83	11.19
-16.0	0.0	0.0	0.0	0.0	0.0	0.0	0.0	0.0
-20.0	1.12	0.03	0.366E-03	1.22	29.70	31.97	32.24	15.82
-24.0	1.39	0.05	0.570E-03	1.90	37.84	39.90	40.23	20.23
-24.0	1.31	0.05	0.504E-03	1.68	35.38	37.52	37.83	18.91
-20.0	1.26	0.03	0.470E-03	1.57	34.06	36.23	36.53	18.19
-16.0	0.82	0.02	0.198E-03	0.66	21.22	23.52	23.71	11.12
16.0	1.01	0.02	0.300E-03	1.00	26.65	28.95	29.19	14.14
20.0	1.19	0.03	0.420E-03	1.41	32.03	34.25	34.54	17.09
24.0	0.0	0.0	0.0	0.0	0.0	0.0	0.0	0.0

TABLE 1 SUMMARY OF DATA FOR RUN U-5

DEPTH = 12 CM HYDRAULIC RADIUS = 4.54 CM SAND SIZE = 0.013 CM

VELOCITY (CM/S)	TEMP. (DEG. C)	VISCOSITY (STOKES)	REYNOLDS NUMBER	SURFACE SLOPE	R2	F	U*(1) (CM/S)	U*(2) (CM/S)	U*(3) (CM/S)
20.0	19.0	0.107E-01	0.225E+05	0.568E-03	0.952E+00	0.051	2.08	1.64	1.39
24.0	19.0	0.107E-01	0.270E+05	0.642E-03	0.997E+00	0.040	2.11	1.22	1.48
26.0	19.0	0.107E-01	0.293E+05	0.704E-03	0.992E+00	0.037	2.18	1.13	1.55
28.0	19.0	0.107E-01	0.315E+05	0.782E-03	0.981E+00	0.035	2.35	1.08	1.63
30.0	19.0	0.107E-01	0.338E+05	0.102E-02	0.996E+00	0.040	2.71	1.24	1.86
30.0	19.0	0.107E-01	0.338E+05	0.100E-02	0.996E+00	0.040	2.68	1.22	1.85
28.0	19.0	0.107E-01	0.315E+05	0.878E-03	0.986E+00	0.040	2.50	1.22	1.73
26.0	19.0	0.107E-01	0.293E+05	0.530E-03	0.999E+00	0.028	1.70	0.85	1.34
24.0	19.0	0.107E-01	0.270E+05	0.656E-03	0.964E+00	0.041	2.14	1.25	1.49
20.0	19.0	0.107E-01	0.225E+05	0.518E-03	0.971E+00	0.046	1.94	1.45	1.33
16.0	19.0	0.107E-01	0.180E+05	0.434E-03	0.981E+00	0.060	1.85	2.12	1.21
12.0	19.0	0.107E-01	0.135E+05	0.322E-03	0.986E+00	0.080	1.95	3.60	1.05
-12.0	20.0	0.104E-01	0.135E+05	0.322E-03	0.914E+00	0.0	0.0	0.0	0.0
-16.0	20.0	0.104E-01	0.185E+05	0.410E-03	0.996E+00	0.057	1.79	1.94	1.18
-20.0	20.0	0.104E-01	0.231E+05	0.602E-03	0.991E+00	0.054	2.17	1.77	1.43
-20.0	20.0	0.104E-01	0.231E+05	0.608E-03	0.990E+00	0.054	2.18	1.80	1.44
-16.0	20.0	0.104E-01	0.185E+05	0.400E-03	0.989E+00	0.056	1.76	1.87	1.17
-12.0	20.0	0.104E-01	0.185E+05	0.400E-03	0.935E+00	0.0	0.0	0.0	0.0
12.0	21.0	0.102E-01	0.185E+05	0.400E-03	0.698E+00	0.0	0.0	0.0	0.0
16.0	21.0	0.102E-01	0.189E+05	0.342E-03	0.979E+00	0.048	1.57	1.51	1.08
20.0	21.0	0.102E-01	0.236E+05	0.538E-03	0.986E+00	0.048	2.01	1.52	1.35
24.0	21.0	0.102E-01	0.283E+05	0.708E-03	0.977E+00	0.044	2.28	1.36	1.55
26.0	20.0	0.104E-01	0.300E+05	0.780E-03	0.980E+00	0.041	2.36	1.27	1.63
28.0	20.0	0.104E-01	0.323E+05	0.860E-03	0.994E+00	0.039	2.46	1.20	1.71
30.0	20.0	0.104E-01	0.346E+05	0.115E-02	0.988E+00	0.046	2.97	1.43	1.98
28.0	20.0	0.104E-01	0.323E+05	0.102E-02	0.984E+00	0.046	2.79	1.46	1.86

TABLE 1 SUMMARY OF DATA FOR RUN U-5

VELOCITY (CM/S)	U*(3) (CM/S)	FR	SE	TAU DYNES/ CM**2)	U50(1) (CM/S)	U50(2) (CM/S)	U50(3) (CM/S)	U50(4) (CM/S)
20.0	1.39	0.03	0.568E-03	1.89	37.77	40.49	40.82	20.19
24.0	1.48	0.05	0.642E-03	2.14	40.38	43.04	43.40	21.59
26.0	1.55	0.06	0.704E-03	2.35	42.46	45.07	45.45	22.70
28.0	1.63	0.07	0.782E-03	2.61	44.96	47.51	47.90	24.03
30.0	1.86	0.08	0.102E-02	3.40	51.97	54.26	54.70	27.73
30.0	1.85	0.08	0.100E-02	3.35	51.53	53.83	54.27	27.49
28.0	1.73	0.07	0.878E-03	2.93	47.89	50.34	50.75	25.58
26.0	1.34	0.06	0.530E-03	1.77	36.37	39.11	39.43	19.44
24.0	1.49	0.05	0.656E-03	2.19	40.86	43.51	43.87	21.85
20.0	1.33	0.03	0.518E-03	1.73	35.91	38.66	38.98	19.20
16.0	1.21	0.02	0.434E-03	1.45	32.61	35.39	35.68	17.40
12.0	1.05	0.01	0.322E-03	1.07	27.69	30.48	30.73	14.72
-12.0	0.0	0.0	0.0	0.0	0.0	0.0	0.0	0.0
-16.0	1.18	0.02	0.410E-03	1.37	31.61	34.40	34.68	16.86
-20.0	1.43	0.03	0.602E-03	2.01	38.98	41.68	42.02	20.85
-20.0	1.44	0.03	0.608E-03	2.03	39.20	41.89	42.23	20.96
-16.0	1.17	0.02	0.400E-03	1.33	31.18	33.98	34.26	16.63
-12.0	0.0	0.0	0.0	0.0	0.0	0.0	0.0	0.0
12.0	0.0	0.0	0.0	0.0	0.0	0.0	0.0	0.0
16.0	1.08	0.02	0.342E-03	1.14	28.62	31.42	31.67	15.23
20.0	1.35	0.03	0.538E-03	1.79	36.66	39.40	39.73	19.60
24.0	1.55	0.05	0.708E-03	2.36	42.59	45.20	45.57	22.77
26.0	1.63	0.06	0.780E-03	2.60	44.90	47.45	47.84	24.00
28.0	1.71	0.07	0.860E-03	2.87	47.36	49.82	50.23	25.30
30.0	1.98	0.08	0.115E-02	3.84	55.53	57.66	58.13	29.59
28.0	1.86	0.07	0.102E-02	3.40	51.97	54.26	54.70	27.73

TABLE 1 SUMMARY OF DATA FOR RUN U-4

DEPTH = 12 CM HYDRAULIC RADIUS = 4.54 CM SAND SIZE = 0.013 CM

VELOCITY (CM/S)	TEMP. (DEG. C)	VISCOSITY (STOKES)	REYNOLDS NUMBER	SURFACE SLOPE	R2	F	U*(1) (CM/S)	U*(2) (CM/S)	U*(3) (CM/S)
24.0	18.0	0.109E-01	0.263E+05	0.138E-02	0.964E+00	0.085	3.54	4.29	2.17
26.0	18.0	0.109E-01	0.285E+05	0.670E-03	0.979E+00	0.035	2.09	1.07	1.51
28.0	18.0	0.109E-01	0.307E+05	0.132E-02	0.975E+00	0.060	3.32	2.10	2.12
30.0	19.0	0.107E-01	0.338E+05	0.980E-03	0.993E+00	0.039	2.63	1.19	1.82
30.0	19.0	0.107E-01	0.338E+05	0.171E-02	0.973E+00	0.068	3.87	2.58	2.41
28.0	19.0	0.107E-01	0.315E+05	0.149E-02	0.995E+00	0.068	3.60	2.58	2.25
26.0	19.0	0.107E-01	0.293E+05	0.160E-02	0.988E+00	0.084	3.82	4.18	2.33
24.0	19.0	0.107E-01	0.270E+05	0.128E-02	0.991E+00	0.079	3.38	3.54	2.08
20.0	19.0	0.107E-01	0.225E+05	0.570E-03	0.971E+00	0.051	2.08	1.65	1.39
16.0	19.0	0.107E-01	0.180E+05	0.584E-03	0.985E+00	0.081	2.62	3.78	1.41
12.0	19.0	0.107E-01	0.180E+05	0.584E-03	0.911E+00	0.0	0.0	0.0	0.0
-12.0	20.0	0.104E-01	0.139E+05	0.334E-03	0.963E+00	0.083	1.98	3.94	1.07
-16.0	20.0	0.104E-01	0.185E+05	0.760E-03	0.981E+00	0.106	2.99	9.53	1.61
-20.0	20.0	0.104E-01	0.231E+05	0.824E-03	0.960E+00	0.073	2.67	3.01	1.67
-24.0	20.0	0.104E-01	0.277E+05	0.138E-02	0.988E+00	0.085	3.55	4.30	2.17
-24.0	20.0	0.104E-01	0.277E+05	0.143E-02	0.992E+00	0.088	3.62	4.70	2.20
-20.0	20.0	0.104E-01	0.231E+05	0.846E-03	0.997E+00	0.075	2.72	3.18	1.70
-16.0	20.0	0.104E-01	0.231E+05	0.846E-03	0.945E+00	0.0	0.0	0.0	0.0
-12.0	20.0	0.104E-01	0.139E+05	0.420E-03	0.973E+00	0.104	2.22	8.69	1.19
12.0	21.0	0.102E-01	0.142E+05	0.220E-03	0.996E+00	0.054	1.27	1.81	0.86
16.0	21.0	0.102E-01	0.189E+05	0.270E-03	0.978E+00	0.038	1.30	1.14	0.96
20.0	21.0	0.102E-01	0.236E+05	0.580E-03	0.975E+00	0.052	2.11	1.68	1.40
24.0	21.0	0.102E-01	0.283E+05	0.110E-02	0.972E+00	0.068	3.08	2.60	1.93
26.0	20.0	0.104E-01	0.300E+05	0.135E-02	0.976E+00	0.071	3.44	2.83	2.14
28.0	20.0	0.104E-01	0.323E+05	0.167E-02	0.994E+00	0.076	3.87	3.24	2.38
30.0	20.0	0.104E-01	0.346E+05	0.180E-02	0.968E+00	0.071	3.99	2.83	2.47
30.0	20.0	0.104E-01	0.346E+05	0.158E-02	0.970E+00	0.063	3.68	2.25	2.32
28.0	20.0	0.104E-01	0.323E+05	0.151E-02	0.982E+00	0.069	3.64	2.65	2.27

TABLE 1 SUMMARY OF DATA FOR RUN U-4

VELOCITY (CM/S)	U*(3) (CM/S)	FR	SE	TAU DYNES/ CM**2)	U50(1) (CM/S)	U50(2) (CM/S)	U50(3) (CM/S)	U50(4) (CM/S)
24.0	2.17	0.05	0.138E-02	4.60	61.27	63.11	63.63	32.57
26.0	1.51	0.06	0.670E-03	2.23	41.33	43.97	44.33	22.10
28.0	2.12	0.07	0.132E-02	4.40	59.80	61.72	62.23	31.81
30.0	1.82	0.08	0.980E-03	3.27	50.85	53.18	53.62	27.14
30.0	2.41	0.08	0.171E-02	5.70	68.89	70.29	70.87	36.50
28.0	2.25	0.07	0.149E-02	4.97	63.92	65.62	66.16	33.94
26.0	2.33	0.06	0.160E-02	5.34	66.49	68.04	68.60	35.27
24.0	2.08	0.05	0.128E-02	4.26	58.76	60.73	61.23	31.27
20.0	1.39	0.03	0.570E-03	1.90	37.84	40.56	40.89	20.23
16.0	1.41	0.02	0.584E-03	1.95	38.34	41.05	41.39	20.50
12.0	0.0	0.0	0.0	0.0	0.0	0.0	0.0	0.0
-12.0	1.07	0.01	0.334E-03	1.11	28.25	31.05	31.30	15.03
-16.0	1.61	0.02	0.760E-03	2.53	44.27	46.83	47.22	23.67
-20.0	1.67	0.03	0.824E-03	2.75	46.27	48.76	49.17	24.72
-24.0	2.17	0.05	0.138E-02	4.61	61.32	63.15	63.67	32.60
-24.0	2.20	0.05	0.143E-02	4.75	62.37	64.15	64.68	33.14
-20.0	1.70	0.03	0.846E-03	2.82	46.94	49.41	49.82	25.08
-16.0	0.0	0.0	0.0	0.0	0.0	0.0	0.0	0.0
-12.0	1.19	0.01	0.420E-03	1.40	32.03	34.82	35.10	17.09
12.0	0.86	0.01	0.220E-03	0.73	22.48	25.20	25.40	11.83
16.0	0.96	0.02	0.270E-03	0.90	25.15	27.91	28.14	13.31
20.0	1.40	0.03	0.580E-03	1.93	38.20	40.91	41.25	20.43
24.0	1.93	0.05	0.110E-02	3.67	54.15	56.34	56.81	28.87
26.0	2.14	0.06	0.135E-02	4.50	60.54	62.42	62.93	32.19
28.0	2.38	0.07	0.167E-02	5.57	68.01	69.46	70.04	36.05
30.0	2.47	0.08	0.180E-02	5.99	70.75	72.03	72.63	37.45
30.0	2.32	0.08	0.158E-02	5.28	66.04	67.61	68.17	35.03
28.0	2.27	0.07	0.151E-02	5.05	64.44	66.10	66.64	34.21

TABLE 1 SUMMARY OF DATA FOR RUN U-3

DEPTH = 12 CM HYDRAULIC RADIUS = 4.54 CM SAND SIZE = 0.013 CM

VELOCITY (CM/S)	TEMP. (DEG. C)	VISCOSITY (STOKES)	REYNOLDS NUMBER	SURFACE SLOPE	R2	F	U*(1) (CM/S)	U*(2) (CM/S)	U*(3) (CM/S)
20.0	21.0	0.102E-01	0.236E+05	0.620E-03	0.983E+00	0.055	2.22	1.85	1.45
24.0	18.0	0.109E-01	0.263E+05	0.860E-03	0.100E+01	0.053	2.61	1.75	1.71
24.0	18.0	0.109E-01	0.263E+05	0.107E-02	0.962E+00	0.066	3.02	2.47	1.91
20.0	18.0	0.109E-01	0.219E+05	0.732E-03	0.981E+00	0.065	2.47	2.41	1.58
-12.0	19.0	0.107E-01	0.135E+05	0.326E-03	0.969E+00	0.081	1.96	3.71	1.05
-16.0	19.0	0.107E-01	0.180E+05	0.428E-03	0.974E+00	0.059	1.84	2.07	1.21
-20.0	19.0	0.107E-01	0.225E+05	0.460E-03	0.991E+00	0.041	1.78	1.26	1.25
-24.0	18.0	0.109E-01	0.263E+05	0.117E-02	0.989E+00	0.072	3.19	2.92	1.99
-24.0	18.0	0.109E-01	0.263E+05	0.137E-02	0.100E+01	0.085	3.53	4.20	2.16
-20.0	19.0	0.107E-01	0.225E+05	0.930E-03	0.989E+00	0.083	2.87	3.96	1.78
-16.0	19.0	0.107E-01	0.180E+05	0.800E-03	0.100E+01	0.111	3.07	13.11	1.65
-12.0	19.0	0.107E-01	0.135E+05	0.610E-03	0.996E+00	0.151	2.68	-12.54	1.44
12.0	21.0	0.102E-01	0.142E+05	0.258E-03	0.960E+00	0.064	1.74	2.32	0.94
16.0	20.0	0.104E-01	0.142E+05	0.258E-03	0.830E+00	0.0	0.0	0.0	0.0
20.0	20.0	0.104E-01	0.231E+05	0.240E-03	0.993E+00	0.021	0.92	0.67	0.90
24.0	20.0	0.104E-01	0.277E+05	0.978E-03	0.985E+00	0.060	2.85	2.13	1.82
24.0	20.0	0.104E-01	0.277E+05	0.690E-03	0.984E+00	0.043	2.23	1.32	1.53
20.0	20.0	0.104E-01	0.277E+05	0.690E-03	0.933E+00	0.0	0.0	0.0	0.0
16.0	20.0	0.104E-01	0.185E+05	0.438E-03	0.958E+00	0.061	1.87	2.15	1.22

TABLE 1 SUMMARY OF DATA FOR RUN U-3

VELOCITY (CM/S)	U*(3) (CM/S)	FR	SE	TAU DYNES/ CM**2)	U50(1) (CM/S)	U50(2) (CM/S)	U50(3) (CM/S)	U50(4) (CM/S)
20.0	1.45	0.03	0.620E-03	2.07	39.62	42.30	42.65	21.19
24.0	1.71	0.05	0.860E-03	2.86	47.36	49.82	50.23	25.30
24.0	1.91	0.05	0.107E-02	3.56	53.34	55.57	56.03	28.45
20.0	1.58	0.03	0.732E-03	2.44	43.37	45.96	46.34	23.19
-12.0	1.05	0.01	0.326E-03	1.09	27.88	30.67	30.92	14.82
-16.0	1.21	0.02	0.428E-03	1.43	32.36	35.14	35.43	17.27
-20.0	1.25	0.03	0.460E-03	1.53	33.66	36.43	36.73	17.98
-24.0	1.99	0.05	0.117E-02	3.90	56.00	58.11	58.58	29.83
-24.0	2.16	0.05	0.137E-02	4.56	61.03	62.88	63.40	32.44
-20.0	1.78	0.03	0.930E-03	3.10	49.42	51.81	52.23	26.39
-16.0	1.65	0.02	0.800E-03	2.67	45.53	48.05	48.44	24.33
-12.0	1.44	0.01	0.610E-03	2.03	39.27	41.96	42.30	21.00
12.0	0.94	0.01	0.258E-03	0.86	24.53	27.29	27.51	12.97
16.0	0.0	0.0	0.0	0.0	0.0	0.0	0.0	0.0
20.0	0.90	0.03	0.240E-03	0.80	23.58	26.32	26.54	12.44
24.0	1.82	0.05	0.978E-03	3.26	50.79	53.13	53.56	27.11
24.0	1.53	0.05	0.690E-03	2.30	42.00	44.62	44.99	22.46
20.0	0.0	0.0	0.0	0.0	0.0	0.0	0.0	0.0
16.0	1.22	0.02	0.438E-03	1.46	32.77	35.55	35.85	17.49

TABLE 2 SUMMARY OF DATA FOR RUN T-1

VELOCITY PROFILE

TIME (HR-MIN)	VELOCITY (CM/S)	TIME (HR-MIN)	VELOCITY (CM/S)
0.0	20.00	6.22	-22.00
0.07	22.00	6.28	-24.00
0.13	24.00	6.36	-26.00
0.21	26.00	6.45	-28.00
0.30	28.00	6.52	-30.00
0.37	30.00	7.02	-32.00
0.47	32.00	7.11	-34.00
0.56	34.00	7.22	-36.00
1.07	36.00	7.37	-38.00
1.22	38.00	8.04	-40.00
1.49	40.00	8.41	-38.00
2.26	38.00	9.07	-36.00
2.52	36.00	9.22	-34.00
3.07	34.00	9.34	-32.00
3.19	32.00	9.43	-30.00
3.28	30.00	9.52	-28.00
3.37	28.00	9.60	-26.00
3.45	26.00	10.09	-24.00
3.54	24.00	10.17	-22.00
4.02	22.00	10.22	-20.00
4.07	20.00	10.30	-18.00
4.15	18.00	10.37	-16.00
4.22	16.00	10.45	-14.00
4.30	14.00	10.51	-12.00
4.36	12.00	10.56	-10.00
4.41	10.00	11.04	-8.00
4.49	8.00	11.09	-6.00
4.54	6.00	11.15	-4.00
4.60	4.00	11.21	-2.00
5.06	2.00	11.26	0.0
5.11	0.0	11.34	2.00
5.19	-2.00	11.39	4.00
5.24	-4.00	11.45	6.00
5.30	-6.00	11.51	8.00
5.36	-8.00	11.56	10.00
5.41	-10.00	12.04	12.00
5.49	-12.00	12.09	14.00
5.54	-14.00	12.15	16.00
5.60	-16.00	12.22	18.00
6.07	-18.00	12.30	20.00
6.15	-20.00	0.0	22.00

TABLE 2 SUMMARY OF DATA FOR RUN T-2

VELOCITY PROFILE

TIME (HR-MIN)	VELOCITY (CM/S)	TIME (HR-MIN)	VELOCITY (CM/S)
0.0	20.00	6.22	-22.00
0.07	22.00	6.28	-24.00
0.13	24.00	6.36	-26.00
0.21	26.00	6.45	-28.00
0.30	28.00	6.52	-30.00
0.37	30.00	7.02	-32.00
0.47	32.00	7.11	-34.00
0.56	34.00	7.22	-36.00
1.07	36.00	7.37	-38.00
1.22	38.00	8.04	-40.00
1.49	40.00	8.41	-38.00
2.26	38.00	9.07	-36.00
2.52	36.00	9.22	-34.00
3.07	34.00	9.34	-32.00
3.19	32.00	9.43	-30.00
3.28	30.00	9.52	-28.00
3.37	28.00	9.60	-26.00
3.45	26.00	10.09	-24.00
3.54	24.00	10.17	-22.00
4.02	22.00	10.22	-20.00
4.07	20.00	10.30	-18.00
4.15	18.00	10.37	-16.00
4.22	16.00	10.45	-14.00
4.30	14.00	10.51	-12.00
4.36	12.00	10.56	-10.00
4.41	10.00	11.04	-8.00
4.49	8.00	11.09	-6.00
4.54	6.00	11.15	-4.00
4.60	4.00	11.21	-2.00
5.06	2.00	11.26	0.0
5.11	0.0	11.34	2.00
5.19	-2.00	11.39	4.00
5.24	-4.00	11.45	6.00
5.30	-6.00	11.51	8.00
5.36	-8.00	11.56	10.00
5.41	-10.00	12.04	12.00
5.49	-12.00	12.09	14.00
5.54	-14.00	12.15	16.00
5.60	-16.00	12.22	18.00
6.07	-18.00	12.30	20.00
6.15	-20.00	0.0	22.00

TABLE 2 SUMMARY OF DATA FOR RUN T-3

VELOCITY PROFILE

TIME (HR-MIN)	VELOCITY (CM/S)	TIME (HR-MIN)	VELOCITY (CM/S)
0.0	10.00	6.28	-12.00
0.13	12.00	6.43	-14.00
0.28	14.00	7.02	-16.00
0.47	16.00	7.22	-18.00
1.07	18.00	7.60	-20.00
1.45	20.00	8.52	-18.00
2.37	18.00	9.30	-16.00
3.15	16.00	9.51	-14.00
3.36	14.00	10.09	-12.00
3.54	12.00	10.24	-10.00
4.09	10.00	10.37	-8.00
4.22	8.00	10.51	-6.00
4.36	6.00	11.04	-4.00
4.49	4.00	11.17	-2.00
5.02	2.00	11.28	0.0
5.13	0.0	11.39	2.00
5.24	-2.00	11.51	4.00
5.36	-4.00	12.04	6.00
5.49	-6.00	12.17	8.00
6.02	-8.00	12.30	10.00
6.15	-10.00	0.0	12.00

TABLE 2 SUMMARY OF DATA FOR RUN T-4

VELOCITY PROFILE

TIME (HR-MIN)	VELOCITY (CM/S)	TIME (HR-MIN)	VELOCITY (CM/S)
0.0	20.00	4.32	-22.00
0.07	22.00	4.36	-24.00
0.13	24.00	4.41	-26.00
0.19	26.00	4.47	-28.00
0.26	28.00	4.53	-30.00
0.34	30.00	4.58	-32.00
0.41	32.00	5.04	-34.00
0.51	34.00	5.11	-36.00
0.60	36.00	5.21	-38.00
1.09	38.00	5.39	-40.00
1.30	40.00	6.08	-38.00
1.58	38.00	6.28	-36.00
2.17	36.00	6.38	-34.00
2.26	34.00	6.47	-32.00
2.34	32.00	6.56	-30.00
2.39	30.00	7.04	-28.00
2.45	28.00	7.11	-26.00
2.51	26.00	7.19	-24.00
2.56	24.00	7.24	-22.00
3.02	22.00	7.30	-20.00
3.06	20.00	7.38	-18.00
3.09	18.00	7.45	-16.00
3.13	16.00	7.53	-14.00
3.19	14.00	8.00	-12.00
3.24	12.00	8.08	-10.00
3.28	10.00	8.17	-8.00
3.32	8.00	8.28	-6.00
3.36	6.00	8.39	-4.00
3.39	4.00	8.54	-2.00
3.43	2.00	9.34	0.0
3.47	0.0	10.34	2.00
3.51	-2.00	11.13	4.00
3.54	-4.00	11.28	6.00
3.58	-6.00	11.39	8.00
4.02	-8.00	11.51	10.00
4.06	-10.00	12.00	12.00
4.09	-12.00	12.07	14.00
4.13	-14.00	12.15	16.00
4.19	-16.00	12.23	18.00
4.24	-18.00	12.30	20.00
4.28	-20.00	0.0	22.00

TABLE 2 SUMMARY OF DATA FOR RUN T-5

VELOCITY PROFILE

TIME (HR-MIN)	VELOCITY (CM/S)	TIME (HR-MIN)	VELOCITY (CM/S)
0.0	10.00	4.38	-12.00
0.13	12.00	4.47	-14.00
0.26	14.00	4.58	-16.00
0.41	16.00	5.11	-18.00
0.58	18.00	5.38	-20.00
1.28	20.00	6.17	-18.00
2.07	18.00	6.47	-16.00
2.34	16.00	7.04	-14.00
2.47	14.00	7.19	-12.00
2.58	12.00	7.32	-10.00
3.07	10.00	7.45	-8.00
3.15	8.00	8.00	-6.00
3.24	6.00	8.17	-4.00
3.34	4.00	8.38	-2.00
3.41	2.00	9.28	0.0
3.49	0.0	10.47	2.00
3.56	-2.00	11.38	4.00
4.04	-4.00	11.58	6.00
4.11	-6.00	12.15	8.00
4.21	-8.00	12.30	10.00
4.30	-10.00	0.0	12.00

TABLE 2 SUMMARY OF DATA FOR RUN T-6

VELOCITY PROFILE

TIME (HR-MIN)	VELOCITY (CM/S)	TIME (HR-MIN)	VELOCITY (CM/S)
0.0	20.00	4.13	-12.00
0.11	22.00	4.23	-14.00
0.21	24.00	4.34	-16.00
0.30	26.00	4.47	-18.00
0.43	28.00	5.13	-20.00
1.07	30.00	5.53	-18.00
1.39	28.00	6.23	-16.00
1.60	26.00	6.39	-14.00
2.11	24.00	6.54	-12.00
2.21	22.00	7.08	-10.00
2.28	20.00	7.21	-8.00
2.36	18.00	7.36	-6.00
2.41	16.00	7.53	-4.00
2.47	14.00	8.13	-2.00
2.52	12.00	9.04	0.0
2.58	10.00	10.17	2.00
3.04	8.00	11.00	4.00
3.09	6.00	11.17	6.00
3.15	4.00	11.30	8.00
3.21	2.00	11.41	10.00
3.26	0.0	11.53	12.00
3.32	-2.00	12.04	14.00
3.39	-4.00	12.13	16.00
3.47	-6.00	12.21	18.00
3.56	-8.00	12.30	20.00
4.06	-10.00	0.0	22.00

TABLE 2 SUMMARY OF DATA FOR RUN T-7

VELOCITY PROFILE

TIME (HR-MIN)	VELOCITY (CM/S)	TIME (HR-MIN)	VELOCITY (CM/S)
0.0	20.00	4.13	-12.00
0.11	22.00	4.23	-14.00
0.21	24.00	4.34	-16.00
0.30	26.00	4.47	-18.00
0.43	28.00	5.13	-20.00
1.07	30.00	5.53	-18.00
1.39	28.00	6.23	-16.00
1.60	26.00	6.39	-14.00
2.11	24.00	6.54	-12.00
2.21	22.00	7.08	-10.00
2.28	20.00	7.21	-8.00
2.36	18.00	7.36	-6.00
2.41	16.00	7.53	-4.00
2.47	14.00	8.13	-2.00
2.52	12.00	9.04	0.0
2.58	10.00	10.17	2.00
3.04	8.00	11.00	4.00
3.09	6.00	11.17	6.00
3.15	4.00	11.30	8.00
3.21	2.00	11.41	10.00
3.26	0.0	11.53	12.00
3.32	-2.00	12.04	14.00
3.39	-4.00	12.13	16.00
3.47	-6.00	12.21	18.00
3.56	-8.00	12.30	20.00
4.06	-10.00	0.0	22.00

TABLE 2 SUMMARY OF DATA FOR RUN T-8

VELOCITY PROFILE

TIME (HR-MIN)	VELOCITY (CM/S)	TIME (HR-MIN)	VELOCITY (CM/S)
0.0	20.00	4.13	-12.00
0.11	22.00	4.23	-14.00
0.21	24.00	4.34	-16.00
0.30	26.00	4.47	-18.00
0.43	28.00	5.13	-20.00
1.07	30.00	5.53	-18.00
1.39	28.00	6.23	-16.00
1.60	26.00	6.39	-14.00
2.11	24.00	6.54	-12.00
2.21	22.00	7.08	-10.00
2.28	20.00	7.21	-8.00
2.36	18.00	7.36	-6.00
2.41	16.00	7.53	-4.00
2.47	14.00	8.13	-2.00
2.52	12.00	9.04	0.0
2.58	10.00	10.17	2.00
3.04	8.00	11.00	4.00
3.09	6.00	11.17	6.00
3.15	4.00	11.30	8.00
3.21	2.00	11.41	10.00
3.26	0.0	11.53	12.00
3.32	-2.00	12.04	14.00
3.39	-4.00	12.13	16.00
3.47	-6.00	12.21	18.00
3.56	-8.00	12.30	20.00
4.06	-10.00	0.0	22.00

TABLE 2 SUMMARY OF DATA FOR RUN T-9

VELOCITY PROFILE

TIME (HR-MIN)	VELOCITY (CM/S)	TIME (HR-MIN)	VELOCITY (CM/S)
0.0	20.00	4.13	-12.00
0.11	22.00	4.23	-14.00
0.21	24.00	4.34	-16.00
0.30	26.00	4.47	-18.00
0.43	28.00	5.13	-20.00
1.07	30.00	5.53	-18.00
1.39	28.00	6.23	-16.00
1.60	26.00	6.39	-14.00
2.11	24.00	6.54	-12.00
2.21	22.00	7.08	-10.00
2.28	20.00	7.21	-8.00
2.36	18.00	7.36	-6.00
2.41	16.00	7.53	-4.00
2.47	14.00	8.13	-2.00
2.52	12.00	9.04	0.0
2.58	10.00	10.17	2.00
3.04	8.00	11.00	4.00
3.09	6.00	11.17	6.00
3.15	4.00	11.30	8.00
3.21	2.00	11.41	10.00
3.26	0.0	11.53	12.00
3.32	-2.00	12.04	14.00
3.39	-4.00	12.13	16.00
3.47	-6.00	12.21	18.00
3.56	-8.00	12.30	20.00
4.06	-10.00	0.0	22.00

TABLE 2 SUMMARY OF DATA FOR RUN T-10

VELOCITY PROFILE

TIME (HR-MIN)	VELOCITY (CM/S)	TIME (HR-MIN)	VELOCITY (CM/S)
0.0	20.00	4.13	-12.00
0.11	22.00	4.23	-14.00
0.21	24.00	4.34	-16.00
0.30	26.00	4.47	-18.00
0.43	28.00	5.13	-20.00
1.07	30.00	5.53	-18.00
1.39	28.00	6.23	-16.00
1.60	26.00	6.39	-14.00
2.11	24.00	6.54	-12.00
2.21	22.00	7.08	-10.00
2.28	20.00	7.21	-8.00
2.36	18.00	7.36	-6.00
2.41	16.00	7.53	-4.00
2.47	14.00	8.13	-2.00
2.52	12.00	9.04	0.0
2.58	10.00	10.17	2.00
3.04	8.00	11.00	4.00
3.09	6.00	11.17	6.00
3.15	4.00	11.30	8.00
3.21	2.00	11.41	10.00
3.26	0.0	11.53	12.00
3.32	-2.00	12.04	14.00
3.39	-4.00	12.13	16.00
3.47	-6.00	12.21	18.00
3.56	-8.00	12.30	20.00
4.06	-10.00	0.0	22.00

TABLE 2 SUMMARY OF DATA FOR RUN U-1

VELOCITY PROFILE

TIME (HR-MIN)	VELOCITY (CM/S)	TIME (HR-MIN)	VELOCITY (CM/S)
0.0	20.00	4.13	-12.00
0.11	22.00	4.23	-14.00
0.21	24.00	4.34	-16.00
0.30	26.00	4.47	-18.00
0.43	28.00	5.13	-20.00
1.07	30.00	5.53	-18.00
1.39	28.00	6.23	-16.00
1.60	26.00	6.39	-14.00
2.11	24.00	6.54	-12.00
2.21	22.00	7.08	-10.00
2.28	20.00	7.21	-8.00
2.36	18.00	7.36	-6.00
2.41	16.00	7.53	-4.00
2.47	14.00	8.13	-2.00
2.52	12.00	9.04	0.0
2.58	10.00	10.17	2.00
3.04	8.00	11.00	4.00
3.09	6.00	11.17	6.00
3.15	4.00	11.30	8.00
3.21	2.00	11.41	10.00
3.26	0.0	11.53	12.00
3.32	-2.00	12.04	14.00
3.39	-4.00	12.13	16.00
3.47	-6.00	12.21	18.00
3.56	-8.00	12.30	20.00
4.06	-10.00	0.0	22.00

TABLE 2 SUMMARY OF DATA FOR RUN U-2

VELOCITY PROFILE

TIME (HR-MIN)	VELOCITY (CM/S)	TIME (HR-MIN)	VELOCITY (CM/S)
0.0	24.00	4.21	-20.00
0.09	26.00	4.32	-22.00
0.22	28.00	4.54	-24.00
0.47	30.00	5.30	-22.00
1.19	28.00	5.56	-20.00
1.39	26.00	6.11	-18.00
1.51	24.00	6.24	-16.00
1.60	22.00	6.36	-14.00
2.07	20.00	6.47	-12.00
2.15	18.00	6.58	-10.00
2.21	16.00	7.11	-8.00
2.26	14.00	7.24	-6.00
2.32	12.00	7.39	-4.00
2.37	10.00	7.58	-2.00
2.43	8.00	8.45	0.0
2.49	6.00	9.56	2.00
2.54	4.00	10.39	4.00
2.60	2.00	10.56	6.00
3.06	0.0	11.09	8.00
3.11	-2.00	11.21	10.00
3.17	-4.00	11.32	12.00
3.23	-6.00	11.43	14.00
3.30	-8.00	11.53	16.00
3.38	-10.00	12.00	18.00
3.45	-12.00	12.09	20.00
3.53	-14.00	12.21	22.00
4.00	-16.00	12.30	24.00
4.09	-18.00	0.0	26.00

TABLE 2 SUMMARY OF DATA FOR RUN U-3

VELOCITY PROFILE

TIME (HR-MIN)	VELOCITY (CM/S)	TIME (HR-MIN)	VELOCITY (CM/S)
0.0	20.00	4.28	-22.00
0.15	22.00	4.51	-24.00
0.41	24.00	5.26	-22.00
1.17	22.00	5.53	-20.00
1.39	20.00	6.08	-18.00
1.51	18.00	6.21	-16.00
2.02	16.00	6.32	-14.00
2.11	14.00	6.43	-12.00
2.19	12.00	6.54	-10.00
2.26	10.00	7.08	-8.00
2.34	8.00	7.21	-6.00
2.41	6.00	7.36	-4.00
2.49	4.00	7.54	-2.00
2.54	2.00	8.41	0.0
3.00	0.0	9.56	2.00
3.08	-2.00	10.43	4.00
3.13	-4.00	11.02	6.00
3.19	-6.00	11.17	8.00
3.26	-8.00	11.30	10.00
3.34	-10.00	11.43	12.00
3.41	-12.00	11.54	14.00
3.49	-14.00	12.06	16.00
3.56	-16.00	12.17	18.00
4.06	-18.00	12.30	20.00
4.17	-20.00	0.0	22.00

TABLE 2 SUMMARY OF DATA FOR RUN U-4

VELOCITY PROFILE

TIME (HR-MIN)	VELOCITY (CM/S)	TIME (HR-MIN)	VELOCITY (CM/S)
0.0	24.00	4.21	-20.00
0.09	26.00	4.32	-22.00
0.22	28.00	4.54	-24.00
0.47	30.00	5.30	-22.00
1.19	28.00	5.56	-20.00
1.39	26.00	6.11	-18.00
1.51	24.00	6.24	-16.00
1.60	22.00	6.36	-14.00
2.07	20.00	6.47	-12.00
2.15	18.00	6.58	-10.00
2.21	16.00	7.11	-8.00
2.26	14.00	7.24	-6.00
2.32	12.00	7.39	-4.00
2.37	10.00	7.58	-2.00
2.43	8.00	8.45	0.0
2.49	6.00	9.56	2.00
2.54	4.00	10.39	4.00
2.60	2.00	10.56	6.00
3.06	0.0	11.09	8.00
3.11	-2.00	11.21	10.00
3.17	-4.00	11.32	12.00
3.23	-6.00	11.43	14.00
3.30	-8.00	11.53	16.00
3.38	-10.00	12.00	18.00
3.45	-12.00	12.09	20.00
3.53	-14.00	12.21	22.00
4.00	-16.00	12.30	24.00
4.09	-18.00	0.0	26.00

TABLE 2 SUMMARY OF DATA FOR RUN U-5

VELOCITY PROFILE

TIME (HR-MIN)	VELOCITY (CM/S)	TIME (HR-MIN)	VELOCITY (CM/S)
0.0	20.00	4.13	-12.00
0.11	22.00	4.23	-14.00
0.21	24.00	4.34	-16.00
0.30	26.00	4.47	-18.00
0.43	28.00	5.13	-20.00
1.07	30.00	5.53	-18.00
1.39	28.00	6.23	-16.00
1.60	26.00	6.39	-14.00
2.11	24.00	6.54	-12.00
2.21	22.00	7.08	-10.00
2.28	20.00	7.21	-8.00
2.36	18.00	7.36	-6.00
2.41	16.00	7.53	-4.00
2.47	14.00	8.13	-2.00
2.52	12.00	9.04	0.0
2.58	10.00	10.17	2.00
3.04	8.00	11.00	4.00
3.09	6.00	11.17	6.00
3.15	4.00	11.30	8.00
3.21	2.00	11.41	10.00
3.26	0.0	11.53	12.00
3.32	-2.00	12.04	14.00
3.39	-4.00	12.13	16.00
3.47	-6.00	12.21	18.00
3.56	-8.00	12.30	20.00
4.06	-10.00	0.0	22.00

TABLE 2 SUMMARY OF DATA FOR RUN U-6

VELOCITY PROFILE

TIME (HR-MIN)	VELOCITY (CM/S)	TIME (HR-MIN)	VELOCITY (CM/S)
0.0	20.00	4.28	-22.00
0.15	22.00	4.51	-24.00
0.41	24.00	5.26	-22.00
1.17	22.00	5.53	-20.00
1.39	20.00	6.08	-18.00
1.51	18.00	6.21	-16.00
2.02	16.00	6.32	-14.00
2.11	14.00	6.43	-12.00
2.19	12.00	6.54	-10.00
2.26	10.00	7.08	-8.00
2.34	8.00	7.21	-6.00
2.41	6.00	7.36	-4.00
2.49	4.00	7.54	-2.00
2.54	2.00	8.41	0.0
3.00	0.0	9.56	2.00
3.08	-2.00	10.43	4.00
3.13	-4.00	11.02	6.00
3.19	-6.00	11.17	8.00
3.26	-8.00	11.30	10.00
3.34	-10.00	11.43	12.00
3.41	-12.00	11.54	14.00
3.49	-14.00	12.06	16.00
3.56	-16.00	12.17	18.00
4.06	-18.00	12.30	20.00
4.17	-20.00	0.0	22.00

TABLE 2 SUMMARY OF DATA FOR RUN U-7

VELOCITY PROFILE

TIME (HR-MIN)	VELOCITY (CM/S)	TIME (HR-MIN)	VELOCITY (CM/S)
0.0	20.00	4.13	-12.00
0.11	22.00	4.23	-14.00
0.21	24.00	4.34	-16.00
0.30	26.00	4.47	-18.00
0.43	28.00	5.13	-20.00
1.07	30.00	5.53	-18.00
1.39	28.00	6.23	-16.00
1.60	26.00	6.39	-14.00
2.11	24.00	6.54	-12.00
2.21	22.00	7.08	-10.00
2.28	20.00	7.21	-8.00
2.36	18.00	7.36	-6.00
2.41	16.00	7.53	-4.00
2.47	14.00	8.13	-2.00
2.52	12.00	9.04	0.0
2.58	10.00	10.17	2.00
3.04	8.00	11.00	4.00
3.09	6.00	11.17	6.00
3.15	4.00	11.30	8.00
3.21	2.00	11.41	10.00
3.26	0.0	11.53	12.00
3.32	-2.00	12.04	14.00
3.39	-4.00	12.13	16.00
3.47	-6.00	12.21	18.00
3.56	-8.00	12.30	20.00
4.06	-10.00	0.0	22.00

TABLE 2 SUMMARY OF DATA FOR RUN U-8

VELOCITY PROFILE

TIME (HR-MIN)	VELOCITY (CM/S)	TIME (HR-MIN)	VELOCITY (CM/S)
0.0	24.00	4.21	-20.00
0.09	26.00	4.32	-22.00
0.22	28.00	4.54	-24.00
0.47	30.00	5.30	-22.00
1.19	28.00	5.56	-20.00
1.39	26.00	6.11	-18.00
1.51	24.00	6.24	-16.00
1.60	22.00	6.36	-14.00
2.07	20.00	6.47	-12.00
2.15	18.00	6.58	-10.00
2.21	16.00	7.11	-8.00
2.26	14.00	7.24	-6.00
2.32	12.00	7.39	-4.00
2.37	10.00	7.58	-2.00
2.43	8.00	8.45	0.0
2.49	6.00	9.56	2.00
2.54	4.00	10.39	4.00
2.60	2.00	10.56	6.00
3.06	0.0	11.09	8.00
3.11	-2.00	11.21	10.00
3.17	-4.00	11.32	12.00
3.23	-6.00	11.43	14.00
3.30	-8.00	11.53	16.00
3.38	-10.00	12.00	18.00
3.45	-12.00	12.09	20.00
3.53	-14.00	12.21	22.00
4.00	-16.00	12.30	24.00
4.09	-18.00	0.0	26.00

TABLE 2 SUMMARY OF DATA FOR RUN V-1

VELOCITY PROFILE

TIME (HR-MIN)	VELOCITY (CM/S)	TIME (HR-MIN)	VELOCITY (CM/S)
0.0	20.00	4.28	-22.00
0.15	22.00	4.51	-24.00
0.41	24.00	5.26	-22.00
1.17	22.00	5.53	-20.00
1.39	20.00	6.08	-18.00
1.51	18.00	6.21	-16.00
2.02	16.00	6.32	-14.00
2.11	14.00	6.43	-12.00
2.19	12.00	6.54	-10.00
2.26	10.00	7.08	-8.00
2.34	8.00	7.21	-6.00
2.41	6.00	7.36	-4.00
2.49	4.00	7.54	-2.00
2.54	2.00	8.41	0.0
3.00	0.0	9.56	2.00
3.08	-2.00	10.43	4.00
3.13	-4.00	11.02	6.00
3.19	-6.00	11.17	8.00
3.26	-8.00	11.30	10.00
3.34	-10.00	11.43	12.00
3.41	-12.00	11.54	14.00
3.49	-14.00	12.06	16.00
3.56	-16.00	12.17	18.00
4.06	-18.00	12.30	20.00
4.17	-20.00	0.0	22.00

TABLE 3 SUMMARY OF DATA FOR RUN T-1

TOTAL SEDIMENT ADDED = 100 G
0 G ILLITE
0 G KAOLINITE
100 G MONTMORILLIONITE

SUSPENDED SEDIMENT CONCENTRATION

TIME (HR-MIN)	MUD (G/L)	SAND (G/L)	TOTAL (G/L)
0.0	0.120	0.031	0.151
1.000	0.370	0.046	0.416
2.000	0.340	0.140	0.480
3.000	0.410	0.162	0.572
4.000	0.300	0.028	0.328
5.000	0.220	0.011	0.231
6.000	0.210	0.011	0.221
7.000	0.340	0.048	0.388
8.000	0.430	0.374	0.804
9.000	0.450	0.214	0.664
10.000	0.300	0.034	0.334
11.000	0.170	0.007	0.177
12.000	0.250	0.014	0.264
13.000	0.280	0.043	0.323

TABLE 3 SUMMARY OF DATA FOR RUN T-2

TOTAL SEDIMENT ADDED = 200 G
0 G ILLITE
0 G KAOLINITE
200 G MONTMORILLIONITE

SUSPENDED SEDIMENT CONCENTRATION

TIME (HR-MIN)	MUD (G/L)	SAND (G/L)	TOTAL (G/L)
0.0	0.420	0.010	0.430
1.000	0.430	0.043	0.473
2.000	0.550	0.113	0.663
3.000	0.480	0.081	0.561
4.000	0.480	0.016	0.496
5.000	0.390	0.011	0.401
6.000	0.580	0.014	0.594
7.000	0.790	0.027	0.817
8.000	0.940	0.110	1.050
9.000	0.940	0.125	1.065
10.000	0.900	0.024	0.924
11.000	1.050	0.016	1.066

TABLE 3 SUMMARY OF DATA FOR RUN T-3

TOTAL SEDIMENT ADDED = 400 G
0 G ILLITE
0 G KAOLINITE
400 G MONTMORILLIONITE

SUSPENDED SEDIMENT CONCENTRATION

TIME (HR-MIN)	MUD (G/L)	SAND (G/L)	TOTAL (G/L)
0.0	1.230	0.0	1.230
1.000	1.140	0.0	1.140
2.000	0.540	0.0	0.540
3.000	1.220	0.0	1.220
4.000	1.290	0.0	1.290
5.000	1.210	0.0	1.210
6.000	1.020	0.0	1.020
7.000	1.070	0.0	1.070
8.000	0.980	0.0	0.980
9.000	0.940	0.0	0.940
10.000	0.860	0.0	0.860
11.000	0.940	0.0	0.940
12.000	1.060	0.0	1.060
13.000	1.070	0.0	1.070

TABLE 3 SUMMARY OF DATA FOR RUN T-4

TOTAL SEDIMENT ADDED = 400 G
0 G ILLITE
0 G KAOLINITE
400 G MONTMORILLIONITE

SUSPENDED SEDIMENT CONCENTRATION

TIME (HR-MIN)	MUD (G/L)	SAND (G/L)	TOTAL (G/L)
0.0	0.102	0.007	0.109
1.000	0.120	0.029	0.149
2.000	0.121	0.053	0.174
3.000	0.122	0.021	0.143
4.000	0.098	0.005	0.103
5.000	0.114	0.050	0.164
6.000	0.114	0.442	0.556
7.000	0.106	0.052	0.158
8.000	0.108	0.023	0.131
9.000	0.094	0.016	0.110
10.000	0.004	0.014	0.018
11.000	0.0	0.018	0.018
12.000	0.095	0.012	0.107
13.000	0.106	0.022	0.128

TABLE 3 SUMMARY OF DATA FOR RUN T-5

TOTAL SEDIMENT ADDED = 400 G
0 G ILLITE
0 G KAOLINITE
400 G MONTMORILLIONITE

SUSPENDED SEDIMENT CONCENTRATION

TIME (HR-MIN)	MUD (G/L)	SAND (G/L)	TOTAL (G/L)
0.0	1.080	0.0	1.080
1.000	1.230	0.0	1.230
2.000	1.210	0.0	1.210
3.000	0.720	0.0	0.720
4.000	1.040	0.0	1.040
5.000	1.170	0.0	1.170
6.000	1.040	0.0	1.040
7.000	1.070	0.0	1.070
8.000	1.010	0.0	1.010
9.000	0.830	0.0	0.830
10.000	0.200	0.0	0.200
11.000	0.060	0.0	0.060
12.000	1.010	0.0	1.010
13.000	0.990	0.0	0.990
14.000	1.000	0.0	1.000

TABLE 3 SUMMARY OF DATA FOR RUN T-6

TOTAL SEDIMENT ADDED = 400 G
0 G ILLITE
0 G KAOLINITE
400 G MONTMORILLIONITE

SUSPENDED SEDIMENT CONCENTRATION

TIME (HR-MIN)	MUD (G/L)	SAND (G/L)	TOTAL (G/L)
0.0	1.240	0.0	1.240
1.000	1.220	0.0	1.220
2.000	1.280	0.0	1.280
3.000	1.150	0.0	1.150
4.000	1.080	0.0	1.080
5.000	1.140	0.0	1.140
6.000	1.140	0.0	1.140
7.000	0.970	0.0	0.970
8.000	0.850	0.0	0.850
9.000	0.510	0.0	0.510
10.000	0.020	0.0	0.020
11.000	0.260	0.0	0.260
12.000	1.010	0.0	1.010
13.000	1.010	0.0	1.010
14.000	0.770	0.0	0.770

TABLE 3 SUMMARY OF DATA FOR RUN T-7

TOTAL SEDIMENT ADDED = 400 G
0 G ILLITE
400 G KAOLINITE
0 G MONTMORILLIONITE

SUSPENDED SEDIMENT CONCENTRATION

TIME (HR-MIN)	MUD (G/L)	SAND (G/L)	TOTAL (G/L)
0.0	1.330	0.0	1.330
1.000	1.330	0.0	1.330
2.000	1.470	0.0	1.470
3.000	1.250	0.0	1.250
4.000	1.250	0.0	1.250
5.000	1.240	0.0	1.240
6.000	1.150	0.0	1.150
7.000	1.110	0.0	1.110
8.000	1.120	0.0	1.120
9.000	1.050	0.0	1.050
10.000	0.130	0.0	0.130
11.000	0.380	0.0	0.380
12.000	0.630	0.0	0.630

TABLE 3 SUMMARY OF DATA FOR RUN T-8

TOTAL SEDIMENT ADDED = 100 G
40 G ILLITE
40 G KAOLINITE
20 G MONTMORILLIONITE

SUSPENDED SEDIMENT CONCENTRATION

TIME (HR-MIN)	MUD (G/L)	SAND (G/L)	TOTAL (G/L)
0.0	0.510	0.0	0.510
1.000	0.520	0.0	0.520
2.000	0.570	0.0	0.570
3.000	0.490	0.0	0.490
3.500	0.390	0.0	0.390
4.000	0.470	0.0	0.470
5.000	0.470	0.0	0.470
6.000	0.520	0.0	0.520
7.000	0.510	0.0	0.510
8.000	0.380	0.0	0.380
9.000	0.310	0.0	0.310
10.000	0.100	0.0	0.100
11.000	0.150	0.0	0.150
12.000	0.390	0.0	0.390
13.000	0.480	0.0	0.480
14.000	0.590	0.0	0.590

TABLE 3 SUMMARY OF DATA FOR RUN T-9

TOTAL SEDIMENT ADDED = 1800 G
200 G ILLITE
1200 G KAOLINITE
400 G MONTMORILLIONITE

SUSPENDED SEDIMENT CONCENTRATION

TIME (HR-MIN)	MUD (G/L)	SAND (G/L)	TOTAL (G/L)
0.0	4.000	0.0	4.000
1.000	4.060	0.0	4.060
2.000	4.640	0.0	4.640
3.000	3.900	0.0	3.900
3.500	2.800	0.0	2.800
4.000	3.280	0.0	3.280
5.000	3.600	0.0	3.600
6.000	3.620	0.0	3.620
7.000	3.380	0.0	3.380
8.000	3.040	0.0	3.040
9.000	2.280	0.0	2.280
10.000	0.120	0.0	0.120
10.500	0.0	0.0	0.0
11.000	1.040	0.0	1.040
12.000	1.540	0.0	1.540
13.000	2.820	0.0	2.820
14.000	3.560	0.0	3.560
14.150	3.690	0.0	3.690

TABLE 3 SUMMARY OF DATA FOR RUN T-10

TOTAL SEDIMENT ADDED = 400 G
400 G ILLITE
0 G KAOLINITE
0 G MONTMORILLIONITE

SUSPENDED SEDIMENT CONCENTRATION

TIME (HR-MIN)	MUD (G/L)	SAND (G/L)	TOTAL (G/L)
0.0	1.370	0.0	1.370
1.000	1.270	0.0	1.270
2.000	1.450	0.0	1.450
3.000	1.360	0.0	1.360
3.500	0.250	0.0	0.250
4.000	1.270	0.0	1.270
5.000	1.090	0.0	1.090
6.000	1.200	0.0	1.200
7.000	1.190	0.0	1.190
8.000	1.310	0.0	1.310
9.000	0.970	0.0	0.970
10.000	0.0	0.0	0.0
11.000	0.080	0.0	0.080
12.000	1.040	0.0	1.040
13.000	1.460	0.0	1.460
14.000	1.530	0.0	1.530

TABLE 3 SUMMARY OF DATA FOR RUN U-1

TOTAL SEDIMENT ADDED = 3000 G
0 G ILLITE
1500 G KAOLINITE
1500 G MONTMORILLIONITE

SUSPENDED SEDIMENT CONCENTRATION

TIME (HR-MIN)	MUD (G/L)	SAND (G/L)	TOTAL (G/L)
0.0	0.0	0.0	0.0
1.000	11.200	0.0	11.200
2.000	11.200	0.0	11.200
3.000	9.650	0.0	9.650
4.000	5.950	0.0	5.950
5.000	6.300	0.0	6.300
6.000	5.050	0.0	5.050
7.000	4.350	0.0	4.350
8.000	2.750	0.0	2.750
9.000	0.400	0.0	0.400
10.000	0.100	0.0	0.100
11.000	4.900	0.0	4.900
12.000	6.100	0.0	6.100
13.000	5.850	0.0	5.850
14.000	7.700	0.0	7.700

TABLE 3 SUMMARY OF DATA FOR RUN U-2

TOTAL SEDIMENT ADDED = 1000 G
0 G ILLITE
500 G KAOLINITE
500 G MONTMORILLIONITE

SUSPENDED SEDIMENT CONCENTRATION

TIME (HR-MIN)	MUD (G/L)	SAND (G/L)	TOTAL (G/L)
0.0	3.540	0.0	3.540
0.500	3.460	0.0	3.460
1.000	3.540	0.0	3.540
1.500	3.700	0.0	3.700
2.000	3.640	0.0	3.640
2.500	3.140	0.0	3.140
3.000	0.280	0.0	0.280
3.500	0.280	0.0	0.280
4.000	1.280	0.0	1.280
4.500	1.660	0.0	1.660
5.000	1.840	0.0	1.840
5.500	1.620	0.0	1.620
6.000	1.240	0.0	1.240
6.500	1.120	0.0	1.120
7.000	0.880	0.0	0.880
7.500	0.540	0.0	0.540
8.000	0.460	0.0	0.460
8.500	0.200	0.0	0.200
9.000	0.060	0.0	0.060
9.500	0.0	0.0	0.0
10.000	0.320	0.0	0.320
10.500	0.240	0.0	0.240
11.000	0.340	0.0	0.340
11.500	0.580	0.0	0.580
12.000	1.400	0.0	1.400
12.500	2.120	0.0	2.120
13.000	2.820	0.0	2.820

TABLE 3 SUMMARY OF DATA FOR RUN U-3

TOTAL SEDIMENT ADDED = 1000 G
0 G ILLITE
500 G KAOLINITE
500 G MONTMORILLIONITE

SUSPENDED SEDIMENT CONCENTRATION

TIME (HR-MIN)	MUD (G/L)	SAND (G/L)	TOTAL (G/L)
0.0	4.200	0.0	4.200
0.500	4.040	0.0	4.040
1.000	4.040	0.0	4.040
1.500	3.900	0.0	3.900
2.000	3.800	0.0	3.800
2.500	3.600	0.0	3.600
3.000	2.080	0.0	2.080
3.500	0.160	0.0	0.160
4.000	0.600	0.0	0.600
4.500	1.100	0.0	1.100
5.000	1.600	0.0	1.600
5.500	1.860	0.0	1.860
6.000	1.760	0.0	1.760
6.500	1.440	0.0	1.440
7.000	1.200	0.0	1.200
7.500	0.980	0.0	0.980
8.000	0.700	0.0	0.700
8.500	0.460	0.0	0.460
9.000	0.300	0.0	0.300
9.500	0.140	0.0	0.140
10.000	0.080	0.0	0.080
10.500	0.460	0.0	0.460
11.000	0.480	0.0	0.480
11.500	0.440	0.0	0.440
12.000	0.560	0.0	0.560
12.500	0.940	0.0	0.940
13.000	1.920	0.0	1.920
13.500	2.520	0.0	2.520
14.000	2.720	0.0	2.720

TABLE 3 SUMMARY OF DATA FOR RUN U-4

TOTAL SEDIMENT ADDED = 1000 G
0 G ILLITE
500 G KAOLINITE
500 G MONTMORILLIONITE

SUSPENDED SEDIMENT CONCENTRATION

TIME (HR-MIN)	MUD (G/L)	SAND (G/L)	TOTAL (G/L)
0.0	3.940	0.0	3.940
0.500	3.980	0.0	3.980
1.000	4.040	0.0	4.040
1.500	4.100	0.0	4.100
2.000	3.800	0.0	3.800
2.500	3.480	0.0	3.480
3.000	2.340	0.0	2.340
3.160	0.400	0.0	0.400
3.500	0.540	0.0	0.540
4.000	1.340	0.0	1.340
4.500	1.740	0.0	1.740
5.000	2.000	0.0	2.000
5.500	1.860	0.0	1.860
6.000	1.540	0.0	1.540
6.500	1.300	0.0	1.300
7.000	1.100	0.0	1.100
7.500	0.700	0.0	0.700
8.000	0.400	0.0	0.400
8.500	0.240	0.0	0.240
9.000	0.140	0.0	0.140
9.500	0.060	0.0	0.060
10.000	0.280	0.0	0.280
10.500	0.220	0.0	0.220
11.000	0.200	0.0	0.200
11.500	0.300	0.0	0.300
12.000	0.820	0.0	0.820
12.500	2.160	0.0	2.160
13.000	2.860	0.0	2.860
13.500	3.500	0.0	3.500
14.000	3.600	0.0	3.600

TABLE 3 SUMMARY OF DATA FOR RUN U-5

TOTAL SEDIMENT ADDED = 1000 G
0 G ILLITE
500 G KAOLINITE
500 G MONTMORILLIONITE

SUSPENDED SEDIMENT CONCENTRATION

TIME (HR-MIN)	MUD (G/L)	SAND (G/L)	TOTAL (G/L)
0.0	2.560	0.0	2.560
0.500	2.360	0.0	2.360
1.000	2.300	0.0	2.300
1.500	2.420	0.0	2.420
2.000	2.340	0.0	2.340
2.500	2.260	0.0	2.260
3.000	1.980	0.0	1.980
3.500	0.260	0.0	0.260
4.000	0.440	0.0	0.440
4.500	0.720	0.0	0.720
5.000	1.380	0.0	1.380
5.500	1.180	0.0	1.180
6.000	0.980	0.0	0.980
6.500	0.840	0.0	0.840
7.000	0.740	0.0	0.740
7.500	0.540	0.0	0.540
8.000	0.480	0.0	0.480
8.500	0.400	0.0	0.400
9.000	0.340	0.0	0.340
9.500	0.160	0.0	0.160
10.000	0.040	0.0	0.040
10.500	0.200	0.0	0.200
11.000	0.280	0.0	0.280
11.500	0.300	0.0	0.300
12.000	0.480	0.0	0.480
12.500	0.900	0.0	0.900
13.000	1.380	0.0	1.380
13.500	1.720	0.0	1.720
14.000	1.880	0.0	1.880
14.500	1.880	0.0	1.880

TABLE 3 SUMMARY OF DATA FOR RUN U-6

TOTAL SEDIMENT ADDED = 1000 G
0 G ILLITE
500 G KAOLINITE
500 G MONTMORILLIONITE

SUSPENDED SEDIMENT CONCENTRATION

TIME (HR-MIN)	MUD (G/L)	SAND (G/L)	TOTAL (G/L)
0.0	2.860	0.0	2.860
0.500	2.680	0.0	2.680
1.000	2.680	0.0	2.680
1.500	2.460	0.0	2.460
2.000	2.460	0.0	2.460
2.500	2.240	0.0	2.240
3.000	0.660	0.0	0.660
3.500	0.340	0.0	0.340
4.000	0.700	0.0	0.700
4.500	0.920	0.0	0.920
5.000	1.280	0.0	1.280
5.500	1.260	0.0	1.260
6.000	1.160	0.0	1.160
6.500	0.920	0.0	0.920
7.000	0.760	0.0	0.760
7.500	0.540	0.0	0.540
8.000	0.460	0.0	0.460
8.500	0.300	0.0	0.300
9.000	0.160	0.0	0.160
9.500	0.040	0.0	0.040
10.000	0.180	0.0	0.180
10.500	0.260	0.0	0.260
11.000	0.240	0.0	0.240
11.500	0.240	0.0	0.240
12.000	0.500	0.0	0.500
12.500	1.100	0.0	1.100
13.000	1.400	0.0	1.400
13.500	1.500	0.0	1.500
14.000	1.400	0.0	1.400

TABLE 3 SUMMARY OF DATA FOR RUN U-7

TOTAL SEDIMENT ADDED = 1000 G
0 G ILLITE
500 G KAOLINITE
500 G MONTMORILLIONITE

SUSPENDED SEDIMENT CONCENTRATION

TIME (HR-MIN)	MUD (G/L)	SAND (G/L)	TOTAL (G/L)
0.0	3.080	0.0	3.080
0.500	2.880	0.0	2.880
1.000	2.940	0.0	2.940
1.500	3.100	0.0	3.100
2.000	3.060	0.0	3.060
2.500	3.000	0.0	3.000
3.000	2.700	0.0	2.700
3.500	0.200	0.0	0.200
4.000	0.320	0.0	0.320
4.500	0.740	0.0	0.740
5.000	0.940	0.0	0.940
5.500	1.100	0.0	1.100
6.000	0.820	0.0	0.820
6.500	0.760	0.0	0.760
7.000	0.600	0.0	0.600
7.500	0.460	0.0	0.460
8.000	0.360	0.0	0.360
8.500	0.220	0.0	0.220
9.000	0.240	0.0	0.240
9.500	0.100	0.0	0.100
10.000	0.0	0.0	0.0
10.500	0.080	0.0	0.080
11.000	0.200	0.0	0.200
11.500	0.160	0.0	0.160
12.000	0.400	0.0	0.400
12.500	0.860	0.0	0.860
13.000	1.360	0.0	1.360
13.500	2.080	0.0	2.080
14.000	2.500	0.0	2.500

TABLE 3 SUMMARY OF DATA FOR RUN U-8

TOTAL SEDIMENT ADDED = 1000 G
0 G ILLITE
500 G KAOLINITE
500 G MONTMORILLIONITE

SUSPENDED SEDIMENT CONCENTRATION

TIME (HR-MIN)	MUD (G/L)	SAND (G/L)	TOTAL (G/L)
0.0	3.280	0.0	3.280
0.500	3.240	0.0	3.240
1.000	3.440	0.0	3.440
1.500	3.380	0.0	3.380
2.000	3.200	0.0	3.200
2.500	0.720	0.0	0.720
3.000	1.200	0.0	1.200
3.500	0.300	0.0	0.300
4.000	0.780	0.0	0.780
4.500	1.200	0.0	1.200
5.000	1.560	0.0	1.560
5.500	1.760	0.0	1.760
6.000	1.620	0.0	1.620
6.500	1.440	0.0	1.440
7.000	1.180	0.0	1.180
7.500	0.720	0.0	0.720
8.000	0.340	0.0	0.340
8.500	0.160	0.0	0.160
9.000	0.120	0.0	0.120
9.500	0.020	0.0	0.020
10.000	0.360	0.0	0.360
10.500	0.240	0.0	0.240
11.000	0.240	0.0	0.240
11.500	0.320	0.0	0.320
12.000	0.960	0.0	0.960
12.500	1.820	0.0	1.820
13.000	2.040	0.0	2.040
13.500	2.580	0.0	2.580
14.000	2.780	0.0	2.780

TABLE 3 SUMMARY OF DATA FOR RUN V-1

TOTAL SEDIMENT ADDED = 1400 G
0 G ILLITE
750 G KAOLINITE
750 G MONTMORILLIONITE

SUSPENDED SEDIMENT CONCENTRATION

TIME (HR-MIN)	MUD (G/L)	SAND (G/L)	TOTAL (G/L)
0.0	3.820	0.0	3.820
0.500	3.680	0.0	3.680
1.000	3.700	0.0	3.700
1.500	3.500	0.0	3.500
2.000	2.080	0.0	2.080
2.500	3.280	0.0	3.280
3.000	0.580	0.0	0.580
3.120	0.160	0.0	0.160
3.500	0.800	0.0	0.800
4.000	0.940	0.0	0.940
4.500	1.200	0.0	1.200
5.000	3.280	0.0	3.280
5.500	1.280	0.0	1.280

APPENDIX B: PHOTOGRAPHS OF THE EXPERIMENTAL RUNS

The figures in this appendix are the ones referred to in Appendix A.

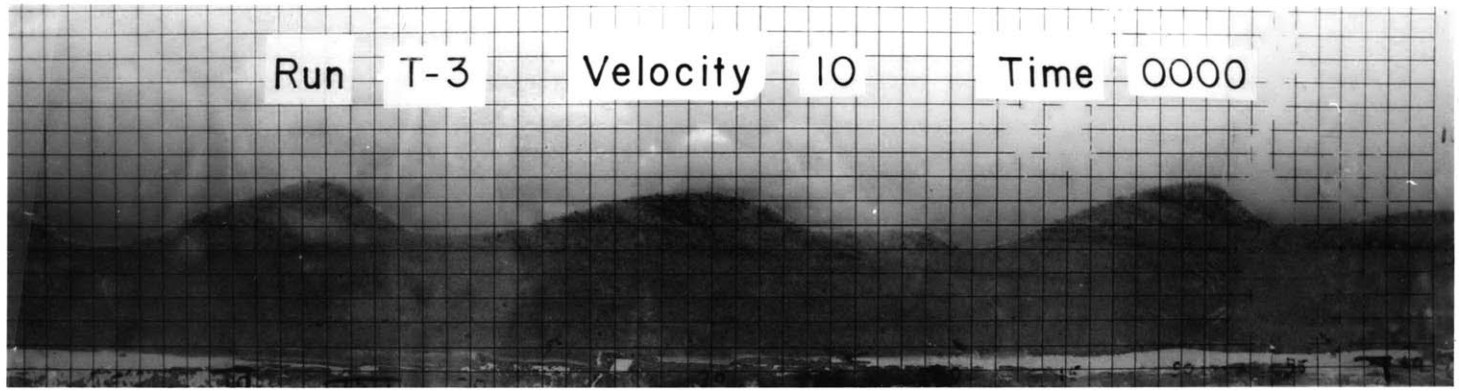

Figure 1:

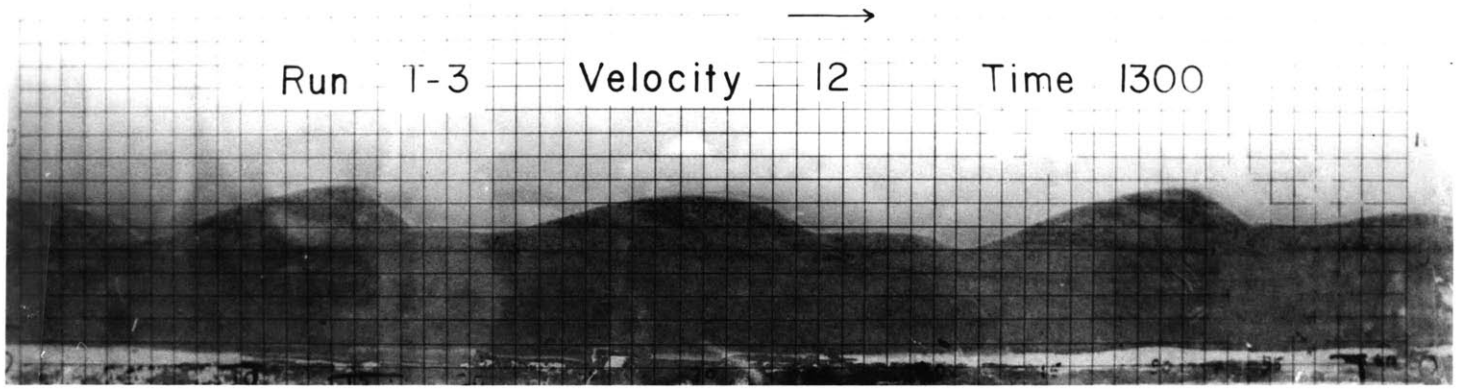

Figure 2:

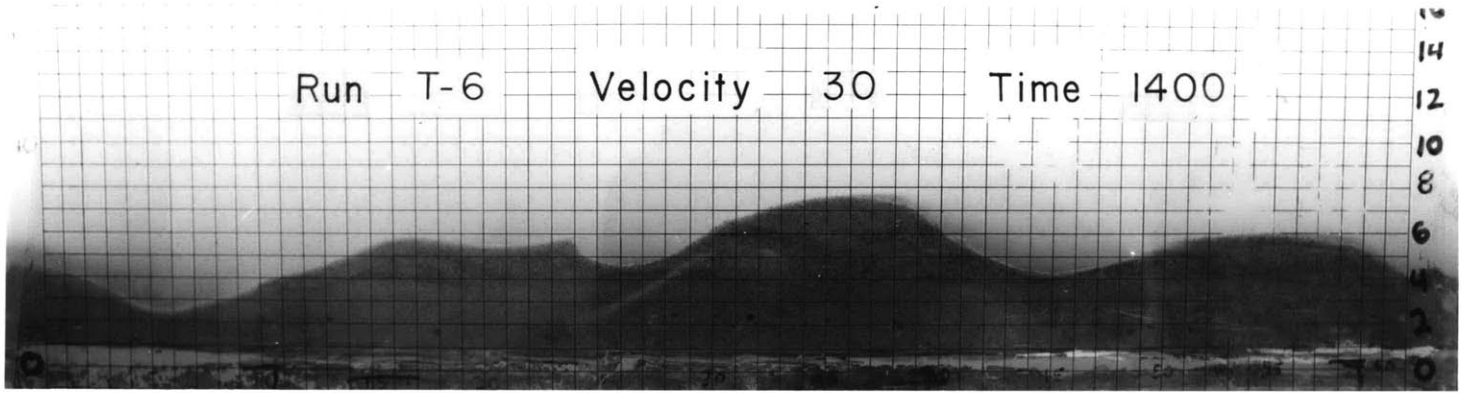

Figure 3:

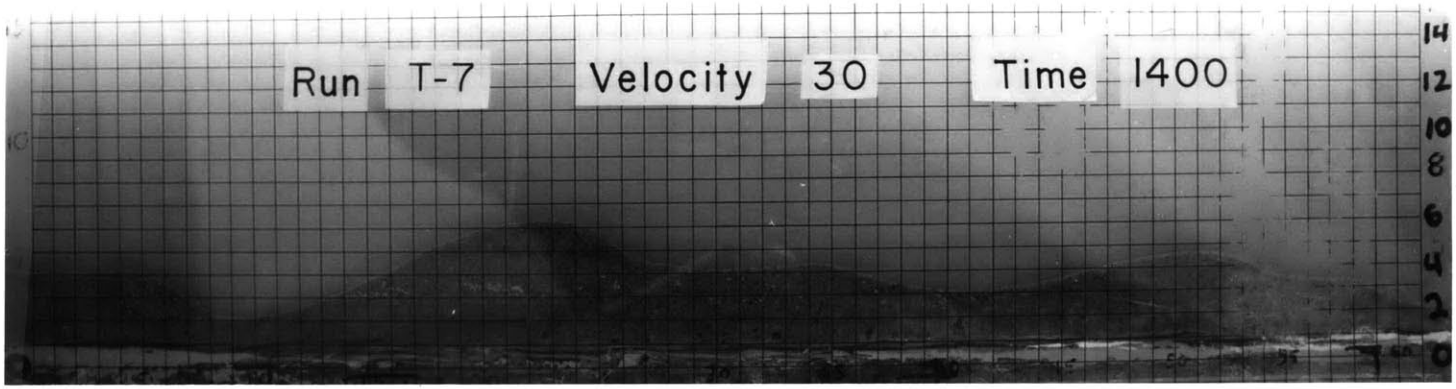

Figure 4:

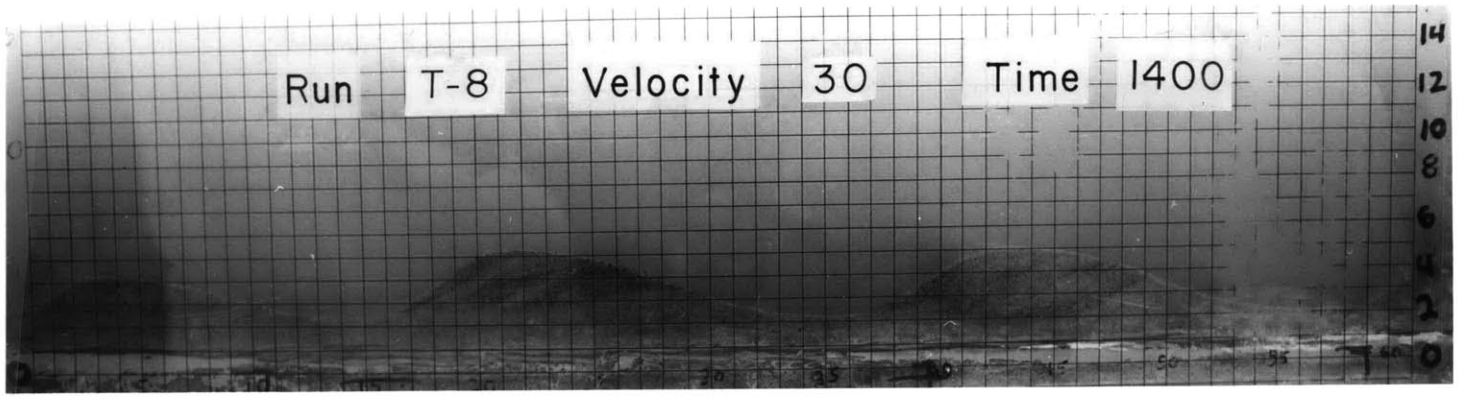

Figure 5:

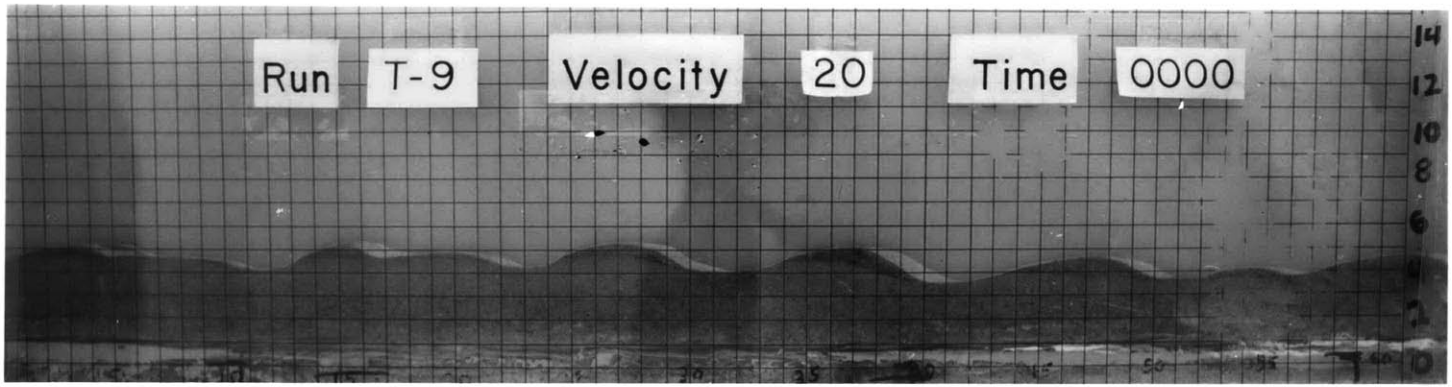

Figure 6:

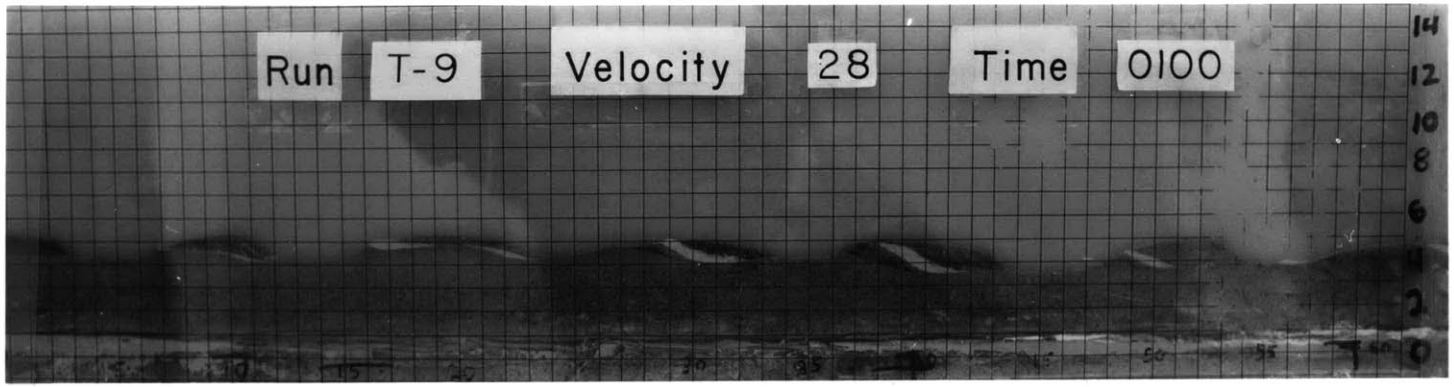

Figure 7:

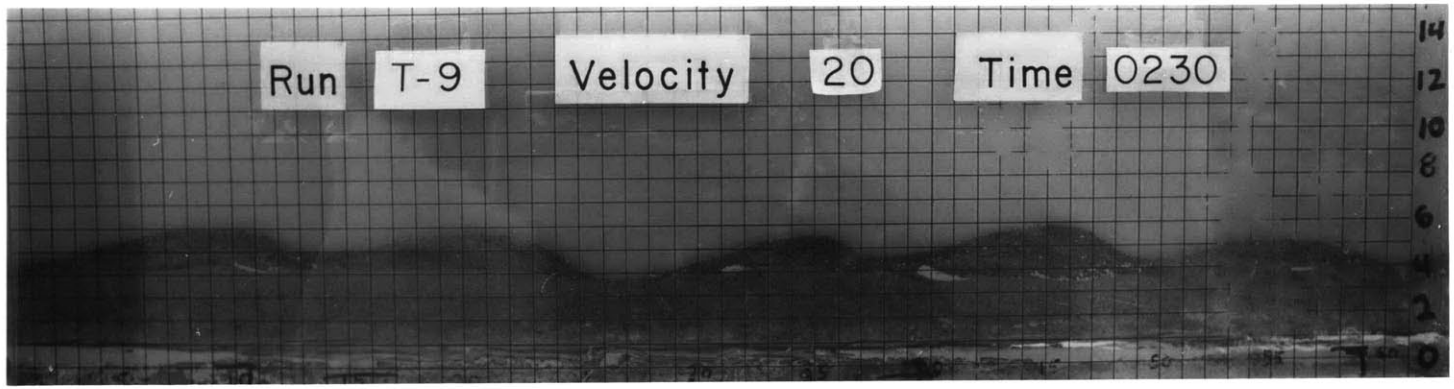

Figure 8: Flow right to left.

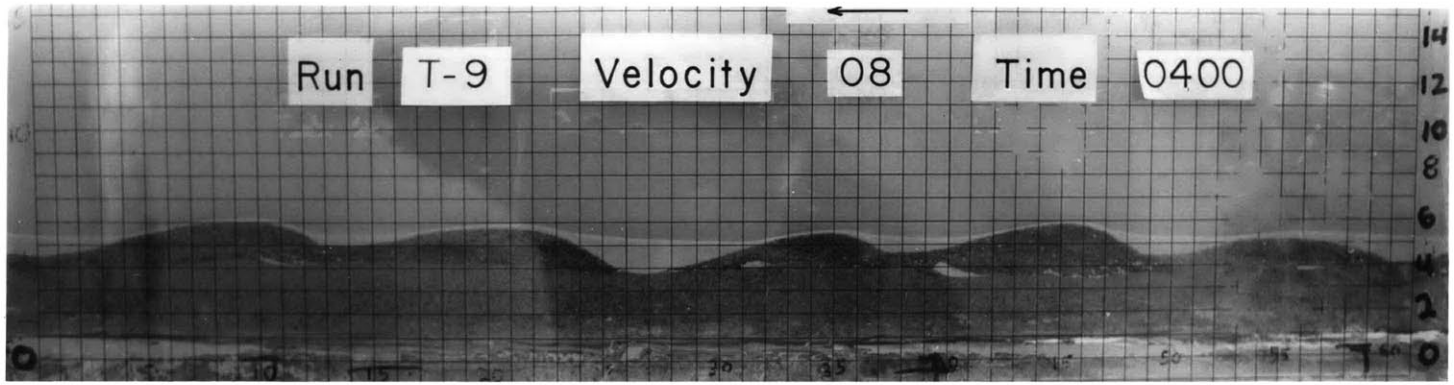

Figure 9: Flow right to left.

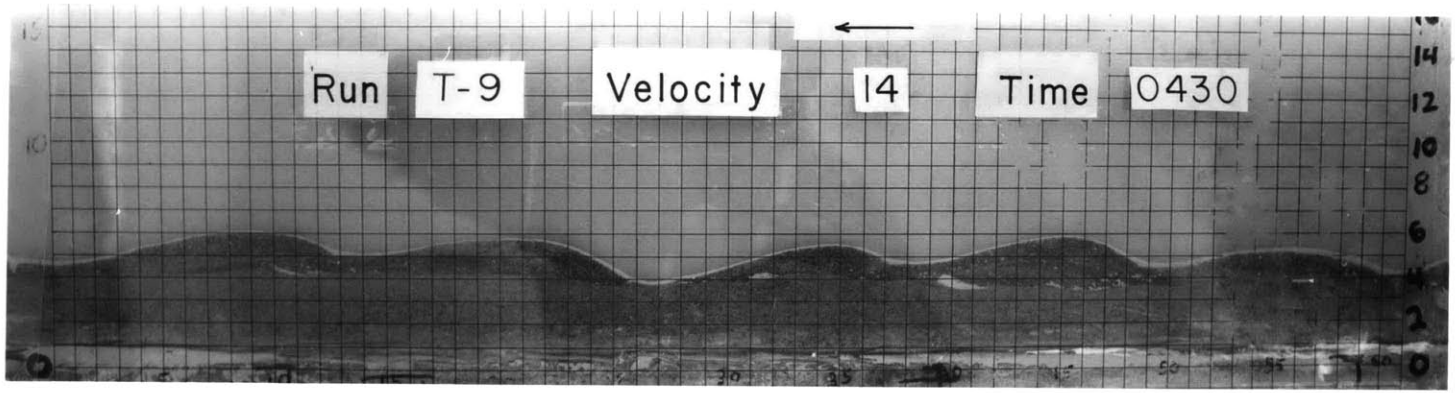

Figure 10: Flow right to left.

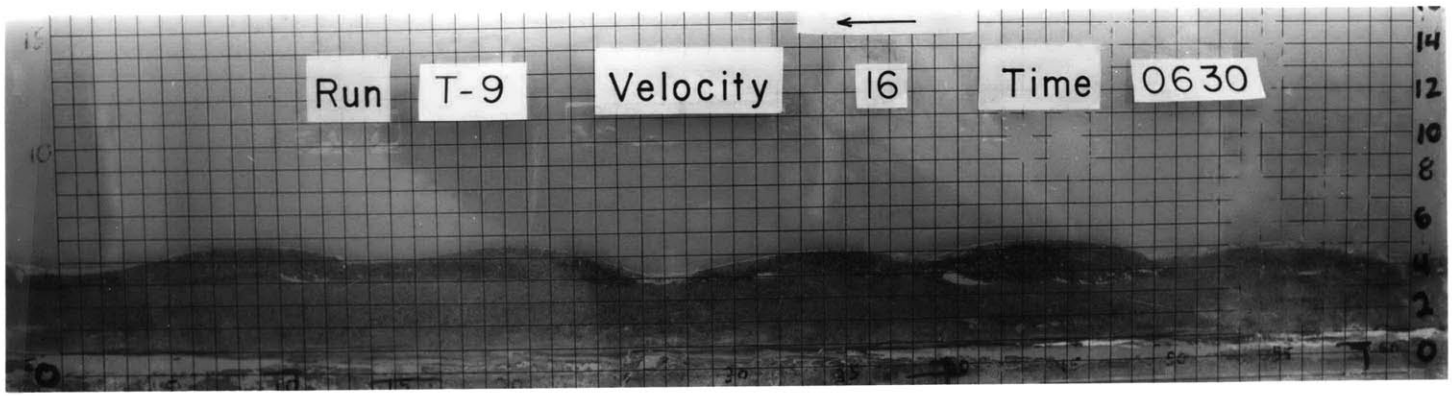

Figure 11: Flow right to left.

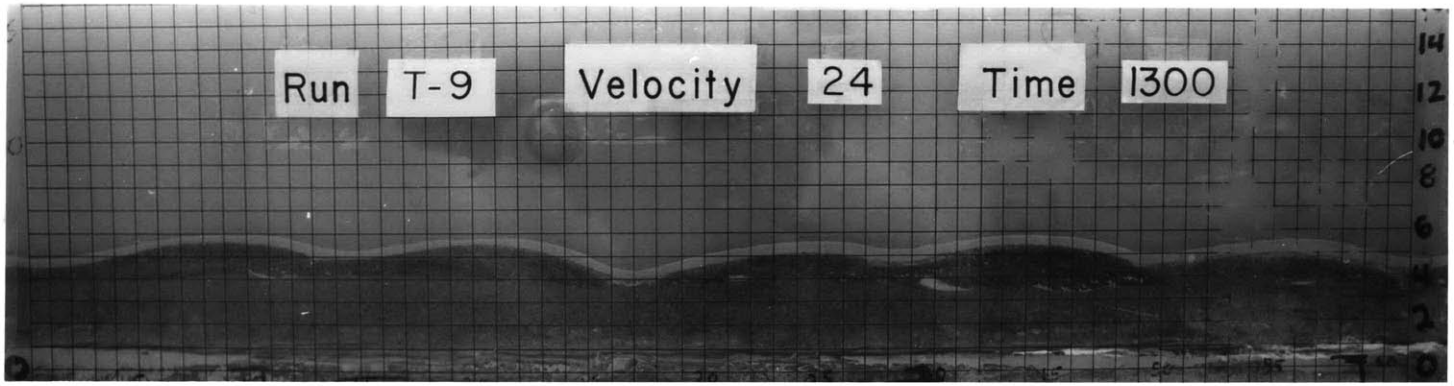

Figure 12:

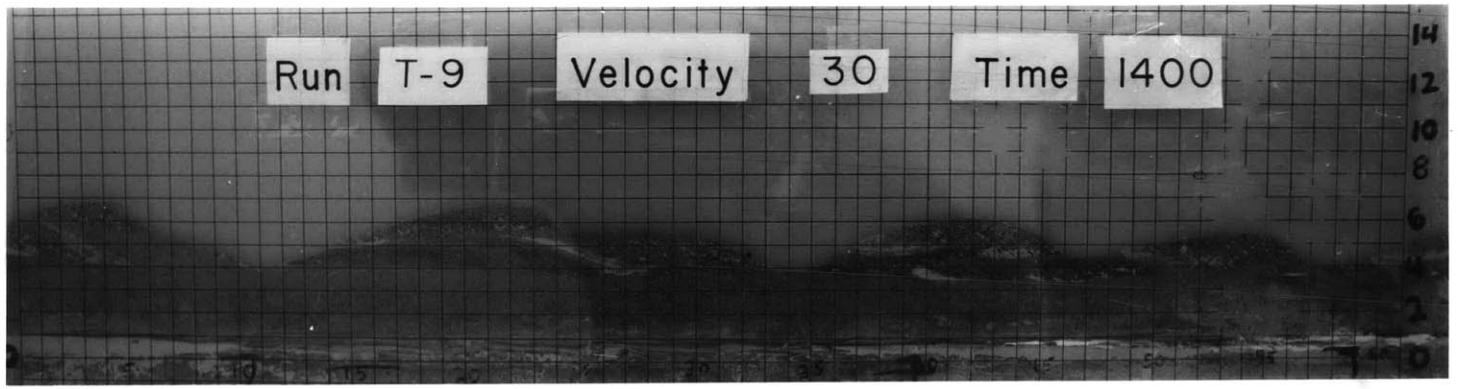

Figure 13:

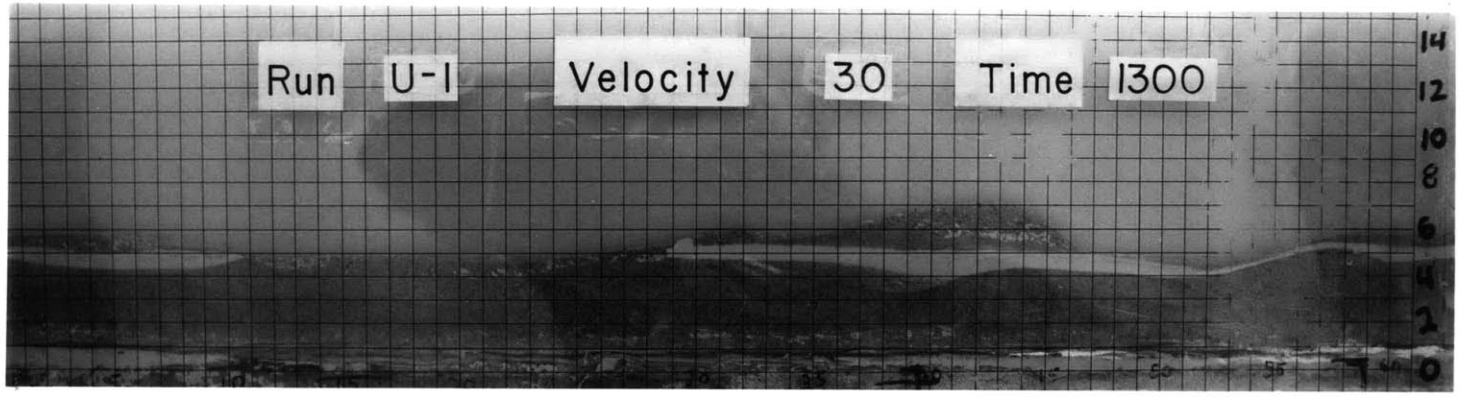

Figure 14:

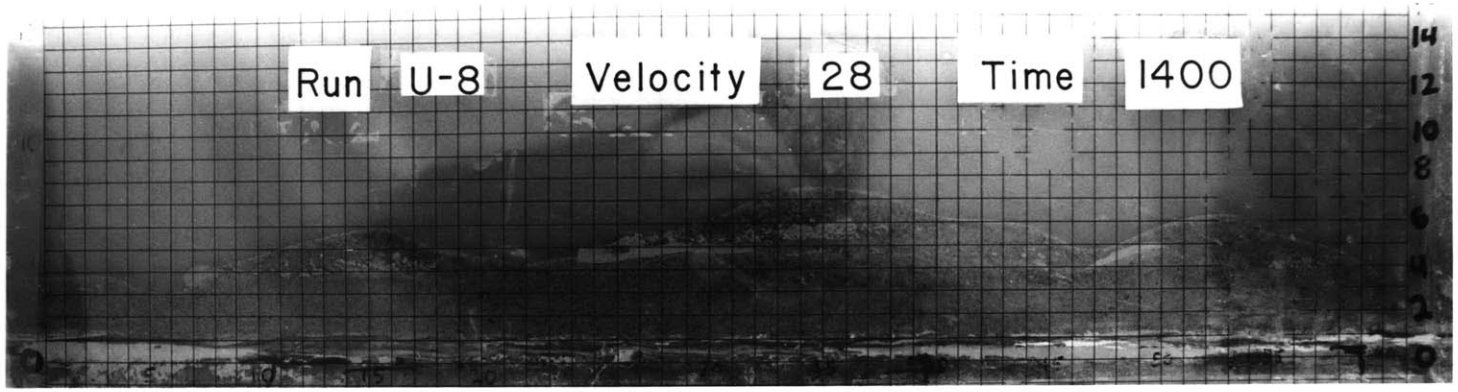

Figure 15:

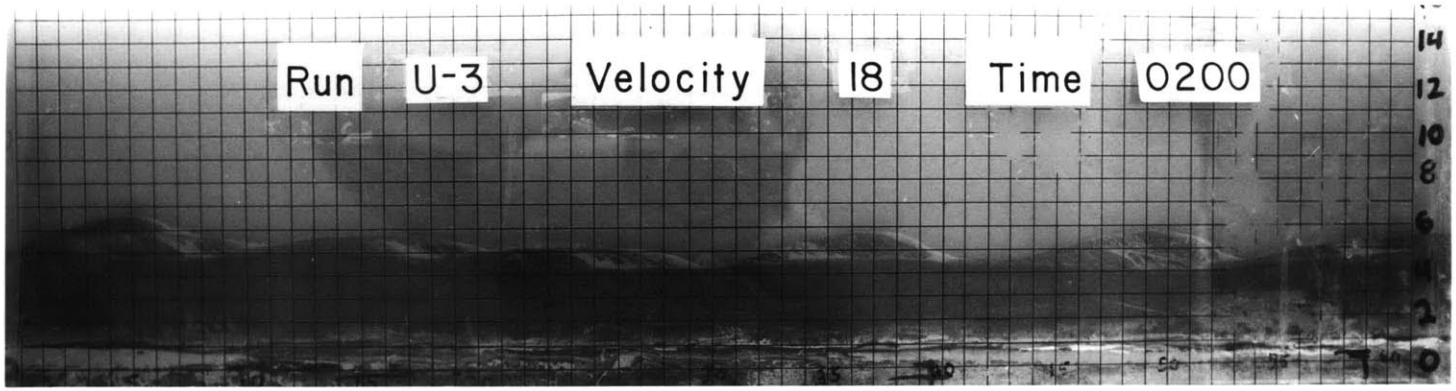

Figure 16:

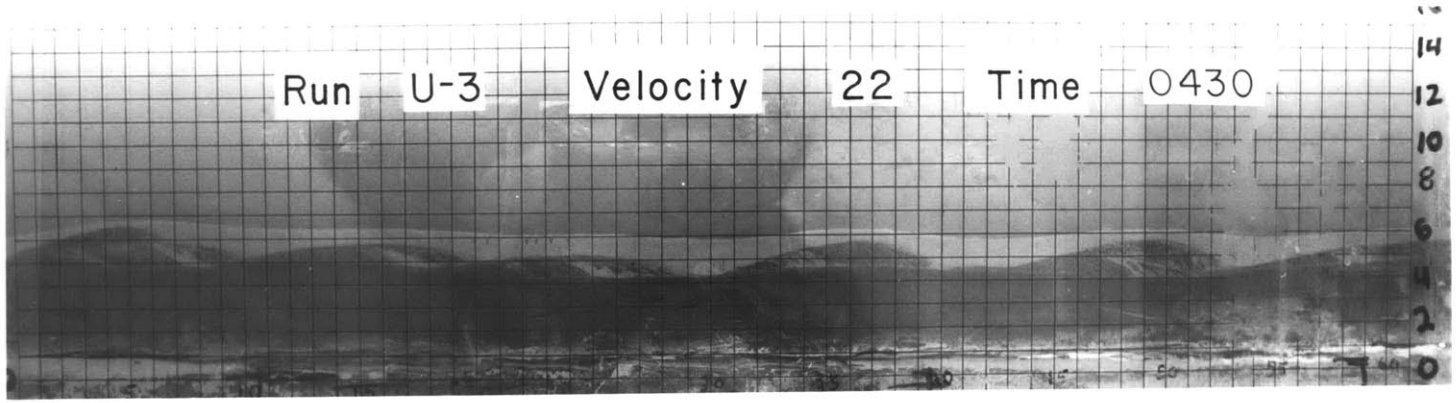

Figure 17: Flow right to left.

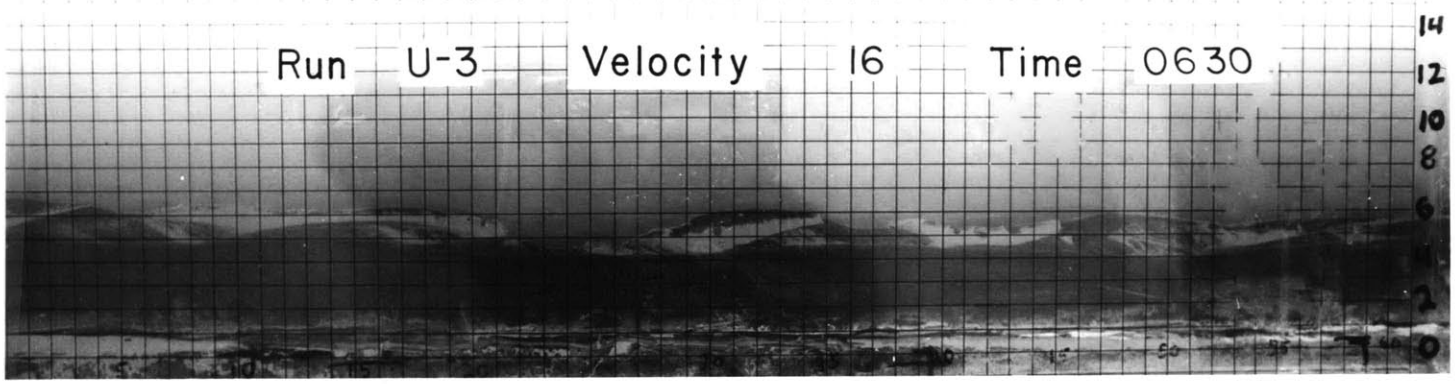

Figure 18: Flow right to left.

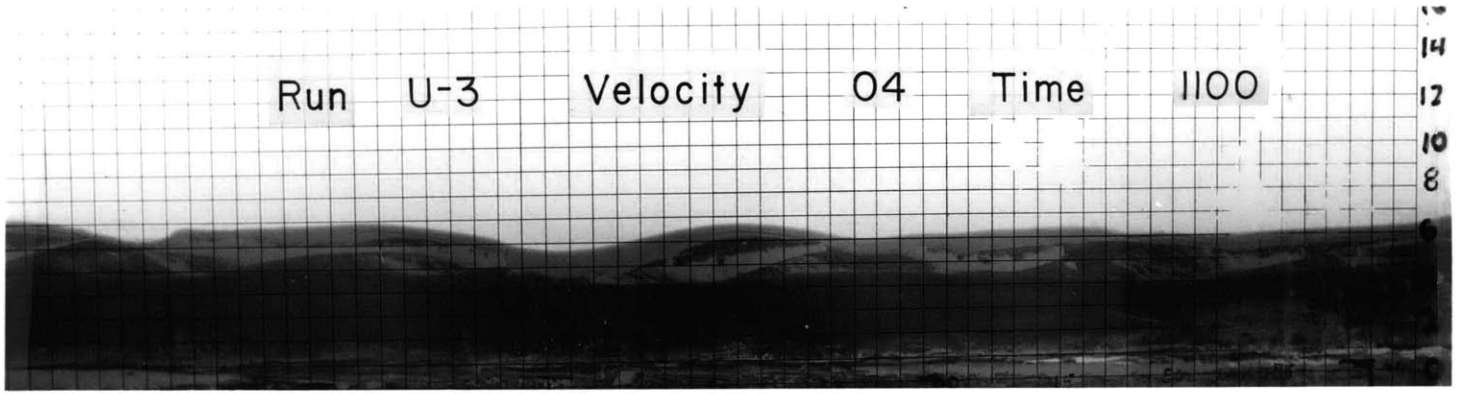

Figure 19:

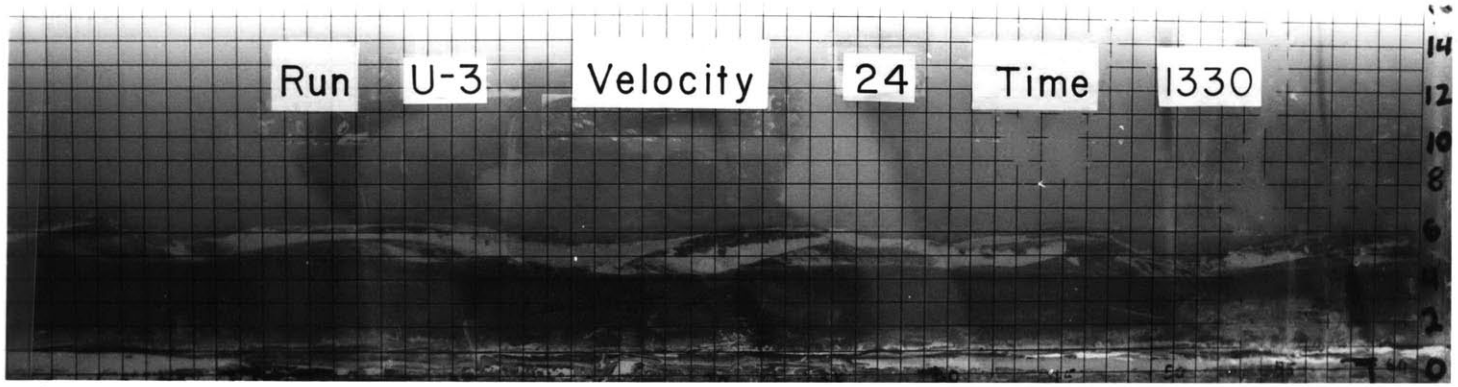

Figure 20:

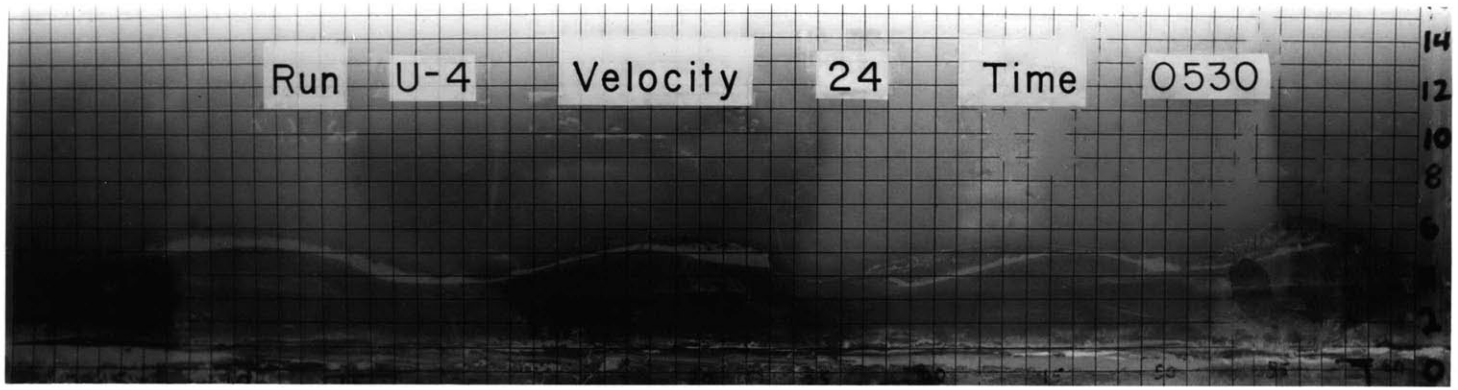

Figure 21: Flow right to left.

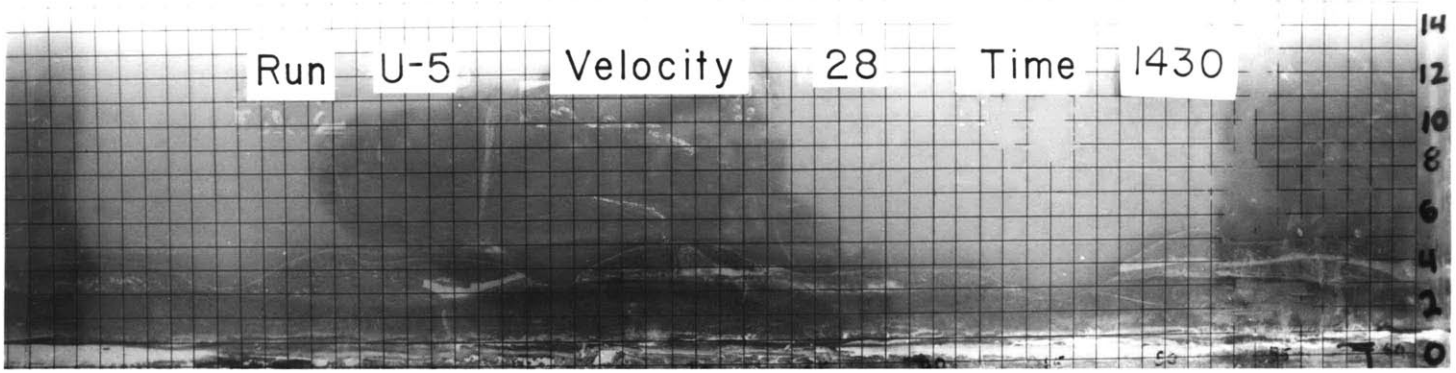

Figure 22:

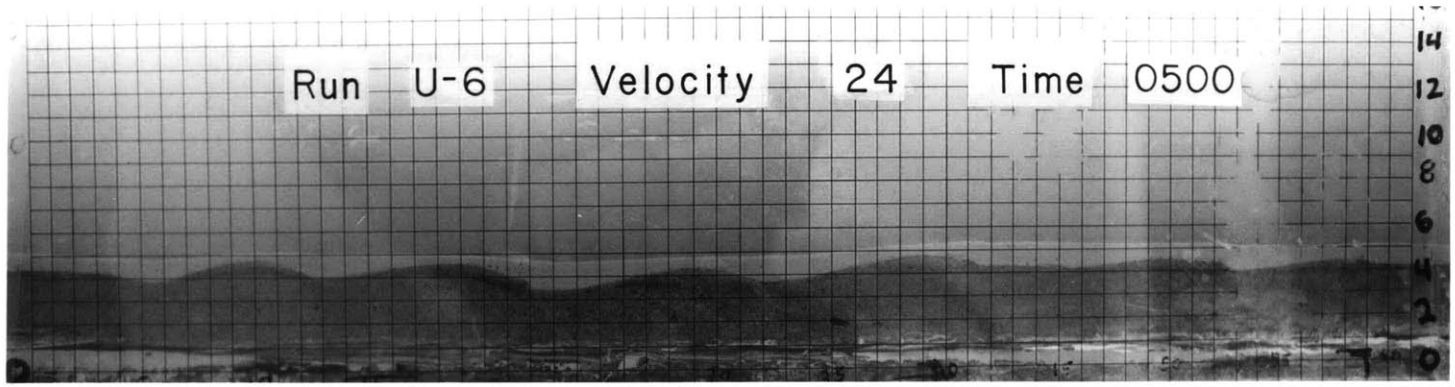

Figure 23: Flow right to left.

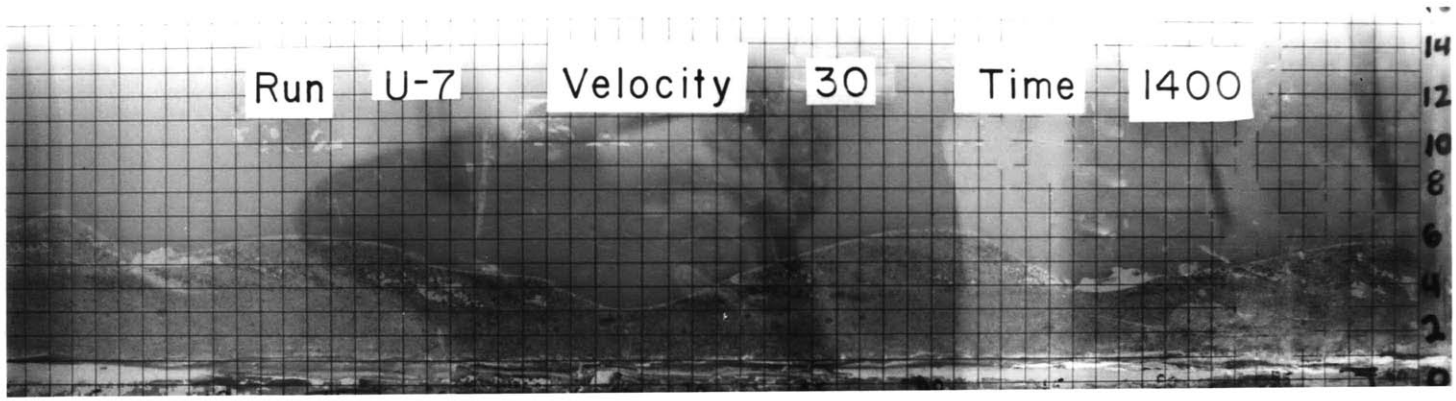

Figure 24:

APPENDIX C: LISTINGS OF THE COMPUTER PROGRAMS USED IN THE INVESTIGATIONS

The first program listed (p. 175-180) computes the velocity profile for a tidal cycle. The second program computes the values of u_*, u_{50}, and τ_0. This program also prints the tables given in Appendix A.

```
C PROGRAM TO DETERMINE AT WHICH VALUES OF TIME THE VELOCITY IN A TIDAL
C CYCLE GIVEN A FUNCTION AND THE MAX AND MIN VALUES OF THE VELOCITY
C READ IN DATA
      REAL MN,MX
      INTEGER OB,OA,PB,PA,QC,QA,QB
      DIMENSIONV(61),VP(121),THETA(201),VEL(201),VC(121),VELC(201)
     1THETAC(201),VINT(201),VELCP(201),VINTP(201),TIME(201),TINT(201),
     2IWORK(201)
 1005 WRITE(6,6)
    6 FORMAT(48H1 NEW RUN OF TIDAL SIMULATION CURRENT VELOCITIES)
      READ(5,1) IHC,VMAX,VMIN,VINC,TAU,VELINT
      WRITE(6,2) VMAX,VMIN,VINC,TAU,VELINT
      READ(5,3) IB,IA,JB,JA,KC,KA,KB,LB,LA,MB,MA,NC,NA,NB,OB,OA,PB,PA,
     1QC,QA,QB
      WRITE(6,4) IB,IA,JB,JA,KC,KA,KB,LB,LA,MB,MA,NC,NA,NB,OB,OA,PB,PA,
     1QC,QA,QB
    1 FORMAT (11,5F6.2)
    2 FORMAT(6H VMAX=,F6.2,6H VMIN=,F6.2,6H VINC=,F6.2,
     25H TAU=,F6.2,8H VELINT=,F6.2)
    3 FORMAT(21I3)
    4 FORMAT(4H IB=,I3,3HIA=,I3,3HJB=,I3,3HJA=,I3,3HKC=,I3,3HKA=,I3,3HKB
     2=,I3,2HLB,I3,3HLA=,I3,3HMB=,I3,3HMA=,I3,3HNC=,I3,3HNA=,I3,3HNB=,I3
     3,3HOB=,I3,3HOA=,I3,3HPB=,I3,3HPA=,I3,3HQC=,I3,3HQA=,I3,3HQB=,I3)
C GENERATE V, K IS LENGTH OF V
      PI=3.141593
      V(1)=VMAX
      I=1
   22 V(I+1)= V(I)-VINC
      IF(V(I+1).GT.VMIN) GO TO 20
   21 K=I+1
      GO TO 27
   20 I= I+1
      GO TO 22
C REORDER AND EXPAND V TO VP, NK IS LENGTH OF VP
   27 I=1
      J=1
```

```
   32 IF(V(I)-VELINT) 30,30,31
   31 I=I+1
      GO TO 32
   30 I=I+1
      J=0
      M=0
   35 I=I-1
      J=J+1
      VP(J)=V(I)
      IF(M) 33,33,34
   33 IF(I.GT.1) GO TO 35
      JMAX= J
      M=1
   36 I= I+1
      J=J+1
      VP(J)= V(I)
      IF(I.LT.K) GO TO 36
      GO TO 35
   34 IF(V(I).NE.VELINT)  GO TO 35
      NK= J
      THETA(1)=0.0
      DO 40 I=2,201
   40 THETA(I)= THETA(I-1)+PI/100.0
      DO 42 I=1,201
   42 VEL(I)=IB*SIN(IA*THETA(I))+JB*COS(JA*THETA(I))+KC*SIN(KA*THETA(I))
     2*COS(KB*THETA(I))+LB*SIN(LA*THETA(I))+MB*COS(MA*THETA(I))+NC*SIN(N
     3A*THETA(I))*COS(NB*THETA(I))+OB*SIN(OA*THETA(I))+PB*COS(PA*TH
     4ETA(I))+QC*SIN(QA*THETA(I))*COS(QB*THETA(I))
C FINE MAX AND MIN OF VEL
      MN=0.0
      MX=0.0
      DO 2000 I=1,200
      IF(VEL(I).GT.MX)  GO TO 4000
      IF(VEL(I).LT.MN) GO TO 5000
      GO TO 2000
 4000 MX=VEL(I)
```

```
      IMX=I
      GO TO 2000
 5000 MN=VEL(I)
      IMN=I
 2000 CONTINUE
C TESTING FOR ZEROES
      VEL(201) = VEL(1)
   50 NZ=0
   52 DO 54 I=1,200
      IF(VEL(I)) 55,53,56
   55 IF(VEL(I+1)) 54,54,53
   56 IF(VEL(I+1)) 53,54,54
   53 NZ=NZ+1
   54 CONTINUE
      IF(NZ.NE.2) GO TO 1000
      WRITE(6,500) NZ
  500 FORMAT (5H NZ= ,I3)
C NORMALIZE
      IF(ABS(VEL(IMX)).GE.ABS(VEL(IMN))) GO TO 60
      Q= VMAX/ABS(VEL(IMN))
      DO 61 I=1,201
   61 VEL(I)= -1.0*Q*VEL(I)
      L=IMN
      K= IMX
      IMN=K
      IMX=L
      GO TO 62
   60 Q= VMAX/VEL(IMX)
      DO 63 I=1,201
   63 VEL(I)= Q*VEL(I)
   62 IF(ABS(VMAX).EQ.ABS(VMIN)) GO TO 69
      R= VMIN/VEL(IMN)
      DO 66 I=1,201
      IF(VEL(I).GT.0.0) GO TO 66
      VEL(I)= R*VEL(I)
   66 CONTINUE
```

```
C SETTING NEAREST VALUE OF VEL EQUAL TOCORRESPONDING VP
   69 L= IMX
      I=1
      DO 70 J= JMAX,NK
   74 IF(ABS(VEL(L)-VP(J)).GT.ABS(VEL(L+1)-VP(J)))  GO TO 71
      VC(I) = VP(J)
      VELC(I) = VEL(L)
      THETAC(I)=THETA(L)
      I=I+1
      L= L+1
      IF(L.GT.200) L=1
      GO TO 70
   71 L=L+1
      IF(L.GT.200) L=1
      GO TO 74
   70 CONTINUE
      DO 72 J=2,JMAX
   76 IF(ABS(VEL(L)-VP(J)).GT.ABS(VEL(L+1)-VP(J))) GOTO 73
      VC(I)=VP(J)
   77 VELC(I)= VEL(L)
      THETAC(I)= THETA(L)
      I=I+1
      L= L+1
      IF(L.GT.200)   L=1
      GO TO 72
   73 L=L+1
      IF(L.GT.200)   L=1
      GO TO 76
   72 CONTINUE
      K=0
      R=0.0
      J= NK-JMAX+1
      DO 88 I=1,NK
      VELCP(I) = VELC(J)
      VINTP(I)= THETAC(J) +R*PI
      J= J+1
```

```
      IF(J.GT.NK) J=2
      IF(K.EQ.1)  GO TO 88
      IF(THETAC(J).GT. THETAC(J-1))  GO TO 88
      R= 2.0
      K=1
   88 CONTINUE
C COMPUTE INTERVALS
      DO 80 MS=2,NK
   80 VINT(MS) = (VINTP(MS)-VINTP(MS-1))/2.0+VINTP(MS-1)
      VINT(1)= VINT(NK)- 2.0*PI
      PUNCH 5,IB,IA,JB,JA,KC,KA,KB,LB,LA,MB,MA,NC,NA,NB,
     2OB,OA,PB,PA,QC,QB,QA,VMAX,VMIN,VELINT
    5 FORMAT (21I1,3F6.2)
      DO 94 J=1,NK
      Q=0.0
      TINT(J)= (VINT(J)-VINT(1))*TAU/(2.0*PI)
      TIME(J)=TINT(J)
 6400 IF(TIME(J).LT.1.0)  GO TO 6500
      TIME(J)=TIME(J)-1.0
      Q= Q+1.0
      GO TO 6400
 6500 TIME(J)= 0.6*TIME(J) +Q
      WRITE(6,910) J,VELCP(J),J,TINT(J),J,TIME(J),J,VP(J)
  910 FORMAT (7H VELCP(,I3,3H)= ,F12.7,6H TINT(,I3,3H)= ,F12.7,
     26H TIME(,I3,3H)= ,F12.7,4H VP(,I3,3H)= ,F12.7)
      PUNCH15,VELCP(J),TINT(J),TIME(J),VP(J)
   15 FORMAT (4F12.7)
   94 CONTINUE
      IX=1
      IY=1
      CALL QKRPLT(TINT,VP,NK,IX,IY,IWORK)
      GO TO 1002
 1000 WRITE (6,1001) NZ
 1001 FORMAT(27H ERROR TOO MANY ZEROES,NZ= ,I3)
 1002 IF (IHC.NE.1)  GO TO 1005
    7 ~~STOP~~ END
```

END

```
      REAL MEAN,MEAN3
      REAL MULT1,MULT2
      REAL NU
      DIMENSION X(5,5),XT(5),MEAN(5),MEAN3(5),SLOP(2),SLOP3(2),Y(5),
     1Y3(3)
      DIMENSION WATER(18,3),TIME(30)
      DIMENSION TINT(100),VP(100),TISD(100),SD1(100),SD2(100),SDT(100)
      DIMENSION AB(30,30),ITAB(3)
      COMMON SLOM
      COMMON DIA
      COMMON U501,U502,U503,U504,UB3,TAU
      COMMON FR,RW,RB,RP,KQ
      COMMON U5011,U5012,U5021,U5022,U5031,U5032
      COMMON KC
      COMMONX,XT,MEAN,MEAN3,SLOP,SLOP3,Y,Y3,R23,R25
      COMMON RHO,NU,DE,DEP,RE,R,TAUT,TAUB,TAUW,UB,Z,FT,FW,FB,T,C,UB2,
     1TAU2
      DATA ITAB/1,2,3/
      DATA WATER/10.0,11.0,12.0,13.0,14.0,15.0,16.0,17.0,18.0,19.0,20.0
     1,21.0,22.0,23.0,24.0,25.0,26.0,27.0,13.48,13.14,12.79,12.45,12.10,
     211.76,11.49,11.21,10.94,10.66,10.39,10.16,9.93,9.71,9.48,9.25,
     39.07,8.88,1.011444,1.011312,1.0111169,1.011015,1.01085,1.0106741,
     41.010432,1.010290,
     51.010082,1.009865,1.009638,1.009401,1.009155,1.008899,1.008634,
     61.008360,1.008077,1.007785/
      Y(1)=0.0
      Y(2)=100.0
      Y(3)=200.0
      Y(4)=300.0
      Y(5)=400.0
C READ IN DATA CARDS
C READ IN CARD WITH NUMBER OF RUNS
      READ (5,2) NR
      DO 30 I=1,NR
C READ IN CONTROL CARD FOR EACH RUN
      READ(5,3) TITLE,NDS,CDV,DIA
```

```
      DO 40 J=1,NDS
C READ IN CONTROL CARD FOR SLOPE MEASUREMENTS
      READ (5,4) V,DE,T,DEP
C READ IN SLOPE MEAS
      DO 99 N=1,5
   99 READ (5,5) (X(M,N),M=1,5)
      DO 80 L=1,18
      IF(T.EQ.WATER(L,1)) GO TO 90
   80 CONTINUE
   90 NU= WATER(L,2)/10.0**3
      RHO=WATER(L,3)
      CALL SLOPE
      IF(KQ.EQ.0) GO TO 550
      AB(1,J)=V
      AB(2,J)= T
      AB(3,J)= NU
      AB(4,J)= RE
      AB(5,J)= SLOT
      AB(6,J)= R25
      AB(11,J)= V
      DO 500 MN=7,10
  500 AB(MN,J)=0.0
      DO 520 MN=12,19
  520 AB(MN,J)=0.0
      GO TO 40
  550 AE=DE
      VU= ABS(V)
      SLOT =ABS(SLOP(2))
      R2=R25
      CALL CALC(AE,SLOT,VU)
    2 FORMAT(I3)
    3 FORMAT(A4,I2,I1,F5.3)
    4 FORMAT (F5.2,4F5.3)
    5 FORMAT (5(2X,F4.2))
      AB(1,J)= V
      AB(2,J)= T
```

```
      AB(3,J)=NU
      AB(4,J) = RE
      AB(5,J) = SLOT
      AB(6,J) = R2
      AB(7,J) = FT
      AB(8,J) = UB
      AB(9,J) = UB2
      AB(10,J) = UB3
      AB(11,J) = V
      AB(12,J) = UB3
      AB(13,J) =FR
      AB(14,J) = SLOM
      AB(15,J) = TAU
      AB(16,J) = U501
      AB(17,J) = U502
      AB(18,J) = U503
      AB(19,J) = U504.
   40 CONTINUE
      WRITE(6,100) ITAB(1),TITLE
  100 FORMAT(1H ,////,45X,6HTABLE ,I2,25H SUMMARY OF DATA FOR RUN ,A4,
     1//)
      WRITE(6,130) DIA
  130 FORMAT(1H ,36X,57HDEPTH = 12 CM    HYDRAULIC RADIUS = 4.54 CM    SAN
     1D SIZE = ,F5.3, 3H CM,//)
      WRITE(6,110)
  110 FORMAT(1H ,15X,8HVELOCITY,5X,5HTEMP.,5X,9HVISCOSITY,5X,
     18HREYNOLDS,5X,7HSURFACE,9X,2HR2,8X,1HF,5X,5HU*(1),4X,5HU*(2),4X,
     25HU*(3),/,16X,6H(CM/S),5X,8H(DEG. C),4X,8H(STOKES),7X,6HNUMBER,
     37X,5HSLOPE,25X,6H(CM/S),3X,6H(CM/S),3X,6H(CM/S),//)
      DO 190 M=1,NDS
  190 WRITE(6,120) (AB(K,M),K=1,10)
  120 FORMAT(1H ,16X,F5.1,7X,F4.1,5X,E10.3,3X,E10.3,3X,E10.3,3X,E10.3,
     13X,F5.3,2X,3(F6.2,3X))
      WRITE(6,150)
  150 FORMAT(1H1)
      WRITE(6,100)ITAB(1),TITLE
```

```
      WRITE(6,140)
  140 FORMAT(1H ,22X,8HVELOCITY,3X,5HU*(3),4X,2HFR,9X,2HSE,7X,3HTAU,
     15X,6HU50(1),3X,6HU50(2),3X,6HU50(3),3X,6HU50(4), /,24X,6H(CM/S),
     23X,6H(CM/S),23X,6HDYNES/,4(3X,6H(CM/S)),/,62X,6HCM**2),//)
      DO 180 M=1,NDS
  180 WRITE(6,160) (AB(K,M),K=11,19)
  160 FORMAT(1H ,24X,F5.1,5X,F4.2,3X,F4.2,3X,E10.3,3X,F5.2,4X,
     14(F6.2,3X))
      WRITE(6,150)
   30 CONTINUE
      READ (5,800) NRV
  800 FORMAT(I2)
      DO 820 M=1,NRV
      READ(5,802) TITLE,NV
  802 FORMAT(A4,I2)
      NQ=NV/2
      DO 810 MV=1,NV
  810 READ(5,804) TINT(MV),VP(MV)
  804 FORMAT(24X,2F12.7)
      WRITE(6,100) ITAB(2),TITLE
      WRITE(6,220)
  220 FORMAT(1H ,56X,17H VELOCITY PROFILE, //,38X,2(4HTIME,9X,8HVELOCITY
     114X), /,36X,2(8H(HR-MIN),8X,6H(CM/S),13X),//)
      DO 812 MV=1,NQ
  812 WRITE(6,806) TINT(MV),VP(MV),TINT(MV+NQ),VP(MV+NQ)
  806 FORMAT (1H ,35X,F5.2,11X,F6.2,14X,F5.2,11X,F6.2)
      WRITE(6,150)
  820 CONTINUE
      READ(5,900) NRC
  900 FORMAT(I2)
      DO 910 K=1,NRC
      READ(5,902) TITLE,NC,MULT1,MULT2,ITS,ILL,KAOL,MONT
  902 FORMAT(A4,I2,2F5.3,4I4)
      DO 920 N=1,NC
      READ(5,904) TIME(N),SD1(N),SD2(N)
  904 FORMAT(3F10.4)
```

```
      SD1(N)=SD1(N)*MULT1
      SD2(N)=SD2(N)*MULT2
  920 SDT(N)=SD1(N)+SD2(N)
      WRITE(6,100) ITAB(3),TITLE
      WRITE(6,360) ITS
  360 FORMAT(1H ,50X,23HTOTAL SEDIMENT ADDED = ,I4,2H G)
      WRITE (6,370) ILL
  370 FORMAT(1H ,50X,I4,9H G ILLITE)
      WRITE(6,380) KAOL
  380 FORMAT(1H ,50X,I4,12H G KAOLINITE)
      WRITE(6,390) MONT
  390 FORMAT (1H ,50X,I4,19H G MONTMORILLIONITE,//)
      WRITE(6,300)
  300 FORMAT (1H ,47X,32HSUSPENDED SEDIMENT CONCENTRATION,///,40X,4HTIME
     1,13X,3HMUD,10X,4HSAND,10X,5HTOTAL,/,38X,8H(HR-MIN),10X,5H(G/L),9X,
     25H(G/L),11X,5H(G/L),/)
      DO 940 ND=1,NC
  940 WRITE(6,950) TIME(ND),SD1(ND),SD2(ND),SDT(ND)
  950 FORMAT(1H ,38X,2(F6.3,10X,F6.3,8X))
      WRITE (6,150)
  910 CONTINUE
      END
      SUBROUTINE FINDFW
      REAL MEAN,MEAN3
      REAL NU
      DIMENSION X(5,5),XT(5),MEAN(5),MEAN3(5),SLOP(2),SLOP3(2),Y(5),
     1Y3(3)
      DIMENSION TABLE (132,2)
      COMMON SLOM
      COMMON DIA
      COMMON U501,U502,U503,U504,UB3,TAU
      COMMON FR,RW,RB,RP,KQ
      COMMON U5011,U5012,U5021,U5022,U5031,U5032
      COMMON KC
      COMMONX,XT,MEAN,MEAN3,SLOP,SLOP3,Y,Y3,R23,R25
      COMMON RHO,NU,DE,DEP,RE,R,TAUT,TAUB,TAUW,UB,Z,FT,FW,FB,T,C,UB2,
```

```
      1TAU2
       DATA TABLE /2.5,2.55,2.6,2.65,2.7,2.725,2.75,2.775,2.8,2.825,2.85,
      12.875,2.9,2.925,2.95,2.975,3.0,3.025,3.05,3.075,3.1,3.15,3.2,3.25,
      23.3,3.35,3.4,3.45,3.5,3.6,3.65,3.7,3.8,3.85,3.9,3.95,4.0,4.05,4.1,
      34.15,4.2,4.3,4.4,4.45,4.5,4.6,4.65,4.7,4.8,4.85,4.9,5.0,5.1,5.2,
      55.27,5.34,5.4,5.6,5.7,5.8,5.87,5.94,6.0,6.1,6.2,6.4,6.5,6.6,6.8,
      66.9,7.0,7.2,7.4,7.5,7.6,7.8,7.9,8.0,8.2,8.4,8.5,8.6,8.8,9.0,9.1,
      79.2,9.4,9.6,9.8,10.0,10.5,11.0,11.25,11.5,11.75,12.0,12.25,12.5,
      812.75,13.0,13.25,13.5,13.75,14.0,14.4,14.7,15.0,15.5,16.0,16.5,
      917.0,17.4,17.7,18.0,18.5,19.0,19.5,20.0,20.5,21.0,22.0,22.5,23.0,
      123.5,24.0,24.5,25.0,26.0,27.0,28.0,29.0,30.0,3.32,3.31,3.30,3.29,
      23.28,3.27,3.26,3.25,3.24,3.23,3.22,3.21,3.20,3.19,3.18,3.17,3.16,
      23.15,3.14,3.13,3.12,3.11,3.10,3.09,3.08,3.07,3.06,3.05,3.04,3.02,
      33.01,3.00,2.99,2.98,2.97,2.96,2.95,2.94,2.93,2.92,2.91,2.90,2.89,
      42.88,2.87,2.86,2.85,2.84,2.83,2.82,2.81,2.80,2.79,2.78,2.77,2.76,
      52.75,2.74,2.73,2.72,2.71,2.70,2.69,2.68,2.67,2.66,2.65,2.64,2.63,
      62.62,2.61,2.60,2.59,2.58,2.57,2.56,2.55,2.54,2.53,2.52,2.51,2.50,
      72.49,2.28,2.47,2.26,2.45,2.44,2.43,2.42,2.41,2.40,2.39,2.38,2.37,
      82.36,2.35,2.34,2.33,2.32,2.31,2.30,2.29,2.28,2.27,2.26,2.25,2.24,
      92.23,2.22,2.21,2.20,2.19,2.18,2.17,2.16,2.15,2.14,2.13,2.12,2.11,
      12.10,2.09,2.08,2.07,2.06,2.05,2.04,2.03,2.02,2.01,2.00/
       KC=0
       Z= Z/100000.0
C CHECK TO ENSURE THAT Z IS IN RANFE OF TABLE
       IF(Z.LT.TABLE(1,1)) GO TO 50
       IF(Z.GT.TABLE(128,1)) GO TO 50
       I=66
       INDEX=33
       GO TO 121
   10  I=I+INDEX
   11  IF(INDEX-1) 12,14,12
   12  INDEX=INDEX-INDEX/2
  121  IF(Z-TABLE(I,1)) 13,16,10
   13  J=I
       I=I-INDEX
       GO TO 11
```

```
   14 IF(Z-TABLE(I,1)) 15,16,15
   15 IF(ABS(Z-TABLE(I,1)).GT.ABS(Z-TABLE(J,1))) I=J
   16 FW= TABLE(I,2)/100.0
      Z= Z*100000.0
      GO TO 90
   50 KC=1
   90 RETURN
      END
      SUBROUTINE CALC (QE,SLO,V)
      REAL MEAN,MEAN3
      REAL NU
      DIMENSION X(5,5),XT(5),MEAN(5),MEAN3(5),SLOP(2),SLOP3(2),Y(5),
     1Y3(3)
      COMMON SLOM
      COMMON DIA
      COMMON U501,U502,U503,U504,UB3,TAU
      COMMON FR,RW,RB,RP,KQ
      COMMON U5011,U5012,U5021,U5022,U5031,U5032
      COMMON KC
      COMMONX,XT,MEAN,MEAN3,SLOP,SLOP3,Y,Y3,R23,R25
      COMMON RHO,NU,DE,DEP,RE,R,TAUT,TAUB,TAUW,UB,Z,FT,FW,FB,T,C,UB2,
     1TAU2
      R=(QE*14.6)/(2.0*QE+14.6)
      RE= V*QE/NU
      FR=V**2/11760.0
      SLOM= SLO*(1.0-FR**2*SLO)
      FT= (7840.0*R*SLOM)/V**2
      Z=RE/FT
C FIND FW
      CALL FINDFW
      IF(KC.EQ.0) GO TO 90
      FB=0.0
      FW=0.0
   90 FB= FT+2.0*QE/14.6*(FT-FW)
C FIND UB
      UB=SQRT(V**2*FB/8.0)
```

```
      TAUB= (UB/RHO)**2
      TAUT=(V**2*FT/8.0)/(RHO**2)
      TAUW=(V**2*FW/8.0)/RHO**2
      RW= TAUW
      RB= TAUT
      RP= RW/RB
      C=SQRT(8.0/FT)
      UB2= ((.13-.3*ALOG10(QE/30.5))/((C      )-7.66*ALOG10(QE/30.5)-
     111.0))*30.5
      TAU2= (UB2/RHO)**2
      UB3= SQRT(980.0*R*SLOM*(1.0/(1.0+.18*(12.0/30.5)/((14.6/30.5)
     2**2))))
      XU=.01176
      U501= UB3*(5.75*ALOG10(UB3*50.0/XU)+5.5)
      U502=UB3*5.75*ALOG10(30.2*50.0/DIA)
      U503= UB3*(17.66+ALOG10(50.0/(35.45*DIA)))
      U504= UB3*((3.33-.13/(UB3/30.5))*ALOG(50.0/30.5)+14.3)
      TAU = (UB3/RHO)**2
   99 RETURN
      END
      SUBROUTINE SLOPE
      REAL MEAN,MEAN3
      REAL NU
      DIMENSION X(5,5),XT(5),MEAN(5),MEAN3(5),SLOP(2),SLOP3(2),Y(5),
     1Y3(3)
      COMMON SLOM
      COMMON DIA
      COMMON U501,U502,U503,U504,UB3,TAU
      COMMON FR,RW,RB,RP,KQ
      COMMON U5011,U5012,U5021,U5022,U5031,U5032
      COMMON KC
      COMMONX,XT,MEAN,MEAN3,SLOP,SLOP3,Y,Y3,R23,R25
      COMMON RHO,NU,DE,DEP,RE,R,TAUT,TAUB,TAUW,UB,Z,FT,FW,FB,T,C,UB2,
     1TAU2
      A=0.0
      B=0.0
```

```
      G=0.0
      D=0.0
      E=0.0
      A3=0.0
      B3=0.0
      C3=0.0
      D3=0.0
      E3=0.0
C COMPUTE MEAN OF SLOPE MAEASUTEMENTS
      DO 10 J=1,5
      XT(J)=0.0
      DO 20 K=1,5
      XT(J)= XT(J)+X(K,J)
   20 CONTINUE
      MEAN (J)= XT(J)/5.0
   10 CONTINUE
C FIND SLOPE
      SD5=0.0
      SD3=0.0
      NPTS=5
      NCOEFF=2
      CALL LSFIT (NPTS,NCOEFF,Y,MEAN,SLOP)
C CALCULATE R2
      DO 60 K=1,5
      E=E+MEAN(K)*Y(K)
      A=A+MEAN(K)
      B=B+Y(K)
      G= G+MEAN(K)**2
      D=D+Y(K)**2
   60 CONTINUE
      R25=(E-(A*B/5.0))**2/((G-A**2/5.0)*(D-B**2/5.0))
      DO 30 I=1,3
      Y3(I)=Y(I+1)
   30 MEAN3(I)=MEAN(I+1)
      NPTS=3
      CALL LSFIT (NPTS,NCOEFF,Y3,MEAN3,SLOP3)
```

```
      DO 70 K=1,3
      E3= E3+MEAN3(K)*Y3(K)
      A3=A3+MEAN3(K)
      B3=B3+Y3(K)
      C3=C3+MEAN3(K)**2
      D3=D3+Y3(K)**2
   70 CONTINUE
      R23=(E3-(A3*B3/3.0))**2/((C3-A3**2/3.0)*(D3-B3**2/3.0))
      KQ=0
      IF(R25.GE.0.98)  GO TO 90
      IF(R23.GE.0.98) GO TO 89
      IF(R25.GE.R23)  GO TO 88
      R25= R23
      SLOP(2)= SLOP3(2)
   88 IF(R25.GE.0.95) GO TO 90
      KQ=1
      GO TO 90
   89 R25=R23
      SLOP(2)= SLOP3(2)
   90 RETURN
      END
```

APPENDIX D: PROCEDURE USED FOR CALCULATING THE SHEAR VELOCITY

All of the methods for determining u_* involve the energy slope. This was determined by measuring the water-surface elevation at five separate points and determining the water-surface slope. The energy slope was then calculated using equation 8. The accuracy of the determination of S_w is critical to the determination of u_*. A measure of the precision of the slope fit by the least-squares program is given by the value of r^2:

$$r^2 = \frac{[\Sigma x_i y_i - (\Sigma x_i y_i/n)]^2}{[\Sigma x_i^2 - (\Sigma x_i)^2/n]\ [\Sigma y_i^2 - (\Sigma y_i)^2/n]} \qquad \text{(A1)}$$

where x is the surface elevation measurement, y the horizontal distance measurement, and n the number of observations. The closer the value of r^2 to 1.0 the more precise the fit. If the initial fit using the five points gave a value of r^2 greater than or equal to 0.98 the fit was accepted. If r^2 was less than 0.98, another fit using only the central three points was made. This was done because it was noted that, particularly at high velocities, the two end points sometimes deviated considerably from the trend of the central three. The same criterion for the value of r^2 was applied to this fit. If neither of the values of r^2 was greater than 0.95, the slopes were

rejected and no determination of u_* was made. For values of r^2 between 0.95 and 0.98, the slope with the higher r^2 was used. It is hoped that by using this procedure, only valid values of S_w were used.

The sidewall procedure described by Johnson involves separating the cross-section of the flume into areas dominated by either the resistance of the bottom or the resistance of the sidewalls. This is done by dividing the Reynolds number of the flow by the Darcy-Weisback friction factor. The friction factor for the sidewalls can then be read from the graph shown by Vanoni (1975). Once the fraction factor of the sidewalls is known, the friction factor of the bottom may be calculated from:

$$f_{bottom} = f_{flume} - \frac{b}{2d} (f_{flume} - f_{sidewall}) \qquad (A2)$$

Substituting f_{bottom} into:

$$R = \frac{f_{bottom} u^2 S_E}{8g} \qquad (A3)$$

yields the hydraulic radius associated with the bottom. The shear velocity may then be calculated from equation 7. It was found that for the higher velocities, the area dominated by the bottom resistance was only 6 cm wide. This means that all of the visual and photographic observations were made in the area dominated by the sidewall resistance at all but the lowest

velocities. Observations taken during low-velocity periods seem to indicate that depositional activity was fairly uniform over the entire width of the channel. In general, the values of u_* calculated by this method appear to be higher than one would expect.

It was hoped that the method of Richardson and Simons (equation 14) would give acceptable results since the equation was developed specifically for rippled beds. In general the results for the lower velocities seem reasonable, but at higher velocities the values fluctuate widely with very minor changes in slope, sometimes giving completely ridiculous results.

The third method, that of Williams, involves a simple correction to the measured energy slope to take into account the sidewall effects, (equation 19). U*(3) is then determined by substitution into equation 7. Results of these calculations are given in Table 1 of Appendix A.